[redacted]

Russian Original Vol. 33, No. 3, September, 1972

March, 1973

File in NTB/NED

SATEAZ 33(3) 837-922 (1972)

SOVIET ATOMIC ENERGY

АТОМНАЯ ЭНЕРГИЯ
(ATOMNAYA ÉNERGIYA)

TRANSLATED FROM RUSSIAN

CONSULTANTS BUREAU, NEW YORK

SOVIET ATOMIC ENERGY

Soviet Atomic Energy is a cover-to-cover translation of *Atomnaya Énergiya*, a publication of the Academy of Sciences of the USSR.

An arrangement with Mezhdunarodnaya Kniga, the Soviet book export agency, makes available both advance copies of the Russian journal and original glossy photographs and artwork. This serves to decrease the necessary time lag between publication of the original and publication of the translation and helps to improve the quality of the latter. The translation began with the first issue of the Russian journal.

Consultants Bureau journals appear about six months after the publication of the original Russian issue. For bibliographic accuracy, the English issue published by Consultants Bureau carries the same number and date as the original Russian from which it was translated. For example, a Russian issue published in December will appear in a Consultants Bureau English translation about the following June, but the translation issue will carry the December date. When ordering any volume or particular issue of a Consultants Bureau journal, please specify the date and, where applicable, the volume and issue numbers of the original Russian. The material you will receive will be a translation of that Russian volume or issue.

Subscription
$75.00 per volume (6 Issues) — Single Issue: $30
2 volumes per year — Single Article: $15
(Add $5 for orders outside the United States and Canada.)

CONSULTANTS BUREAU, NEW YORK AND LONDON

227 West 17th Street
New York, New York 10011

Davis House
8 Scrubs Lane
Harlesden, NW10 6SE
England

Published monthly. Second-class postage paid at Jamaica, New York 11431.

SOVIET ATOMIC ENERGY

A translation of *Atomnaya Énergiya*

March, 1973

Volume 33, Number 3 September, 1972

CONTENTS

	Engl.	Russ.
REVIEWS		
The Status of the Radioactive Waste Disposal Problem – B. S. Kolychev, V. V. Kulichenko, and F. V. Rauzen	837	723
ARTICLES		
Strength of Construction Elements in the Fuel Channel of the Beloyarsk Atomic Power Station Reactors – I. Ya. Emel'yanov, O. A. Shatskaya, E. Yu. Rivkin, and N. Ya. Nikolenko	842	729
Automation of Nuclear Power Plants and Discrete Power Drives – I. Ya. Emel'yanov, V. V. Voskoboinikov, and V. P. Perfil'ev	848	735
Use of Surface Roughness to Improve Heat Transfer from Rod Type Fuel Elements – O. S. Vinogradov and P. I. Puchkov	853	741
Radiation-Induced Swelling of some Transition Metal Borides – T. M. Guseva, V. P. Gol'tsev, and V. A. Ol'khovikov	858	747
Testing Two Assemblies of Thermionic Converters in the Water-Cooled Water-Moderated Reactor – A. A. Batalov, V. M. Zaitsev, N. V. Zvonov, I. V. Kazin, V. F. Kondrat'ev, V. N. Kuznetsov, A. P. Rodnikov, S. V. Ryabikov, V. F. Tikhonov, and N. A. Shapkin	863	753
Neutron Production in Various Materials with 46 MeV Alpha Particles – V. K. Daruga and E. S. Matusevich	868	757
Neutron Yield Spontaneous Fission of Even–Even Curium Isotopes – L. I. Prokhorova, V. G. Nesterov, G. N. Smirenkin, G. V. Grishin, E. A. Nikitin, V. N. Polynov, and V. V. Rachev	875	767
ABSTRACTS		
Averaging Cross Sections and Reciprocal Velocities to Calculate the Eigennumbers of the Nonsteady-State Boltzmann Equation – B. D. Abramov	879	771
Perturbation of γ-Radiation Field when Objects in Filler are Examined – F. M. Zav'yalkin	880	772
Instrumental Activation Determination of Trace Amounts of Copper – I. A. Miranskii and R. Sh. Ramazanov	881	772
Track-Delineating Autoradiography in Metallographic Inspection of Targets of the Transuranium Elements – V. G. Polyukhov, V. N. Syuzev, Yu. V. Chushkin, and M. M. Antipina	882	773
Yields of Ge^{68} in Irradiation of Gallium by Protons and Deuterons, and Irradiation of Zinc by α-Particles – P. P. Dmitriev, N. N. Krasnov, G. A. Molin, and M. V. Panarin	883	774
Resolving Power of Electron Microscope Autoradiography for α-Emitters – V. N. Chernikov, A. P. Zakharov, and V. M. Luk'yanovich	884	775

CONTENTS

(continued)

	Engl.	Russ.
LETTERS TO THE EDITOR		
New Device for In-Pile Measurements of Internal Friction and Shear Modulus of Specimens – V. S. Karasev, É. U. Grinik, V. S. Landsman, and A. I. Efimov	886	777
Measurement of the Spectral and Angular Distributions of Back-Scattered Electrons – P. L. Gruzin, Yu. V. Petrikin, and A. M. Rodin	889	779
Radiative Capture of Neutrons by U^{238} in the 1.2-4.0 MeV Range – Yu. G. Panitkin and V. A. Tolstikov	893	783
Low-Energy Portion of the Spectrum of Prompt Neutrons from the Spontaneous Fission of CF^{252} – L. Jeki, Gy. Kluge, A. Lajtai, P. P. D'yachenko, and B. D. Kuz'minov	896	785
γ-Radiation Field in the Upper Layer on the Black Sea – G. F. Batrakov, B. N. Belyaev, A. S. Vinogradov, K. G. Vinogradova, B. A. Nelepo, and A. G. Trusov	899	785
Average Yield of Neutrons Per Spontaneous Fission of Bk^{249} – V. N. Kosyakov, V. G. Nesterov, B. Nurpeisov, L. I. Prokhorova, G. N. Smirenkin, and I. K. Shvetsov	903	788
INFORMATION: CONFERENCES AND SYMPOSIA		
IV All-Union Conference on Utilization of Neutron Scattering in Solid-State Physics – M. G. Zemlyanov	905	791
IAEA Symposium on Application of Nuclear Activation Techniques in the Natural Sciences – R. G. Gambaryan	907	792
Symposium on Dosimetry Techniques Used in Agriculture, Industry, Biology, and Medicine – V. I. Ivanov	909	793
International Radioecology Conference – R. M. Aleksakhin	912	795
BRIEF COMMUNICATIONS	915	796
BOOK REVIEWS		
G. N. Balasonov – Stimulation and Optimization in Automated Control Systems – Reviewed by A. M. Rozen and Yu. G. Mitskevich	917	797
L. Kh. Éidus – Physicochemical Fundamentals of Radiobiological Processes and Radiation Protection – Reviewed by Yu. V. Sivintsev	919	798
I. B. Rubashov and Yu. S. Bortnikov – Electrogas-Dynamics – Reviewed by V. G. Lapchinskii	920	798
J. Cronin, D. Greenberg, and V. Telegdi – Collection of Physics Problems with Solutions – Reviewed by V. A. Krivonosov, V. G. Lapchinskii, and B. A. Medvedev	922	799

The Russian press date (podpisano k pechati) of this issue was 8/29/1972. Publication therefore did not occur prior to this date, but must be assumed to have taken place reasonably soon thereafter.

THE STATUS OF THE RADIOACTIVE WASTE DISPOSAL PROBLEM*

B. S. Kolychev, V. V. Kulichenko, and F. V. Rauzen

UDC 621.039.7

Decontamination of Atmospheric Discharges

The majority of international authors have stated that the presently existing system of discharge gaseous wastes from atomic power stations and radiochemical plants through high ventilator stacks with subsequent dilution in the atmosphere provides for the elimination of the hazards of radioactive contamination of the atmospheric environment.

Such an opinion is, in particular, stated in paper [1], where the authors come to the conclusion that contamination of the atmosphere, even for a significant world-wide increase of atomic power, will give rise to less than one percent of the permissible level, and thus may appear to be a difficulty of purely local character.

In spite of this, many countries are conducting intensive work on the development of effective methods for decontaminating air discharge of activated gases and aerosols, since the future construction of very powerful nuclear reactors (of several Gigawatts) and of large plants for the processing of irradiated fuels, notably after only a short duration hold-up, will require decontamination of the atmospheric discharge.

The greatest difficulty in this connection is presented by tritium. In an English paper [2] it is stated that in the next few decades, in view of a significant increase in the quantity of tritium (approximately one Curie/year) it will be discharged into the sea along with waste products of low activity so that, as a result of great dilution, the tritium cannot present a serious hazard.

In paper [3] it is reported that tritium can be discharged into the atmosphere along with water vapor obtained in the concentration of liquid wastes (in particular in evaporation at room temperatures with the aid of pulsed blow-through of air).

The authors of paper [1] consider that for radiochemical plant production higher than 10 ton/day it is necessary to find a safer solution to the disposal of tritium. One such solution can be burial at great depths in the earth. This method is beginning to be studied in the Federated German Republic. For the decontamination of aerosol discharges into the atmosphere it is recommended in [1] that use be made of absolute filters of glass fibers, asbestos, and other mineral materials, giving a decontamination coefficient of 10^4. Filters are available for decontamination of gases at high temperatures from 200 to 800°C.

For the removal of iodine use is made of filters of activated cocoanut palm or wood charcoal, sometimes impregnated with potassium iodide, or methyleneamine, or by a molecular sieve with silver. An iodine decontamination coefficient of 10^4 is obtained. This is inadequate for decontamination in gases arising from the processing of short-duration storage of fuels from fast neutron reactors. A significantly higher decontamination coefficient is required here, reaching 10^8.

For decontamination of the discharge of radioactive noble gases the listed methods are those such as extraction by Freon-12 and other solvents, absorption, and diffusion. These methods have been tried on

*Survey of Section IV papers at the International Conference on the Peaceful Uses of Atomic Energy.

Translated from Atomnaya Énergiya, Vol. 33, No. 3, September, 1972, pp. 723-727. Original article submitted April 25, 1972.

a laboratory scale. Reference is made to interesting results with semipermeable membranes. While these methods have not been placed into service they are under consideration for adoption in fuel reprocessing plants as well as for atomic power stations.

Much attention is paid in [4] to the decontamination of iodine and iodomethyl on activated charcoal. Decontamination of noble gases also takes place on activated charcoal. A presentation is made of the relation between the quantity of charcoal in the column, the hold-up time, the velocity of the gas, and the dynamic absorption coefficient.

A brief presentation is given in [5] of the status of decontamination of atmospheric effluents at four nuclear power plants of the Federated German Republic. At the stations of Lingen and Kahle-na-Maine the gases of the primary loop are withdrawn for decontamination from the heat transfer and primary loop water volume. At the nuclear power plants of Lingeln and Gindremingen and air discharge is held up for 40-60 minutes. For the hold-up of xenon use is made of charcoal absorbers with a hold-up time of 15 to 30 days. The run-offs from the primary loop pass through filtration and the discharge into the stack.

At the nuclear power plant at Obregheim the reactor is enclosed in a hermetic container ventilated by a small flow of air (500 m^3/h) which is discharged through a stack after aerosol and iodine filters. Emergency conditions are not specified.

All papers in the area of radioactive gas and aerosol decontamination of air discharges presented at the international conference presented by foreign sources can be viewed as preparations for the near future when, in connection with the evolution of nuclear power, discharges into the air will start to present a significant hazard if necessary measures are not taken in a timely manner for their decontamination.

Processing of Liquid Wastes of Low and Medium Levels of Activity

Results are briefly given in [3] on new work at the Kaderach, Grenoble, and Valduc research centers. For the disposal of radioactive isotopes of cesium use is made of coprecipitation with nickel ferrocyanide. For good sediment separation use is generally made of such a ratio of ferrocyanide to metal as will give a precipitate with the least collodial properties (for nickel, for example, this ratio is 1.5). A recent investigation has shown the advantage of just such a colloidal form of precipitate for ferrocyanides of heavy metals. It was also established that the precipitate is better produced out of purified solution, which excludes the influence of ions of solution on the sorptive properties of the precipitate. The obtained suspension can be preserved for several days until used.

For the decontamination of ruthenium, both a slightly saline solution (3-5 gm/liter) as well as a nitrate (1.5-2.0 N) with a high concentration of magnesium ions (10-25%) have been examined by the following processes:

1. At pH = 2-7 activated metallic iron is introduced into the solution or the solution is filtered through an iron packing. Deposition of the ruthenium takes place on the iron. Subsequently a precipitation of iron ions from the solution is produced, which permits additional removal of ruthenium.

2. Precipitation occurs in a solution at pH = 8-9 by the addition of sulphate of bivalent iron (300-500 mg/liter of iron) and lead sulphate (50-150 mg/liter of lead).

These two processes have been introduced at the French decontamination installations.

3. For the decontamination of concentrated solutions of magnesium nitrate containing several Curies per m^3 of solution a process was developed in which coprecipitation of ruthenium occurs with bivalent iron at the time of its formation. The decontamination coefficient for this reaches 200-300 for solutions which were not decontaminated by the first two methods.

Paper [3] describes the use of zeolites for decontamination of tank water used for the storage of fuel elements of gas–graphite reactors and holding only cesium isotopes. The zeolite is used either in the form of granules in columns or as a powder in deposition filters. A decontamination coefficient is two or three orders of magnitude. For removal of Sr^{90} from solutions use is made of cation exchange resins Duolite CC2 and CC3, giving a decontamination coefficient of 200. In this paper the authors dwell at length on the operations of an earlier described installation for evaporative concentration of low level activity wastes with resulting counterflow with passage over the solution of air at room temperature. This method is considered to be particularly suitable for wastes containing tritium, which is discarded along with the water vapor into the atmosphere.

In [6] it is noted that, in spite of the negligible amount of radioactivity discarded by a medium sized nuclear power plant of a research center into a river (6-7 mCi of β emitter Sr^{90}, Cs^{137}, and Co^{60}; approximately 3 Curie of tritium per month) a concentration of radioactive isotopes was observed: in oysters Zn^{65} (10^{-6} Ci/gm), in fish Co^{60}, in bottom sands and zoster sea-grass ($25 \cdot 10^{-6}$ Ci/gm) also Co^{60}.

In [5] only the most general guidelines are presented for treatment of liquid wastes at the nuclear power plants of the Federated German Republic, consisting of partial treatment with no indication of method and partial discharge to an open drainage system. Also listed is a system for control of radioactive effluents.

Consolidation of Radioactive Wastes, Cementation and Bituminization of Medium Activity Level Wastes

Cementation is viewed as the process by which treatment is completed. Emphasis is placed on its disadvantage in comparison with bituminization from the point of view of volume increase [1] and stability with respect to leaching [4].

Two variants of bituminization are considered in paper [3]:

Evaporative concentration of solutions prior to bituminization occurs in the flow which, for purposes of increasing the surface area for heat transfer, is broken into jets with the aid of polyvinylchloride curtains. In the final product the content of salts reaches 400-600 gms/liter, and the specific activity reaches $2 \cdot 10^{-4}$ Curie/liter. The experimental arrangement has been operated for a period of two years with favorable results. A partial clogging of the curtain gaps, generated by the sludge, has been observed.

At the Valduc research center an installation was constructed with a vertical layer evaporator LUVA-150 for the inclusion in the asphalt of a slurry. The slurry holds 40-50% of dry product with an α activity of $3 \cdot 10^{-3}$ Ci/liter and a $\beta-\gamma$ activity of $10 \cdot 10^{-4}$ Ci/liter. The slurries mix in equal proportion with the liquid concentrate from the evaporator; the concentrate holds 350-400 gm/liter of sodium nitrate with α-activity to 10^{-3}/liter. The slurries contain various hydroxides to 15% diatomaceous earth.

The mixture with slurry and concentrate and asphalt falls separately on the upper part of the arrangement. The obtained product is homogenized by a six-stage pump and is fed to a metallic drum of 100 liter capacity. The water evaporation yield of the installation is 50-60 kg/h, and the finished product is 100 kg/h. Heating of the LUVA-150 device is performed by an organic heat transfer agent.

At Kaderach tests are being conducted with a horizontal thin-layered vaporizer on water emulsified asphalt. In paper [3] a description is given of a process for the inclusion of wastes in a heat-resistant polymer. The concentrate, holding 250-300 gm/liter of dry residue with a specific $\beta-\gamma$ activity of (2-3) $\cdot 10^{-4}$ Ci/liter and an admix for better retention of the Cs^{137} and Sr^{90} are fed to the thin-layered evaporator; the yield of water evaporation is 20 kg/h. The obtained powder with residual water of 0.3% is loaded into a metal drum of 60 liter capacity. Into this is added a mixture of 65% propylene glycol maleophthalate and 35% styrol, and, after homogenization of the mixture, a polymer catalyzer. The fill volume may reach 60%, but in practice it does not exceed 40-50%.

The finished products of such a composition are characterized by high mechanical stability. The combustion temperature in air is 450-500°C.

The radiation stability of the sample is under study. At the present time the samples have an accumulated dose of 10^6 rads. No changes have been observed. The water resistance of samples is characterized by a solubility of 10^{-7} cm/day for Cs^{137} and 10^{-8} cm/day for Sr^{90}. The principal difficulty is the conversion of cobalt to an insoluble state. The indicated process will possibly be used in the future for processing of other powder-like material products: ashes from combustion of dusts from dust extraction filter chambers.

Vitrification of High Activity Wastes

In [7] a report is presented on tests conducted on three different methods of vitrification at the Battelle Northwest Institute. Full-scale high-activity wastes were processed by a crucible and a spray method, and also by a process for obtaining phosphate glass. The crucible process, developed at Oak Ridge, consists of receiving the liquid waste in a crucible where, by stepwise increases in temperature, there sequentially occur the processes of drying, calcination, and sintering. Burial takes place in the selfsame crucible. It is a batch process. The spray process, developed at the Battelle Northwest Institute, is a two-stage continuous process; the liquid waste is dehydrated and calcinated in a sprayer calcinator and the calcinate is admitted to a melter or crucible for melting or sintering. The process of obtaining phosphate glass is composed of two stages: through evaporative boil-down concentration with essentially complete denitrification of a mixture of nitrated wastes with phosphoric acid; and a continuous melt in a platinum furnace from which is produced a continuous pour of phosphate glass into containers destined for burial [8]. At the time of the tests the activity of the wastes was more than 50 MCi. Thirty three tests were conducted. The obtained products were loaded into containers with diameters of 15-30 cm and a height of 244 cm. Heat release from the consolidated products reaches 300 W/liter, which corresponds to an activity of approximately 100,000 Ci/liter.

Besides the described installations there is in operation in Idaho an installation for calcination in a boiling layer, where approximately 8000 m^3 of highly active wastes were processed.

The final products of the test methods are materials which differ from each other with respect to their resistance to leaching of the radioisotopes by water. The least resistant is the calcinate powder obtained in the boiling layer arrangement. More resistant is the sintered calcinate obtained in the crucible process. Higher in its degree of resistance is the microcrystalline ceramic of the spray process. The most resistant is the phosphated glass.

All these products must be stored in an envelope, a pig-iron container. Unfortunately the paper makes no presentation of a comparative evaluation of the tested methods.

Paper [8] presents test results of an arrangement at the Northwest Institute of Battelle and gives a comparative analysis of the best methods. The author comes to the conclusion that no one method produces an optimum solution to all problems, and selection of the vitrification must be determined by the technology of nuclear fuel reprocessing. However, he considers that on the whole these processes and apparatures are adequate for industrial utilization.

At the present time the total volume in England of high activity wastes amount to approximately 500 m^3, containing say 250 MCi of activity. This corresponds to approximately 0.2 m^3 for each 1000 MW-days (electrical) [2]. The vitrification process continues to be examined at the "Fingal" industrial pilot plant at Harwell. Work is in progress on wastes with concentrations 1/10 of those actually obtained in activities at the plant. New data on comparison with earlier published results is not given in the paper.

It should be noted that glass turns out to be the most suitable material for high-level activity wastes. The authors of [1] consider the vitrification process to be complicated and requiring special development for waste products of different composition. A method of bituminization of medium activity wastes is successfully applied in France. The possibility of bituminizing medium activity wastes is demonstrated. The possibility is shown for bituminizing wastes of specific activities to 50 and 100 Ci/liter. Such an approach opens up the possibility of mixing high activity wastes with others and then processing by the bituminization method. Considering the economics of processing wastes, this presents a more reasonable method than does that of vitrification. The cost of consolidation, transportation, and burial in France is 6-10 dollars/kg of irradiated fuel. Misgivings are expressed that future increases in the degree of fuel element burn, and consequently the presence in the wastes of transuranium elements and fission products will lead to increases in cost to 15-25 dollars/kg of fuel.

Storage of Wastes and their Disposal in Seas and Oceans

In [7] results are given of studies in the USA on the use of salt formations as media for the burial of consolidated wastes. Studies have been in progress since 1955. Salt formations are found in 24 states. They possess good structural properties and mechanical and radiation stabilities. The mines are comparatively inexpensive, their thermal properties are better than those of many rocks, and they are generally found at locations having low seismic activities. Most important is the fact that salt strata are not coupled with circulating ground waters and are safely shielded from surface waters. Their utilization for this purpose of burial of consolidated wastes is safer and more advantageous than is utilization for this purpose of other rock and surface soil. Formations selected for the burial are those which are not in use and will not be in use for production of salt or for other industrial requirements. The temperature of layers between two containers at the center of placement must not be higher than 200°C, and the maximum temperature at a location 20 cm from the wall of a hotter container must not be higher than 250°C.

Thus, if we store high activity wastes in a salt mine without the use of forced cooling, then their activity must be limited.

In considering the various means for burial of wastes the French authors [1] as well as the American ones [7] regard salt formations to be acceptable media for the burial of consolidated high activity wastes, and for burial of low activity wastes the depressions of the ocean are suitable.

A detailed report on the behavior of radioactive contaminants in the waters of the oceans and seas is presented by a group of Japanese authors [9]. They studied the behavior of radionuclides in the sea, the dwell-time of these in surface waters, the sorption of them by suspended materials of the sea, and their transfer to sea organisms. Investigated were factors of concentration and escape of Cs^{137}, Sr^{85}, Sr^{90}, Co^{60}, Fe^{59}, and Ru^{106} for organisms, possible norms for the utilization of sea products, and exposure effects of the radionuclides. The authors come to the comforting conclusion that if the selection of waste disposal sites is performed with care then the level of contamination of the surrounding media and the degree of possible hazard to the surrounding population can be shown to be negligibly small in comparison to the hazard connected with the disposal of wastes from the chemical industry.

In another Japanese report [4] data is presented on the sea-burial of cementated wastes. Subjects to the investigation were samples of diameter 50 mm and heights of 70 mm obtained by the inclusion in cement of a 20 percent solution of sodium sulfate containing Cs^{137}. A synthetic seawater was used in the experiment. The experiment showed that the elution of Cs^{137} from the cement block is reduced by pressure changes in the interval from 300-400 kg/cm^2. This is tied to the compression of the cement, resulting in a decrease of volume and porocity. Significant difference in rates of leaching in water were not noticed at temperatures from 26 to 2°C. The authors come to some conclusions as to the reduction of contamination hazard in the surrounding media for burial of radioactive cements at the ocean bottom.

It should be noted that in the considered reports little new information is presented. More detailed technical information is presented in the French papers, but they are concerned primarily with wastes from research centers.

Evidently the prolonged development of industrial installations for the vitrification of wastes of high activity levels has raised speculation as to the necessity for ultimate burial in a consolidated state [2]. This is found to be a direct contradiction of previously expressed analyses, of the point of view of authors of other reports [1, 7], as well as with objective evaluations of the hazards of storing high level activity wastes in liquid in containers.

French authors [1] have recognized the necessity for long term storage of high activity level wastes in consolidated form. They have, because of the same difficulties with vitrification, proposed the possibility of bituminization of high activity wastes after mixing them with wastes of medium activity levels.

LITERATURE CITED

1. Y. Sousselier and J. Pradel (France), IV Geneva Conference (1971), Paper No. 766.
2. A. Preston et al. (England), ibid., Paper No. 542.
3. P. Pohier, Andriot, D. Chan (France), ibid., Paper No. 621.
4. S. Kadoja et al. (Japan), ibid., Paper No. 250.
5. A. Bödege et al. (Federal German Republic), ibid., Paper No. 396.
6. G. Watson (Australia), ibid., Paper No. 800.
7. W. Belter, J. Blomeke, and F. Culler (USA), ibid., Paper No. 839.
8. K. Schneider, A. Blasewitz, and J. L. McElroy, Nuclear Technology, No. 4, 69 (1971).
9. M. Saiki et al. (Japan), IV Geneva Conference (1971), Paper No. 850.

STRENGTH OF CONSTRUCTION ELEMENTS IN THE FUEL CHANNELS OF THE BELOYARSK POWER STATION REACTORS

I. Ya. Emel'yanov, O. A. Shatskaya,
E. Yu. Rivkin, and N. Ya. Nikolenko

UDC 621.039.5.058

The construction of the reactors in the Beloyarsk Atomic Power Station involved the solution of complicated physical, metallographical, and engineering problems. One of these was that of ensuring the necessary strength in the structural elements of the fuel channels. The structural execution of the channels, the manufacturing technology, and the service conditions envisaged made it essential to carry out a careful study of the stress distribution in all the elements of the channel and to estimate the fatigue and corrosion–mechanical strength.

The fuel channels for nuclear superheating of the steam (steam-superheating channels) and the evaporation of the water (evaporating channels) are made in approximately the same form (Fig. 1). The coolant passes into the inlet chamber of the head of the channel and along the down-coming system of pipes; it turns in the tail and after passing through the rising pipe system enters the outlet space of the head. The fuel elements in the evaporating channels are arranged in six rising branches, and in the steam-superheating channels in three down-coming and three rising branches.

In order to compensate the difference in the thermal expansions of the down-coming and rising branches of the channels, tubular compensators are employed. The parts of the channels are made from Kh18N10T and ÉI-847 steels.

The main parameters of channel operation in the steady-state mode are presented in Table 1.

During the heating process, the difference between the temperatures of the coolant at the inlet and outlet of the steam-superheating channels reaches 250-260°C.

TABLE 1. Operating Parameters of the Channels in the Steady-State Mode

Unit	Channel	Temperature, °C		Pressure, kg/cm^2	
		inlet	outlet	inlet	outlet
I	Evaporating	300	330	135	130
	Steam-superheating	315	510	110	95
II	Evaporating	300	335	145	140
	Steam-superheating	335	510	130	110

TABLE 2. Greatest Stresses in the Heads of the Steam-Superheating Channels under Transient Conditions

Mode	Element	Range of temperature variation, °C	Stress, kg/cm^2
Heating	Transitional chamber	260—510	20
	Shell ϕ 34 ×1 mm	260—510	14
Emergency stop	Transitional chamber	510—415	12
	Shell ϕ 34 ×1 mm	510—415	12

Translated from Atomnaya Énergiya, Vol. 33, No. 3, pp. 729-733, September, 1972. Original article submitted May 6, 1971.

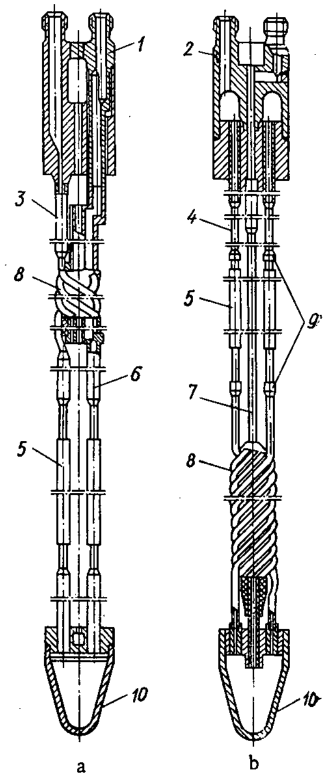

Fig. 1

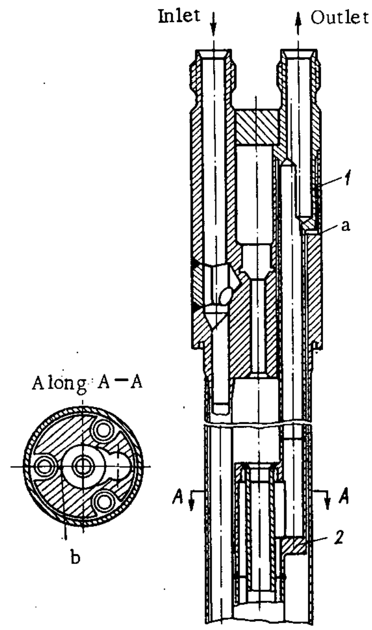

Fig. 2

Fig. 1. Basic arrangement of the steam-superheating (a) and evaporating (b) channels: 1) head of the steam-superheating channel; 2) head of the evaporating channel; 3) three down-coming branches; 4) six rising branches; 5) fuel elements; 6) three rising branches; 7) down-coming branches; 8) compensators; 9) welded joints of tubes; 10) tailpiece.

Fig. 2. Head of steam-superheating channel: 1) shell; 2) transitional box chamber.

Analysis of the Stressed State of the Channel Elements. We analyzed the stressed state of the channel elements both experimentally and by calculation. We determined the stresses in the channel elements due to the action of the internal pressure, and also the thermal stresses, in both the steady and transient modes. The equivalent membrane stresses (determined from the energy theory of strength) due to the action of the internal pressure were limited to $\sigma_{0.2}^{t}/1.65$, where $\sigma_{0.2}^{t}$ is the yield stress of the tube material as the calculated temperature. The local stresses in isolated parts of the joints attaching the channel tubes to the heads and tailpieces exceeded the yield stress. The stresses due to the effects of internal pressure never exceeded the permissible values.

The heads of the channels are fairly large components, through the inlet and outlet spaces of which coolant flows at different temperatures. Whereas in the heads of the evaporating channels the temperature drop between the inlet and outlet is relatively slight, in the heads of the steam-superheating channels it may rise as high as 260°C.

The arrangement of the heads of the steam-superheating channels is illustrated in Fig. 2. In the steady-state mode, substantial thermal stresses were only able to develop in the shell of diameter 34 × 1 mm connecting the outlet conduit with the main part of the channel head. However, calculation showed that the greatest stresses in the shell of diameter 34 × 1 mm amounted to no more than 12.5 kg/mm^2. There is no danger in this from the point of view of strength requirements.

In the heads of the steam-superheating channels and the intermediate box chambers adjacent to those, we also determined the thermal stresses arising in the course of preheating (blowing) and in the case of

Declassified and Approved For Release 2013/02/27 : CIA-RDP10-02196R000300110003-7

TABLE 3. Main Characteristics of the Compensators

Dimensions of compensator tubes, mm	Number of turns	Mean diameter of turn, mm	Pitch of winding, mm	Rising angle of winding, deg	Maximum displacement of compensator, mm
9,4×0,6	5	55	110	32,5	11
9,4×0,6	8	55	110	32,5	42
12×0,6	3	55	110	32	11
12×0,6	9	55	110	32	42

Note: All the compensators were made of Kh18N10T steel.

TABLE 4. Greatest Stresses in the Compensators

Unit	Channel	Dimensions of compensator tubes, mm	Number of turns	Greatest displacements, mm	Stresses, kg/mm²
I	Evaporating	9,4×0,6	5	11	36
		12×0,6	3	11	71
I	Steam-superheating	9,4×0,6	8	42	82
II	Evaporating	9,4×0,6	5	11	36
II	Steam-superheating	12×0,6	9	42	80

an emergency stop. In both the calculated conditions the greatest stresses arose in the shell of diameter 34 × 1 mm at point a, and in the intermediate box chamber at point b (Fig. 2). The greatest stresses arising in the emergency-stop modes of the reactors in the Beloyarsk Atomic Power Station are shown in Table 2.

In the first and second channels of the Beloyarsk Atomic Power Station units, four forms of compensators were employed; the main characteristics of these appear in Table 3.

The characteristics of the compensators were calculated by a method allowing for the intensification of the stresses due to the curvilinear nature of the compensator winding, the influence of internal pressure on the rigidity of the compensator, and the effect of the oval form of the tube in the winding cross section on the stress distribution in the compensator. The calculation showed that the greatest stresses arose in the first upper turn of the compensator (Fig. 1) on the concave side. The greatest nominal elastic stresses are shown in Table 4.

In order to verify the method of calculating the compensators we made some tensometric measurements. We used wire sensors of the resistance type with a base of 5 mm and foil sensors with a base of 1 mm. The calculated and experimental data were in satisfactory agreement.

Fatigue Strength of the Channel Elements. Fatigue tests were applied both to the channels as a whole and also to individual most highly stressed elements, such as the compensators. The channel elements were subjected to fatigue loading in the transient modes (heating and cooling). It was considered that the total number of all transient modes in the service life of one channel was no greater than 300. During the tests we reproduced the most stringent conditions of preheating, in which the greatest stresses developed in the channel elements. This enabled us to extend the results to any combination of transient modes if the number of these were no greater than 300.

Principal attention was directed toward the fatigue strength of the steam-superheating channels, these being more stressed than the evaporating channels.

In testing the full-scale steam-superheating channels, coolant at a temperature of 510°C was passed into the outlet conduit of the channel. Water was sprayed into the channel tailpiece to reduce the temperature of the coolant passing through the down-coming branches of the channels to 260°C. The mixture so formed passed out through the inlet conduit of the channel. During the heat exchanges the temperature at the entrance into the channel fell from 510 to 260°C at a rate of 100 deg/min. The next heating from 260 to 510°C took place at 70 deg/min. After 2120 heat exchanges no damage or loss of hermeticity was observed in the elements of the channel.

The results of the tests showed that, under the more rigorous transient modes, involving temperature change rates of up to 100 deg/min, there was at least a sevenfold reserve relative to the accepted working number of cycles (300).

Analysis showed that the most stressed elements of the channels limiting their fatigue strength were the compensators; a special study was therefore made of the rupture resistance of these under fatigue loading. We tested compensators in the original state and again after heat treatment (vacuum annealing at 850°C for 3-4 h). The results of tests carried out on five-turn compensators made of tube of diameter

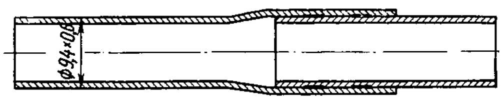

Fig. 3. Weld of the "bell" type.

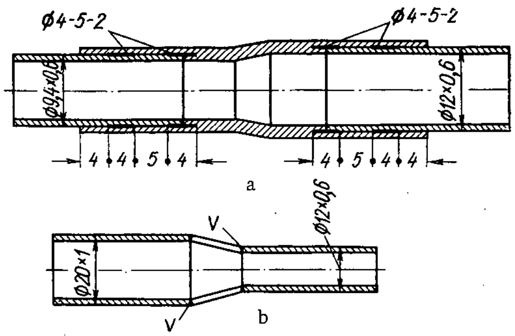

Fig. 4. Gapless welds by roller (a) and argon-arc (b) welding.

9.4 × 0.6 mm and nine-turn compensators made of tube of diameter 12 × 0.6 mm (both in the original and heat-treated states) showed that, for nominal working elastic stresses of σ_{el} = 80 kg/mm^2, the compensators ruptured after 7150-60,000 cycles. This meant that the compensators gave a reserve factor of over 23 with respect to the working number of cycles (300).

Subsequent tests on the compensators carried out at higher stresses (σ_{el} = 95 and 110 kg/mm^2) showed that in this case also the compensators remained perfectly serviceable, giving at least an eightfold reserve with respect to the number of cycles.

The results indicate that the elements of the fuel channels exhibit a reasonable fatigue strength for conventional working loads and the specific number of loading cycles.

Analysis of the Corrosion–Mechanical Strength of the Channel Elements. It is well known that austenitic steels of the 1Kh18N10T type are inclined toward stress corrosion when in contact with water or a water–steam mixture containing oxygen or chloride ions. A special part of the investigation was directed toward the possible occurrence of this type of damage in various elements of the fuel channels.

We studied the corrosion–mechanical strength of the compensators in a test-bed giving a fair simulation of service conditions as regards the parameters of the medium. A water–steam mixture at a temperature of 340°C and pressure of P = 145 kg/cm^2 passed through compensators situated in an electric furnace. Before the tests the compensators were subjected to fatigue loading, involving a displacement which created the maximum nominal elastic working stresses inside them (σ_{el} = 80 kg/mm^2). The number of loading cycles was 6000. The fatigue loading was undertaken in order to simulate the most damaged state of the compensator material which normally occurred at the end of the service life of the channels. The compensators held in the electric furnace were compressed by the same amount.

After holding for 144 h, the temperature of the compensators was reduced to 100 ± 5°C and the pressure to 100 kg/cm^2. At the same time water containing 0.06 mg/liter of chlorine was sprayed into the electric furnace (on the outside of the compensators). On reducing the temperature to 95°C the moisture condensed, while at 105°C it evaporated. During the 24-h holding period the condensation–evaporation cycle was repeated approximately 30-40 times. Afterwards the temperature was raised to 340°C and the pressure to 145 kg/cm^2 and another 144-h holding period ensured. The condensation–evaporation cycle was then repeated once more, and so on.

Under these conditions the compensators failed after 144-1100 h. The nature of the damage was the same: networks of cracks developed on the outer surface, and these developed into open honeycombs. The regions of honeycomb formation lay at a wide variety of points in the compensators. Sometimes several were formed in a single compensator.

The results indicated that the deposition of moisture on the outer surface of the compensators and its subsequent evaporation might cause an increase in the chloride concentration on the surface, together with the development of stress-corrosion processes and ultimate rupture of the compensators.

We studied the corrosion–mechanical strength of welds in the channel tubes in an analogous way. A characteristic feature of the type of weld first used (the so-called bell shape – Fig. 3) was the existence of finite gaps between the tubes being joined. Thermal calculation showed that it was sufficient for there to be only a very slight thermal flux from the direction of the graphite stack of the reactor for an intensive evaporation of moisture to occur in the gaps of the welds washed by the water–steam mixture. As a result of the possible repeated deposition of moisture in the gap and its subsequent evaporation, the chloride concentration increased and corrosion cracking intensified.

The development of failure in welds was simulated under laboratory conditions. The sample with the weld under test was placed in an electric furnace. Through the sample flowed a water–steam mixture at a pressure of 110 kg/cm^2, containing (in the initial state) 0.06 mg/liter of chlorides and up to 8-10 mg /liter of oxygen. The temperature at the outer surface of the weld was kept constant at 340°C. The thermal flux was taken from the electric furnace to the outer surface of the sample (in the same way as the thermal flux from the reactor stack). As criterion of stress-corrosion resistance we took the time which elapsed before the detection of cracks on the weld surface during metallographic examination.

With this type of test, cracks were detected in the "bell" type of weld after 160h. After 700-2000 h, open honeycombs started to form in the welds. The type of damage observed was typical of corrosion cracking.

Comparison between the results of the laboratory tests and individual cases of damage in the channel elements, compensators, and welds of the Beloyarsk Atomic Power Station during actual service indicated that the cause of the damage might well be stress corrosion, intensified by local increases in the chloride concentration at individual points on the surface of these elements.

Methods of Increasing the Life of Channel Elements. According to an analysis of the corrosion–mechanical strength of the fuel channel elements, stress corrosion may very well have been the reason for the failure of some compensators and welds. We accordingly sought ways of protecting the compensators and welds from corrosion cracking.

In order to protect the compensators the following methods were proposed: 1) the removal of residual stresses by austenization (vacuum heating to 1100°C, holding for 3-4 min) or stabilization (vacuum heating to 860°C for 3 h); 2) electrochemical protection by placing an aluminum insertion piece inside the assembly of compensators; 3) the use of protective coatings made of Nichrome or aluminum alloys deposited on the outer surface of the compensators by the gas-flame or plasma techniques.

Compensators protected by one or other of these methods were tested in the same way as the compensators in the original state. The tests showed that neither heat treatment electrochemical protection, nor Nichrome coatings gave the necessary protection from corrosion cracking. The most reliable method of protecting the compensators from stress corrosion was the deposition of aluminum alloys on the outer surface by the gas-flame or plasma methods. The deposition of coatings only slightly reduced the fatigue strength of the compensators by comparison with that in the original state.

Compensators with aluminum alloys deposited on their outer surface have been used in the fuel channels of the Beloyarsk Atomic Power Station for a number of years, and in no case have any of them been found to fail.

The most effective way of increasing the efficiency of welds lies in avoiding conditions capable of leading to a local increase in chloride concentration. One structural principle yielding the desired effect is that of eliminating gaps in the welds. Some typical gapless welds are illustrated in Fig. 4. On testing these welds by a method analogous to that used in testing "bell" welds no cracks appeared even after 15,000 h tests. Gap welds of this kind never failed under service conditions either.

The following conclusions may be drawn from the foregoing analysis:

1. An analysis of the stressed state and the results of fatigue tests carried out on various elements of the fuel channels have shown that, for existing working loads and thermal stresses involving no more than 300 cycles of transient modes, the strength of the channels is perfectly adequate, provided that conditions leading to the development of stress corrosion are avoided.
2. Cases of failure in the compensators and in the welds of the thin-walled tubes noted under service conditions are associated with corrosion cracking arising from a local increase in the chloride concentration on the surface.

3. An effective means of increasing the life of fuel-channel elements is that of depositing protective aluminum alloy coatings on the outer surface of the compensators and using the gapless-weld principle in the construction.

AUTOMATION OF NUCLEAR POWER PLANTS AND DISCRETE POWER DRIVES

I. Ya. Emel'yanov, V. V. Voskoboinikov, and V. P. Perfil'ev

UDC 621.039.56

Utilization of Control Digital Computers and Development of Discrete Control Systems. Further increases in the power output of nuclear power plants and the need to optimize the basic operating conditions of nuclear power plants have led to a drastic expansion in the number of problems to be handled by control systems. These problems include: monitoring the neutron distribution with respect to reactor radius and reactor height; maintaining a specified power ratio for groups of fuel channels; automatic control under all sets of operating conditions; programmed displacement of groups of control devices, etc.

Optimizing control conditions with the above factors taken into proper account depends on the acquisition, processing, and storage of a huge volume of data. Digital computers have therefore become

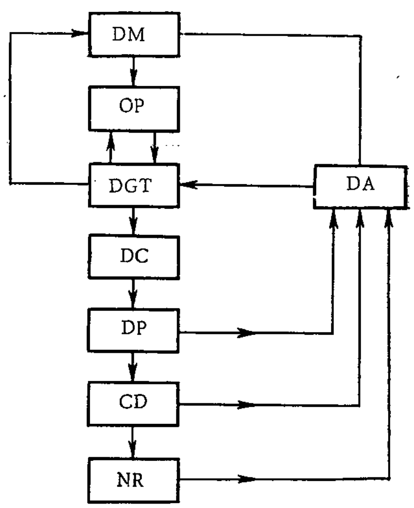

Fig. 1

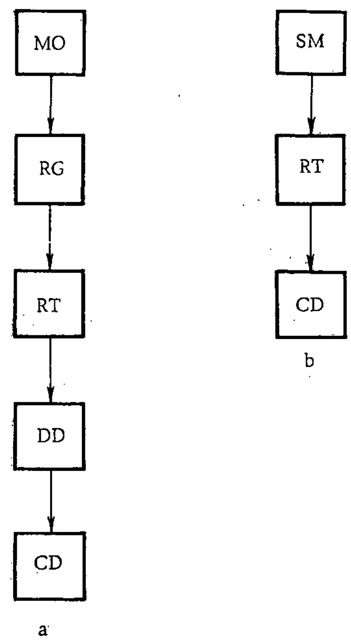

Fig. 2

Fig. 1. Basic layout of digital-computerized nuclear reactor control system: DM) data mapping device. OP) operator; DGT) digital computer; DA) data acquisition device; DC) discrete power drive controls; DP) discrete power drive; CD) control device; NR) nuclear reactor.

Fig. 2. Block diagrams of reactor control and protection system devices: MO) motor; RG) reducing gearbox; RT) rotation transducer; DD) disengaging device; CD) control device; SM) stepping electric motor.

Translated from Atomnaya Énergiya, Vol. 33, No. 3, pp. 735-739, September, 1972. Original article submitted September 16, 1971; revision submitted January 1, 1972.

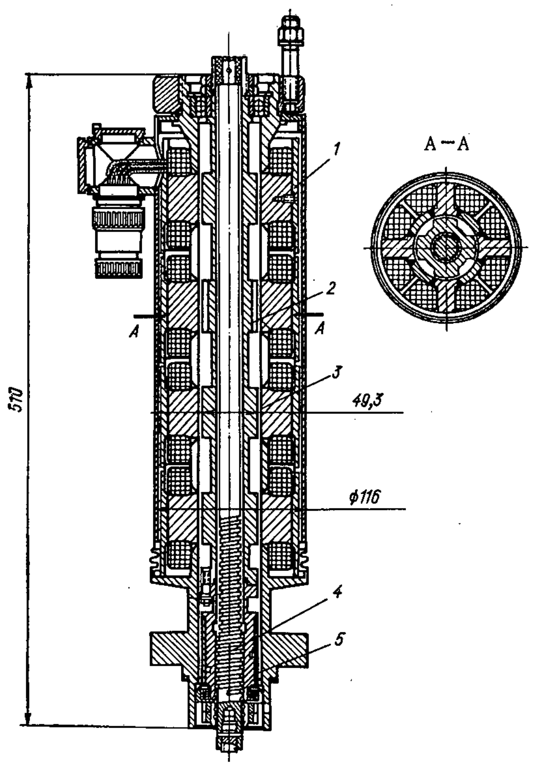

Fig. 3. General view of SM-2 reactor shim rod power drive mechanism: 1) stator; 2) rotor; 3) pressuretight jacket; 4) screw; 5) ball nut.

increasingly more widespread in recent years for use in the automation of nuclear power plants [1]. The use of digital computers imposes additional requirements on the control system, and has been a motive force in the development of discrete control systems and actuators capable of handling the signals emerging from the system computer directly in digital or numerical form.

Typical features of discrete control systems are pulsed control, hard feedback between the amounts of displacement of the control device and the number of control pulses, and no running down of the rotor when power is switched off. Discrete control systems respond very rapidly, and are simple and reliable in operation.

Reliance on a discrete power drive in nuclear reactor control systems favors synchronous displacement over the required range of speeds of groups of control devices (without requiring additional auxiliary devices), or even more complicated matching of the motion of the control devices as dictated by control requirements. This makes it possible to devise complicated variable structures of automatic controllers, and thereby renders the reactor control system more versatile.

Consider a possible basic layout for nuclear reactor control (Fig. 1) using a digital computer in combination with discrete power drives. Generalized data, after processing by the digital computer, are sent to the data mapping device. Note that information on the position of the control device is transmitted conveniently in the form of the number of control pulses.

Modern sophisticated discrete nuclear control systems are characterized by structures with a versatile general-purpose discrete power drive, combining the functions of automatic control, reactivity compensation, and emergency protection responses.

Control signals shaped in the measuring portion of the control system, as well as signals originating in the digital computer and passed through appropriate circuits, arrive at the control units of the actuating part of the reactor control and protection system. These signals govern the control devices which must move in synchronism and alter the reactivity of the power plant in order to arrive at the specified operating conditions. The synchronous displacement of the control devices is achieved by supplying all of the discrete power drives from a common pulse generator. Special attention must be given to nuclear safety considerations when designing control equipment with the aid of a digital computer. Highly reliable independent control circuits capable of shaping the required command pulses to deal with emergency situations and accidents are provided for this purpose.

Discrete Power Drive with Stepping Motors. One of the promising trends in the development of discrete control systems is the use of high-power stepping electric motors with a linear characteristic for the number of pulses plotted against the rotation angle.

A discrete power drive with a stepping electric motor featuring a passive rotor [2-4] has gained wide acceptance in reactor design. The design of the stepping electric motor makes it possible to achieve relatively pressuretight separation of the rotor and stator while retaining clearances acceptable for electrical machinery of that type.

The last point is particularly important in the development of control mechanisms for pressurized water reactors. Among the advantages of power motors are the following:

Declassified and Approved For Release 2013/02/27 : CIA-RDP10-02196R000300110003-7

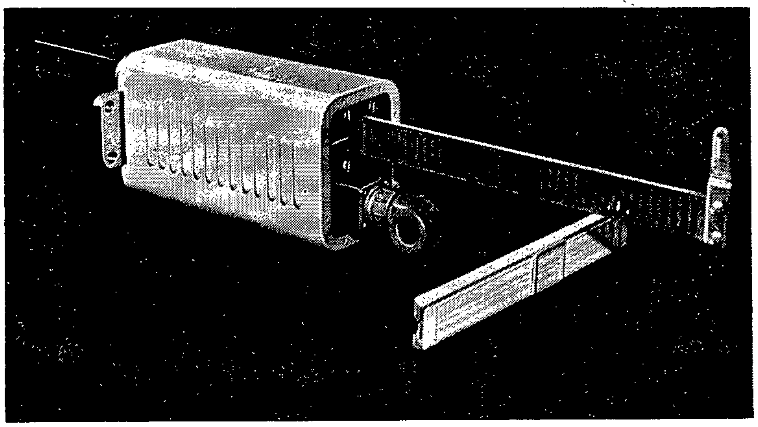

Fig. 4. General view of linear stepping electric motor with flat armature.

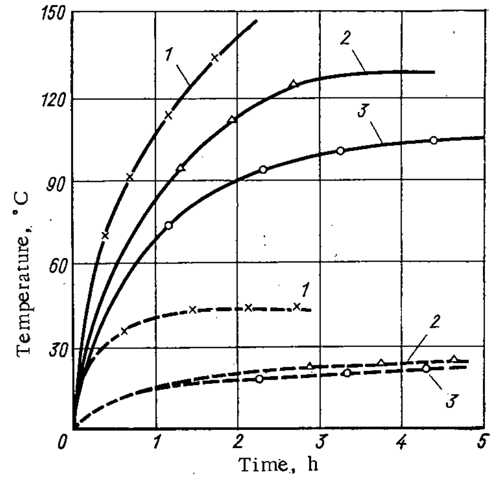

Fig. 5. Temperature of stepping motor windings, as a function of motor design variant.

a) improved reliability of the power drive as the result of significant simplifications of the moving parts;

b) a broad range of speed control;

c) high precision in positioning of the control device;

d) option of reversing the control device and stopping the control device without running down.

In addition, the stepping motor makes it possible to hold the control device back in any position through the forces of the electromagnetic field, thereby making it possible to do without clutches and other restraining devices. Reliable operating conditions are ensured for emergency and scramming operations.

Figure 2 shows the block diagram of power drives with a conventional electric motor (a) and a stepping electric motor (b).

When a stepping electric motor is used, there is no longer any need either for a complex reducing gearbox (the stepping electric motor features frequency speed control and in essential functions as an electrical speed reducer) or for a disengaging device to run the control rod or other control device into the reactor core in scramming operations. The stepping electric motor brings about reliable positioning of the control device in the fixed-setting mode. The control device is inserted rapidly into the reactor core when the control windings are deenergized.

When the stepping motor operates in a leakproof enclosure, there is no need for pressure seals, which would seriously impair the reliability mechanism. The moving parts of the device become simplified still further through the use of a stepping electric motor combined with a rotary type control device. In that case there is no further need for a transducer to convert one form of motions into another.

Translational displacement of the control device can be achieved with the aid of a linear stepping motor in which control pulses are converted to discrete translational displacements of the armature.

In contrast to the stepping motors in general industrial use with a laminated magnetic circuit, the enclosed stepping motors used in the control drives for nuclear reactors usually feature a monolithic magnetic circuit. Moreover, these power drives are frequently operated at elevated temperatures, in radiation environments, and under vibratory loads. Those specific operating conditions necessitate requirements on the design, parameter calculations, and fabrication technology of the machines.

A four-phase stepping motor in which two phases are under voltage simultaneously has been found optimum for actuating reactor control and protection systems mechanisms.

As an example, consider the design of a stepping motor used in the power drive of the shim rod of the SM-2 pressurized water reactor [5]. A general view of the device is shown in Fig. 3.

The shim rod is immersed in the water of the reactor primary loop. The rod is displaced by the action of a four-phase (four-section) enclosed stepping motor. A ball nut and screw linkage is used to convert the rotation into linear drive. The motor rotor, immersed in the primary-loop water, is separated from the stator by a nonmagnetic stainless steel jacket. The stepping motor features the following technical data:

Clearance between enclosing jacket and rotor poles	0.2 mm
Working clearance on jacket side	0.6 mm
Material:	
of stator magnetic path	electrical engineering steel
of rotor	magnetically soft stainless steel grade 0Kh17T (GOST 5949-61)
of jacket	stainless nonmagnetic steel grade Kh18N9T (GOST 5949-61)
Number of rotor positions per revolution	16
Angular pitch of rotor	22°30'
Each step of motor corresponds to percentage reactivity change	0.001%

At the present time, some experience has been accumulated in the development and operation of heavy-duty stepping electric motors employed in nuclear reactor control mechanisms. For example, the stepping motor for the SM-2 reactor shim rod drive under discussion here has been in service for ten years. It was mounted on the reactor lid at a site of enhanced moisture, where the temperature of the surrounding air reaches 40°C and brings about displacement of the control rods operating in the primary-loop water under 50 atm pressure. The operating conditions of the shim rod drive are as follows: axial load on ball nut and screw pair up to 70 kg; rate of rod advance 1.25 mm/sec; frequency of control pulses to 25 Hz; operating current to 5 A.

When the stepping motors in the power drives of reactor shim rods are in service, they are inspected externally once a month and the strength of the winding insulation is checked. The shim rod drives are demounted, disassembled, and washed out once every two to three years, mainly because of fouling of the ball nut. As a result, operating experience with stepping electric motors on the SM-2 reactor has demonstrated the high reliability of those motors in service.

Instead of using a nonmagnetic jacket to provide a pressuretight enclosure for the rotor of the stepping motor and separate it from the stator, enclosed stepping motors are fabricated by welding the pole-pieces to the pressuretight enclosure. This makes it possible to maintain the normal operating clearance for machinery of that type, while improving the performance characteristics.

In the enclosed power drive with stepping motor, the only components in contact with the reactor primary loop are the motor rotor and bushings, and that explains the high reliability of those enclosed power drives.

As an example of a linear stepping motor, we consider the motor designed to displace an automatic control rod (Fig. 4). This motor features four phases (sections) each of which carries a single control winding. The magnetic circuits of the motor stator form a groove in which a flat armature is free to move on swing-link guides. Grooves forming a toothed indexing sector are cut on the armature. The same serrations are cut on the poles of sections of the stator in the stepping motor.

The chief problem encountered in the development of linear stepping motors is reduction of armature weight. In the linear motor in question, the armature weight accounts for ~2% of the maximum static force. The frequency with which that type of motor is switched on and off brings about a speed of armature travel amounting to as much as several tens of steps per second. The armature–stator coupling is achieved solely by the forces of the magnetic field. This accounts for the high reliability of this particular type of power drive.

Heat Conditions Affecting the Performance of Stepping Motors. The supply voltage of the motor windings is increased significantly [6] under operating conditions which produce an increase in the amount of heat released in the monolithic magnetic curcuit, and a sharp increase in the heating of the motor steel. Moreover, the stepping motors employed in reactor design frequently perform at elevated ambient temperatures (temperature of the primary-loop water, temperature in the zone in which the power drives of the reactor control and protection system operate, etc.).

These circumstances call for particularly careful analysis of heat and heat-transfer conditions in the development of stepping motors. Special measures are taken in the design of electric motors for nuclear reactor control mechanisms to achieve the best transfer of the heat generated in the motor as it works. These measures include the utilization of special filling compounds to remove the heat from the control windings, etc. An example of the effect of different design measures on heat removal from a stepping motor, we can consider the overheating curves of the stepping motor used in the automatic control mechanism shown in Fig. 5 for breaking conditions (broken curves) and operating conditions (continuous curves).

Curves 1 depict the performance of a motor without the special filling compound. Curves 2 refer to a motor whose stator is encapsulated in an epoxy compound with alumina powder filler, to improve conduction of heat from the winding coils; this measure lowered the overheating temperature to 130°C. An aluminum radiator was also set on the epoxy-encapsulated motor, so that the overheating temperature was reduced further to 105°C (curves 3).

Note that reliance on forced cooling of control devices is not always optional (the motor must be designed in a refractory variant in this case). Refractory insulation for winding conductors capable of withstanding operating temperature of 500-600°C is now available [7].

A single article cannot possibly find room for discussion of the wide range of topics pertaining to the development of discrete power drives for nuclear reactor control systems. It must be stressed, in conclusion, that the fast pace of development of nuclear power calls for concentrated efforts in the area of further improvement and heightened effectiveness of discrete control systems as one of the promising trends in the automation of nuclear power facilities.

LITERATURE CITED

1. I. Ya. Emel'yanov and R. G. Porotikova, Atomnaya Tekhnika za Rubezhom, No. 11, 9 (1970).
2. Discrete Electric Power Drive with Stepping Motors [in Russian], Énergiya, Moscow (1971).
3. M. D. Labzin, Maritime Electric Power Drives with Stepping Electric Motors [in Russian], Sudostroenie, Moscow (1971).
4. A. M. Bamdas et al., Actuating Electric Motors and Automatic Control Components of Nuclear Reactor Servomechanisms [in Russian], Atomizdat, Moscow (1971).
5. S. M. Fainberg et al., Paper No. 320 (USSR) Presented to the III Geneva Conference on the Peaceful Uses of Atomic Energy (1964).
6. V. I. Shubin, V.P. Perfil'ev, and Z. N. Osadchenko, Bulletin of the Committee on Inventions and Discoveries, Council of Ministers of the USSR [in Russian], No. 21 (1969), p. 52.
7. Chemistry and Practical Applications of Organosilicon Compounds [in Russian], Khimiya, Leningrad (1968).

USE OF SURFACE ROUGHNESS TO IMPROVE HEAT TRANSFER FROM ROD TYPE FUEL ELEMENTS

O. S. Vinogradov and P. I. Puchkov

UDC 621.039.548

Studies have been made on roughness as a feasible means of intensifying heat transfer from bundles of tubes or rods in a longitudinal flow pattern [1-5]. There is a great variety in: the technology of roughening, shapes, and relative dimensions of elements of surface roughness; the distribution of these elements over the surface; and designs of bundles (layouts, remote-control techniques, relative lengths, etc.). Even greater variety is observed in investigations carried out in round pipes, and in annular and plane channels. Therefore there is a need for investigators to find optimum shapes and dimensions of roughness and, to whatever extent possible, simplify the technology of roughening surfaces.

While the effect of the relative dimensions of surface roughness on heat transfer and on the resistance of bundles of pipes can be generalized even by empirical formulas, the effect of shapes and of various technological factors on heat removal (e.g., contact with the heat-emitting surface) does not lend itself to generalization.

Difficulties therefore arise in attempts to transfer results of investigations carried out on bundles or assemblies of other structure to specific designs of rod type fuel elements. The authors of the present article carried out a special investigation of the effect of surface roughness on one of the available designs of fuel assemblies for gas-cooled reactors.

The experiments were run in an apparatus with a closed circulation loop, using various gases under pressure to $6 \cdot 10^6$ Pa and gas temperature to 725°K without cooling.

The working sector (Fig. 1) consisted of the vertical body of the channel accommodating two mockups of assemblies of rod type fuel elements. The top mockup was not heated, and set up full-scale hydrodynamic conditions for the lower heated mockup which comprised the experimental structure.

The mockup consisted of a central support rod providing a mounting for the top and bottom heads with special lugs, brackets, and grids to support the fuel elements. The latter were simulated by thin-walled stainless steel tubes welded to the lugs and grids of the heads, and acting as busses conducting the electrical current. The heads and all of the parts resting on the heads were made of copper. The basic geometric dimensions of the working sector and of the mockup are given below.

Three mockups of fuel assemblies were investigated: one with smooth-walled tubes (bundle 1) and two with rough walls (bundles 2 and 3). Roughness in the form of a single-start helical thread cut with a profile close to triangular on the surface of the tubes was produced on the tubes. A microscope was employed to check the dimensions and shape of the roughness. The roughness dimensions are cited in Table 1.

TABLE 1. Dimensions of Roughness

Parameter	Bundle 2	Bundle 3
Height $h \cdot 10^3$, m	0,024±0,005	0,065±0,01
Pitch $s \cdot 10^3$, m	0,15±0,01	0,44±0,01
Relative height h/d_{eq}	0,00095	0,0026
Pitch/height ratio s/h	6,25	6,75

Translated from Atomnaya Énergiya, Vol. 33, No. 3, pp. 741-745, September, 1972. Original article submitted October 7, 1971.

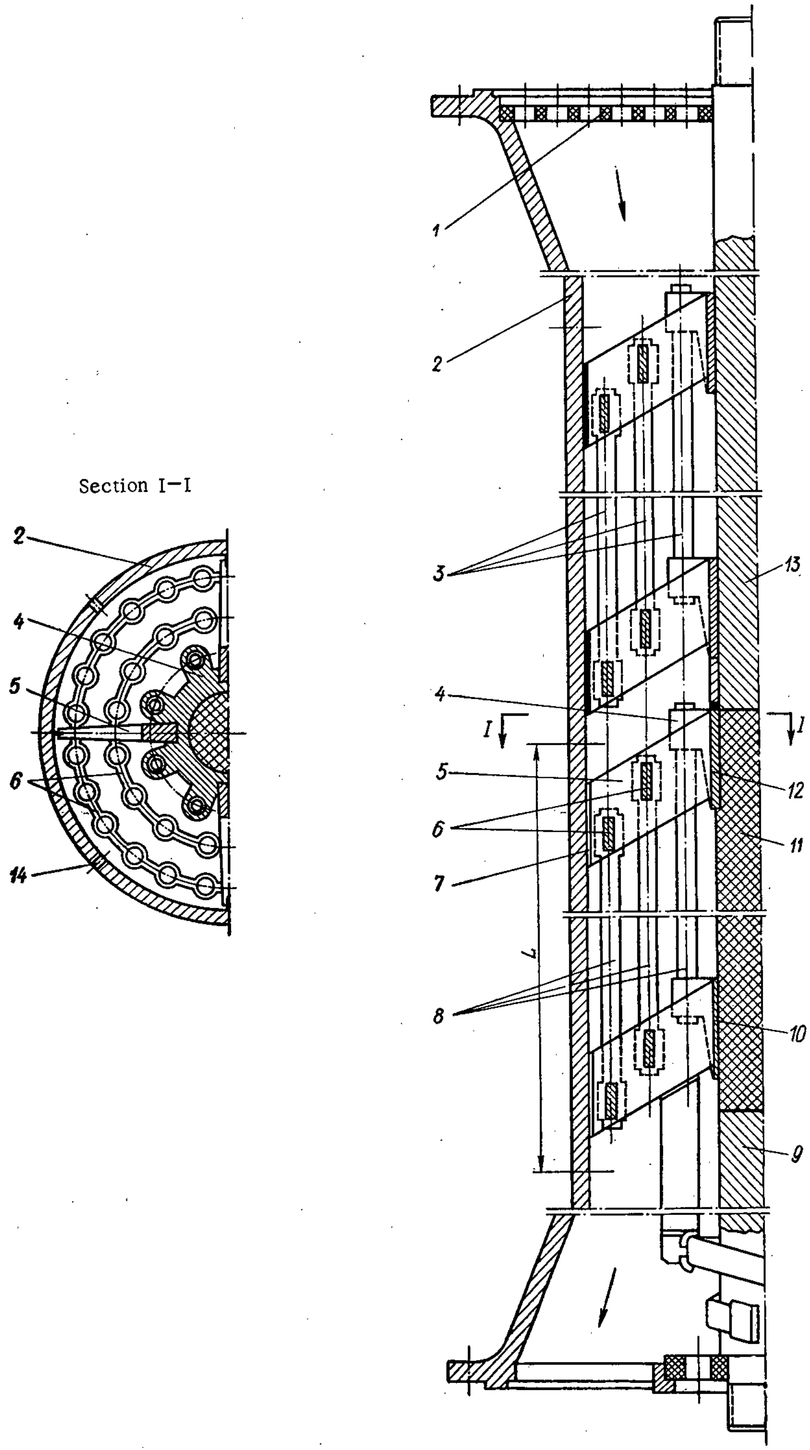

Fig. 1. Working sector: 1) top grid; 2) channel body; 3) copper tubes in unheated mockup; 4) lugs; 5) brackets; 6) grids; 7) Paronit insulating inserts; 8) tubular fuel elements; 9) copper rod; 10) bottom head; 11) support asbestos-cement rod; 12) top head; 13) copper conducting rod; 14) bleedoffs for static pressure.

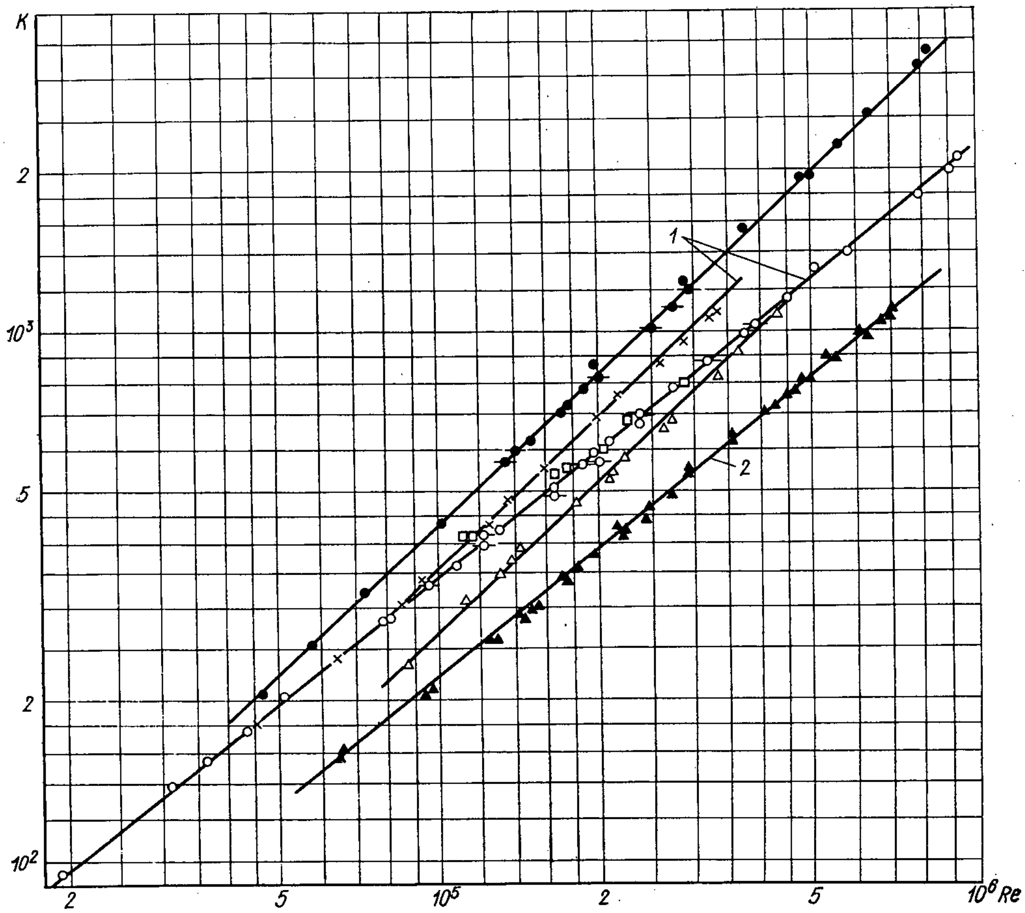

Fig. 2. Effect of roughness on heat emission. Mockups of rod type fuel elements, K = f(Re). Smooth rods: ○) air, $\overline{T}_{st} \approx 375°K$, $\psi = 1.2$–1.3; -○-) air, $\overline{T}_{st} \approx 500°K$, $\psi = 1.6$; □) CO_2, $\overline{T}_{st} \approx 725°K$, $\psi \approx 1.3$; rough rods: ×) air, $h/d_{eq} = 0.00095$, $\overline{T}_{st} \approx 375°K$, $\psi \approx 1.25$, $h/d_{eq} = 0.0026$; ●) air, $\overline{T}_{st} \approx 375°K$, $\psi = 1.2$–1.3; -●-) CO_2, $\overline{T}_{st} \approx 725°K$, $\psi \approx 1.3$; 1) calculation based on Eq. (5). Annular channels, Nu = f(Re): ▲) smooth surface; Δ) roughness, $h/d_{eq} = 0.0016$; 2) calculations based on Eq. (3).

The experiments were conducted using air and carbon dioxide gas at the average tube surface temperature $\overline{T}_{st} = 375°$-$725°K$, gas temperature $\overline{T}_g = 300°$-$575°K$, temperature ratio $\psi = \overline{T}_{st}/\overline{T}_g = 1.2$-$1.6$, and Reynolds numbers $Re = 2 \cdot 10^4$-10^6.

Basic Geometric Dimensions of the Working Sector and Mockup

Channel inner diameter, d_2	0.1055 m
Total length of one assembly, L	0.575 m
Heated length of tubes, L_H	0.520 m
Number of tubes, N	48
Outer diameter of tubes, d_1	$5 \cdot 10^{-3}$
Total heat-emitting surface area, F	$0.393\ m^2$
Free cross-sectional area (minus head), Ω	$7.32 \cdot 10^{-3}\ m^2$
Equivalent diameter, d_{eq}	$25.2 \cdot 10^{-3}$ m

The surface temperature was measured with Chromel–Alumel thermocouples embedded in the tubes. When the temperature of the outer surface of the tubes was calculated, a correction was introduced for the temperature drop in the wall, not exceeding 2% of the temperature head. Eight calorimetric tubes (two in each row) accommodated five thermocouples distributed over the length of the structure, while the

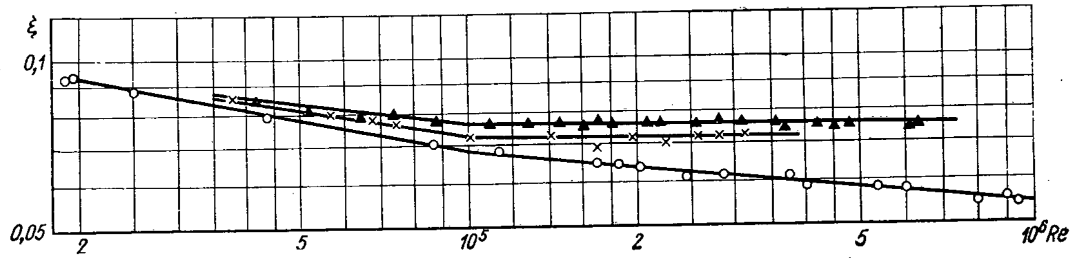

Fig. 3. Effect of roughness on resistance: ○) mockup with smooth rods; ×, ▲) rough rods, h/d_{eq} = 0.00095 and 0.0026 respectively; —— calculation based on Eq. (6).

remaining tubes accommodated one thermocouple each, corresponding to the position of the middle thermocouple in the calorimetric tubes.

The average temperature of the surface of the calorimetric tubes in each row $\overline{T}_{st_i}$ and the coefficient of the temperature field for each row $\varphi = \overline{T}_{st_i}/\overline{T}_{c_i}$, where $\overline{T}_{c_i}$ are the readings of the middle thermocouple down the tube length, were calculated from the thermocouple readings.

The surface temperature of the tubes in the entire bundle were calculated from the formula

$$\overline{T}_{st} = \frac{\sum_{i=1}^{3} \varphi_i \overline{T}_{c_i} n_i}{\sum_{i=1}^{3} n_i}, \tag{1}$$

where $\overline{T}_{c_i}$ is the arithmetic mean of the readings of the central thermocouples of all the tubes in the i-th row; n_i is the number of tubes in the i-th row.

The stream temperature $\overline{T}_g$ was calculated as the arithmetic mean of the thermocouple readings at the entrance to the working sector and at the exit from the sector, and was decisive in the assignment of physical constants. The heat loading was calculated on the basis of the electric power level, and was verified against the heating up of the gas. The imbalance was less than 5%. The results of the experiments were processed in dimensionless form:

$$\mathrm{Nu} = \frac{\alpha d_{eq}}{\lambda}; \quad \mathrm{Re} = \frac{w d_{eq}}{\nu}; \quad \xi = \frac{2\Delta P}{\rho w^2} \frac{d_{eq}}{L}. \tag{2}$$

The effect of the temperature ratio on heat emission was taken into account by introducing the correction $\psi^{-0.55}$, which has been accepted in the literature.

Figure 2 shows results of experiments on heat emission in the form of the dependence K = f(Re), where $K = \mathrm{Nu}/\mathrm{Pr}^{0.4}\,\psi^{-0.55}$. Curves typical of heat emission from rough surfaces are plotted, and the interval on which no influence of roughness is detected shows up clearly in the case of surface asperities of small relative dimensions ($h/d_{eq} \approx 0.00095$), as well as an interval manifesting a pronounced effect of surface roughness (at $\mathrm{Re} \geq 8 \cdot 10^4$). For comparison, Fig. 3 shows experimental results on heat emission in air from a smooth tube and a rough tube (h/d_{eq} = 0.0016) with outer diameter $d_{eq} = 5 \cdot 10^{-3}$ m, immersed in a channel of inner diameter d_2 = 0.064 m; this curve depicts the dependence Nu = f(Re). An annular channel with unilateral internal heating, and the ratio d_2/d_1 = 12.8, is formed in this case.

Experimental data on heat emission from a smooth-walled tube are in excellent agreement with B. S. Petukhov's formula [6]:

$$\mathrm{Nu}_1 = 0.86\,\mathrm{Nu} \quad (d_1/d_2)^{-0.16}\zeta, \tag{3}$$

where Nu_{rt} is the heat transfer to air in a round tube as calculated on the basis of the formula

$$\mathrm{Nu}_{rt} = 0.0186\ \mathrm{Re}^{0.8}\psi^{-0.5}. \tag{4}$$

The difference in the exponent applied to ψ is 0.5 and 0.55, which is insignificant, yielding an error no greater than 0.5% (ψ = 1.15). The effect of surface roughness on heat emission from the tube in the annular channel is similar to its effect in assemblies of rod type fuel elements.

TABLE 2. Values of the Coefficients in Eqs. (5) and (6)

Bundles	Formula (5)			Formula (6)		
	Re range	c	m	Re range	c_1	m_1
Bundle 1, smooth	$2\cdot10^4$—10^6	0,035	0,8	$2\cdot10^4$—10^5 10^5—10^6	0,68 0,215	—0,2 —0,1
Bundle 2, h/d_{eq} = 0.00095	$4\cdot10^4$—$8\cdot10^4$ $8\cdot10^4$—$4\cdot10^5$	0,035 0,0056	0,8 0,96	10^5—$4\cdot10^5$	0,072	0
Bundle 3, h/d_{eq} = 0.0026	$3\cdot10^4$—10^6	0,0068	0,96	$3\cdot10^4$—10^5 10^5—10^6	0,34 0,076	—0,13 0

Results of experiments on the hydraulic drag presented by fuel assemblies in an isothermal air flow pattern are plotted in Fig. 3. That diagram also shows drag curves typical of surfaces of low relative roughness, which degenerate into straight lines independent of Reynolds numbers in the range Re $\geq 10^5$.

Heat emission from the fuel assemblies investigated is described by the empirical formula

$$Nu = c\,Re^m\,Pr^{0.4}\psi^{-0.55}, \tag{5}$$

while the hydraulic drag

$$\xi = c_1 Re^{m_1}. \tag{6}$$

Values of the numbers c, m, c_1, and m_1 are listed in Table 2 for the range of variation of Reynolds numbers of interest here.

Note the slightly greater increase in heat emission (up to 80%) compared to the increase in drag (to 40%) in response to surface roughness. The underlying reason is that the bulk of the drag presented by the assembly is accounted for by the massive heads, so that even an appreciable increase in the friction factor of the fuel rods caused by surface roughness would make no substantial contribution to increasing the drag of the fuel assembly as a whole, while the increase in heat emission is due primarily to swirling of the laminar sublayer on the rod surfaces by roughness elements (asperities). Consequently, roughness makes it possible to raise markedly the thermal characteristics of fuel assemblies in gas-cooled reactors. Surface roughness can also be used to advantage in intensifying heat transfer in components of heat-power equipment.

LITERATURE CITED

1. N. Kattchee and W. Mackewicz, Ékspress Informatsiya, Teploénergetika, No. 46 (1964).
2. E. Adam, Kernenergie, 9, No. 1, 1 (1966).
3. G. Grunwald, Kernenergie, 9, No. 11, 345 (1966).
4. Sutherland, Internat. J. of Heat and Mass Transfer, 10, No. 11, 1589 (1967).
5. G. A. Dreitser and É. K. Kalinin, Inzh.-Fiz. Zh., 15, No. 3, 408 (1968).
6. B. S. Petukhov and L. N. Roizen, Teplofiz. Vys. Temp., 2, No. 1, 78 (1964).

RADIATION-INDUCED SWELLING OF SOME TRANSITION METAL BORIDES

T. M. Guseva, V. P. Gol'tsev, and V. A. Ol'khovikov

UDC 621.039.516.22

Owing to the recent tendency towards higher power ratings and longer runs in nuclear reactors, greater service reliability is being demanded from neutron-absorbing materials. The most commonly used absorbing compositions are the diborides of chromium and titanium and the hexaborides of europium and samarium; these have higher boron contents than other borides [1].

One of the main effects of neutron irradiation limiting the service life of absorbing elements on boron-containing materials, is their expansion (swelling) at high temperatures. It is therefore of practical importance to establish the relations between swelling, burnup, and temperature.

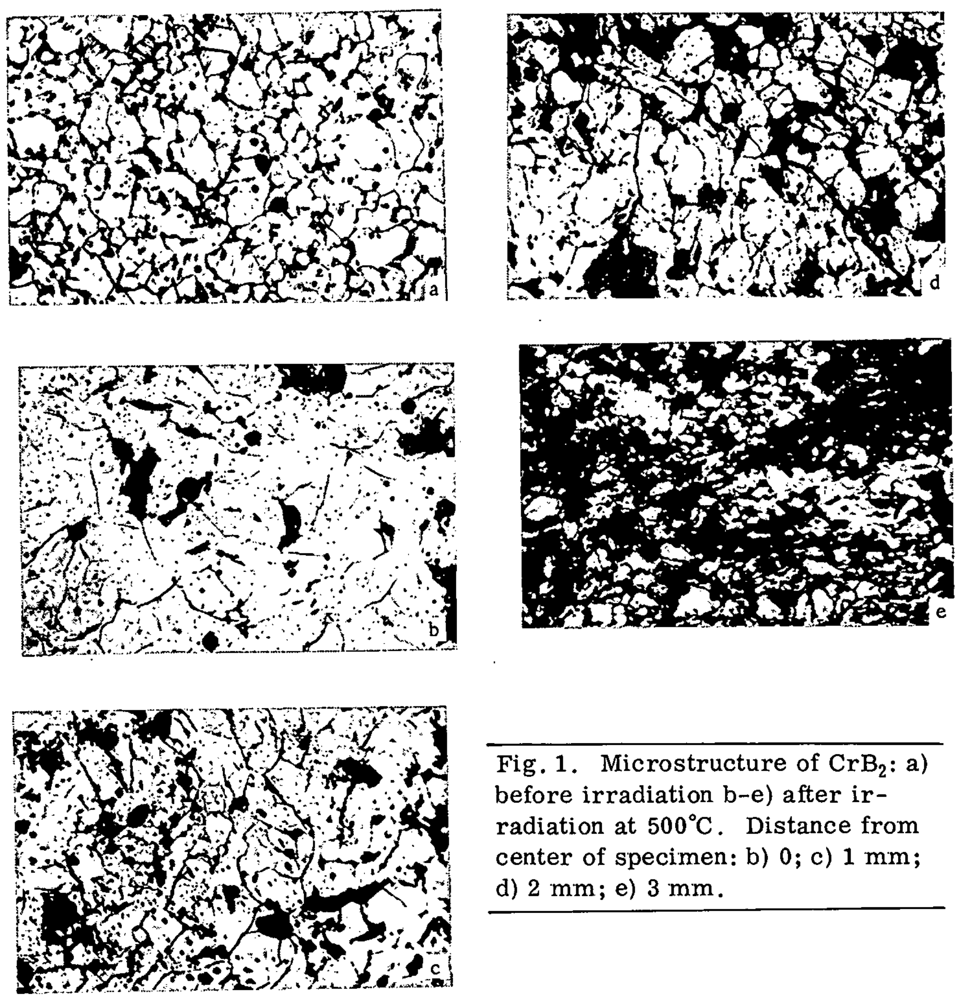

Fig. 1. Microstructure of CrB_2: a) before irradiation b–e) after irradiation at 500°C. Distance from center of specimen: b) 0; c) 1 mm; d) 2 mm; e) 3 mm.

Translated from Atomnaya Énergiya, Vol. 33, No. 3, pp. 747–752, September, 1972. Original article submitted May 18, 1971; revision submitted March 1, 1972.

Declassified and Approved For Release 2013/02/27 : CIA-RDP10-02196R000300110003-7

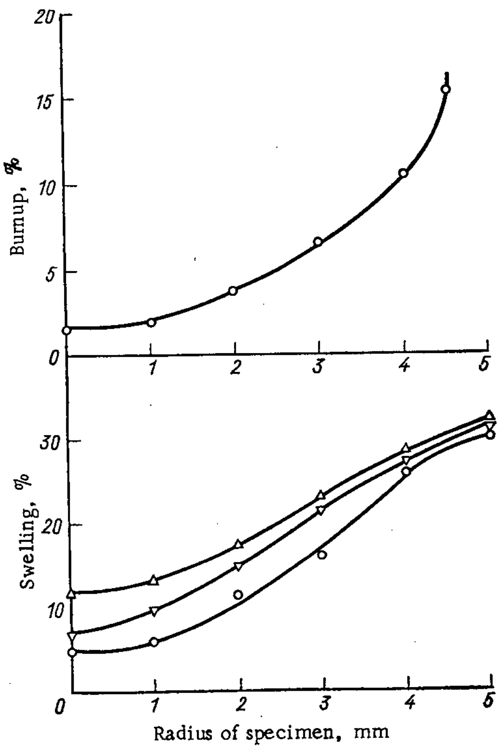

Fig. 2. Burnup (calculated) and swelling (measured) in various radial cross sections of CrB_2 specimen: ○) 500°C; ▽) 650°C; △) 1050°C.

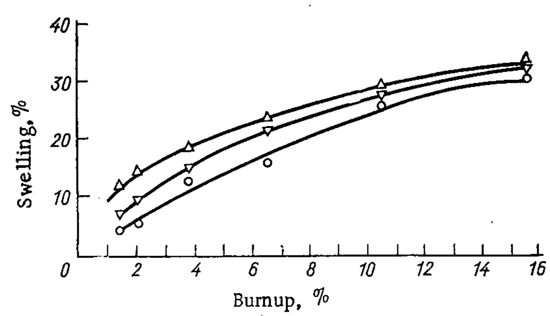

Fig. 3. Swelling vs burnup in chromium diboride at the following temperatures: ○) 500°C; △) 650°C; ▽) 1050°C.

MATERIALS AND METHOD

The materials chosen for testing were compositions based on chromium diboride CrB_2 and a combination of chromium and titanium diborides, $Cr(Ti)B_2$. Specimens of both compositions, in the form of tablets, 10 mm in diameter and 5 mm in depth, were prepared by hot-pressing the borides at 1850-2050°C. According to chemical analysis results, the CrB_2 contained 25-28 wt.% of boron, and the $Cr(Ti)B_2$ contained 22 wt.%; in both cases the boron was 80% enriched with B^{10}. X-ray and metallographic phase analyses revealed that the former material had one single phase with the CrB_2 structure, while the latter was a solid solution of chromium diboride in titanium diboride, isomorphic with TiB_2. The microstructure of both materials were homogeneous throughout the specimens. The initial porosity (approximately 6-7%) was uniformly distributed over the cross section (Fig. 1a).

The specimens were sealed into capsules of Kh16N15MZB stainless steel and irradiated for 5500 h in a water-cooled channel in an SM-2 reactor with fluxes of $5 \cdot 10^{14}$ neutrons/cm^2 · sec of thermal neutrons and $1 \cdot 10^{14}$ neutrons/cm^2 · sec of fast neutrons; the water pressure was 50 atm and the temperature was 50°C. The mean specimen temperature were 400 and 500°C; the temperature reached was monitored by means of diamond indicators by the usual method [2]. The heating of the specimens was due to energy emission caused by the (n, α) reaction of B^{10} and the absorption of γ-quanta from the core. The required specimen temperature were maintained by making radial gaps between the specimens and the interior surfaces of the capsules to act as heat resistances.

RESULTS AND DISCUSSION

The swelling of boron-containing materials is due to the following processes which are caused by burnup of B^{10}.

1) The total volume of the products of the nuclear reactions is greater than that of the original absorber (solid swelling).
2) Gas atoms accumulate, gas pores form, and subsequently grow at high temperatures.
3) Microfissures and cavities appear owing to the presence of internal stresses developing during irradiation and also by the coalescence of gas pores.

Solid swelling is a small effect and depends linearly on the burnup [3], whereas gas swelling depends markedly on the burnup and temperature and can be very appreciable. Many authors (e.g., Barnes [4], have shown that the amount of gas swelling is proportional to the volume of gas pores in the reactor materials.

Owing to self-screening, and hence to the concentration of impurity atoms, the burnup in absorbing materials depends on the specimen thickness; burnup is maximal in the surface layers, and much less marked in the central region. Obviously the porosity or swelling, which is a function of the burnup, will

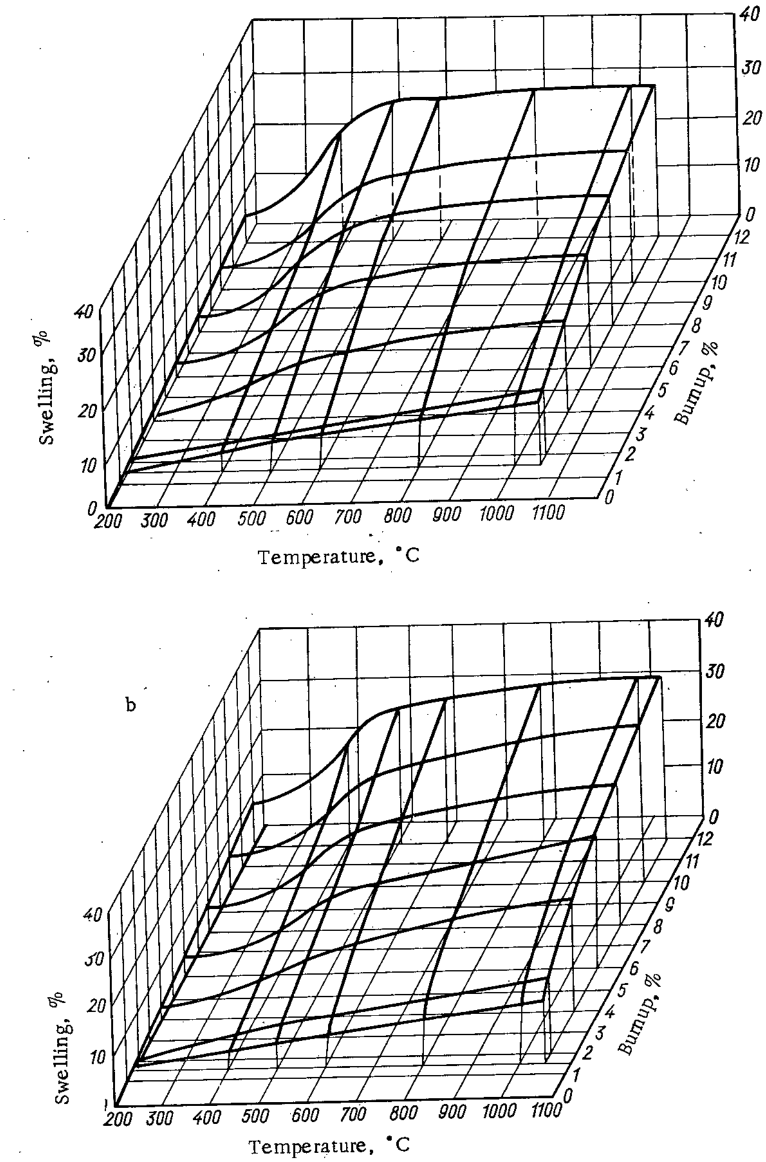

Fig. 4. Complete graph of radiation swelling; a) CrB_2; b) $Ti(Cr)B_2$.

vary similarly over the cross section of the specimen (see Fig. 1b-e). Thus in a single absorber there may be several burnup values and several corresponding degrees of swelling. If we know the way in which the burnup varies over the cross section of the specimen, and if we determine the variation of the swelling over the cross section of the same specimen, then we can establish the relation between swelling and burnup in isothermal conditions (owing to the high thermal conductivities of chromium and titanium borides, the temperature difference does not exceed 20-30°C).

The variation in the burnup of boron over the cross section of a specimen is given by

$$n = \frac{n_0}{e^{-\sigma(n_0 x - \varphi_0 t)} - e^{-\sigma n_0 x} + 1}, \qquad (1)$$

where n is the concentration of B^{10} nuclei, n_0 is the initial concentration of B^{10}, σ is the cross section of the absorber, φ_0 is the neutron flux, and x is the distance over the cross section of the specimen.

We can assess the variation of the swelling over the cross section of the specimen from the variations in its density or porosity. The most convenient method of studying successive layers of swelling is

TABLE 1. Swelling and Porosity of Irradiated Chromium and Titanium Borides

Properties	CrB_2				$Ti(Cr)B_2$			
	not irradiated	irradiated at 500°C	irradiated and annealed at		not irradiated	irradiated at 500°C	irradiated and annealed at	
			650°C	1050°C			780°C	1050°C
Initial:								
density, gm/cm³	5,34	4,31	4,17	4,18	4,53	3,76	3,57	3,25
porosity (impregnation), %	7,30	26,0	29,0	28,0	5,80	21,8	25,8	32,5
porosity (metallographic), %	7,0	27,0	30,0	30,0	6,0	24,0	28,0	34,0
Changes in:								
density, %	—	19,0	21,9	21,7	—	17,0	21,2	28,2
porosity (impregnation), %	—	18,7	21,7	20,7	—	16,0	20,0	26,7
porosity (metallographic), %	—	20,0	23,0	23,0	—	18,0	22,0	28,0

Note. Swelling is given as mean value, i.e., averaged over whole specimen. Mean burnups of B^{10} for CrB_2 are 6.1-6.5%; for $Ti(Cr)B_2$, 7.5-7.8%.

metallography in conjunction, for example, with the method of secants [5]. In this method, the whole area of a transverse polished section of the irradiated specimen is divided into a reasonable number (in our case, six) of concentric rings of equal width. The porosity is measured in each of the chosen sections, and from its variation the swelling is calculated for the corresponding parts of the cross section (after subtraction of the porosity before irradiation):

$$\frac{\Delta V}{V_0}=\frac{\Delta V}{V}\cdot\frac{I}{I-\frac{\Delta V}{V}}, \tag{2}$$

where ΔV is the change in pore volume in the irradiated specimen, and V and V_0 are the volumes of the irradiated and original specimens. We found that pores less than 0.1μ in size but within the resolving power of the optical microscope contributed less than 1% to the total porosity, and could therefore be neglected in the subsequent calculations.

Figure 2 shows graphs of the burnup and swelling, found metallographically, in cross sections at various radii (0 corresponds to the center of the specimen) in a CrB_2 specimen irradiated at 500°C and annealed at 650-1050°C. The mean values of the burnup and swelling, averaged over the whole specimen and found by graphical integration of the curves in Fig. 2, agree with the mean values of the burnup and swelling found directly by chemical analysis of the boron content and by hydrostatic weighing (see Table 1). Simultaneously we notice a correlation between the swelling and the porosity changes of the irradiated specimens, found by vacuum impregnation with a liquid of known density.

From the graphs in Fig. 2 we can plot the swelling of chromium diboride vs the burnup, using the corresponding value for the same cross section of the specimen (Fig. 3).

In designing control rods it is necessary to know the changes in the dimensions of the cores of absorber elements operating over long periods ar various temperatures. On the other hand, for given dimensions it is necessary to find the operating time under given irradiation conditions in which the core of an absorber element will not swell and cause catastrophic damage to the whole structure. To solve these problems we suggest the use of a complete radiation swelling diagram, i.e., a three-dimensional graph of the swelling vs the burnup and the temperature. On comparing the data in Table 1 and Fig. 3 we easily verify that the total swelling of the specimen for some average burnup is closely correlated with the swelling of that cross section of the specimen for which the burnup exactly coincides with the mean value. On this basis we can use the results of a layerwise determination of the burnup and corresponding swelling to plot graphs of the swelling over a wide range of burnup and temperatures (Fig. 4).

From the swelling diagram it follows that for small amounts of burnup (1-2%) the swelling increases linearly or nearly linearly with the temperature. At moderate degrees of burnup (2-6%) the swelling increases monotonically with temperature; the greatest rate of swelling ($\partial\Delta V/\partial t$) is observed at 400-600°C. At high burnup (over 6%), the temperature dependence of the swelling has three sections: a slight increase up to 400-500°C, a sharp rise at 500-600°C, and finally a slow increase at temperatures up to 1000°C.

LITERATURE CITED

1. W. Ray et al., Nucl. Sci. and Engng, 4, No. 3, 386 (1960).
2. N. F. Pravdyuk et al., in: Effects of Nuclear Radiations on Materials [in Russian], Izd-vo Akad. Nauk SSSR, Moscow (1962), p. 184.
3. S. T. Konobeevskii, Action of Irradiation on Materials [in Russian], Atomizdat, Moscow (1967).
4. R. Barnes, Nucl. Materials, 11, 12, 135 (1964).
5. E. V. Panchenko et al., Laboratory Metallography [in Russian], Metallurgiya, Moscow (1965).

TESTING TWO ASSEMBLIES OF THERMIONIC CONVERTERS IN THE WATER-COOLED WATER-MODERATED REACTOR

A. A. Batalov, V. M. Zaitsev,
N. V. Zvonov, I. V. Kazin,
V. F. Kondrat'ev, V. N. Kuznetsov,
A. P. Rodnikov, S. V. Ryabikov,
V. F. Tikhonov, and N. A. Shapkin

UDC 621.039.578:537.58

In recent years contributors to the scientific literature have frequently discussed the possibility of making reactors allowing the direct conversion of thermal atomic energy into electrical power by means of the thermionic technique [1, 2]. One version of this type of reactor, the thermionic converter, is a system in which the fuel elements simultaneously act as electrical-generating elements, so that electrical power is obtained directly in the active zone of the reactor.

The combination of the nuclear process and current generation within a single element leads to a certain complication of the fuel-element construction, and this in turn requires careful and meticulous design of the single converter channel. The final stage in a development of this kind involves carrying out reactor tests on assemblies of electrical-generating elements with the aim of achieving a comprehensive verification of the physical ideas and technological principles forming the basis for such a construction.

In this paper we shall present certain data regarding loop tests carried out on two assemblies of reactor-type thermionic converters in a water-cooled, water-moderated reactor [3].

It is well known that there are two concepts of electrical-generating elements which may be involved when making reactors with thermionic converters of the inbuilt type [4]. The first is based on an electrical-generating channel with its length equal to the height of the active zone, containing several electrical-generating elements connected in series inside the channel ("garland" arrangement). In this case the output voltage in the channel is summed, and, owing to the short length of the individual modules, the relative electrical losses will be small. Serious disadvantages of this type of construction include the existence of intermodule commutative connections in the active zone of the reactor, the necessity of the electrical matching of the elements working in different thermal modes, and the general substantial complication of the construction.

The second concept is based on a single long element extending along the height of the active zone (single-fuel-element scheme), the current being taken from the ends lying outside the active zone; this

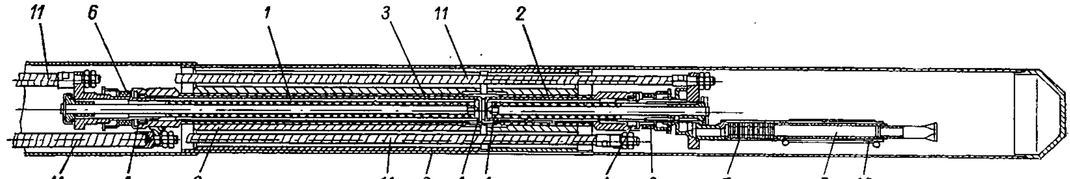

Fig. 1. Electrical-generating part of the assembly.

Translated from Atomnaya Énergiya, Vol. 33, No. 3, pp. 753-756, September, 1972. Original article submitted December 27, 1971.

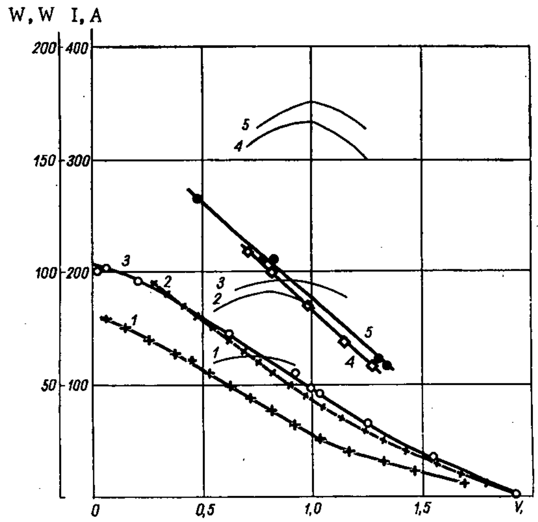

Fig. 2

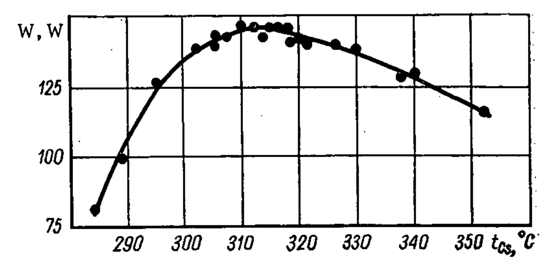

Fig. 3

Fig. 2. Volt–ampere and power characteristics of the TÉP-I: 1) 1000 kW, 12.8 W/cm^2; 2) 1250 kW, 16 W/cm^2; 3) 1500 kW, 19.2 W/cm^2; 4) 1750 kW, 22.4 W/cm^2; 5) 2000 kW, 26 W/cm^2.

Fig. 3. Typical relationship between the power of the TÉP-I and the cesium vapor pressure (N = 1500 kW).

greatly simplifies the construction and the technology of its execution. A characteristic feature of the operation of a cylindrical single-fuel-element thermionic converter is the considerable influence of the ohmic losses on the electrical output power. The effect of these losses is that, with increasing length of the electrical-generating elements L (other construction elements maining constant), the power W developed is not proportional to L but tends to a certain limiting value W_{lim} as $L \to \infty$. In order to simplify the model of the isothermal electrical-generating element for optimum values of the useful load, this relationship may be written

$$W = W_{\lim}\ thk,$$

where $k = L[(j_0/E - V_0)(\rho_c/\delta_c + \rho_a/\delta_a)]^{1/2}$; j_0, V_0 are the current density and voltage at optimum load, E is the no-load voltage, ρ_c, ρ_a, δ_c, and δ_a are the specific electrical resistance and thickness of the electrodes of the thermionic converter respectively.

It follows from the relationship that there is a certain "critical" length L_{cr} which it is energetically undesirable to exceed because of the inordinate increase in the ohmic losses at the electrodes, the smaller L_{cr}, the greater the specific current take-off j_0. Thus, for the single-fuel-element version of the electrical-generating element, the requirement of relatively small losses and a reasonable size of the active zone of the reactor limits the range of suitable materials and the temperatures of the emitting cathode shell.

Since, for practical geometrical dimensions of a single-fuel-element electrical-generating unit, the range of acceptable electrical powers lies between 2 and 5 W/cm^2, it is desirable to use molybdenum as emitter material, the thermionic characteristics of this element having been fully studied. In this case, the single-fuel-element version may compete successfully (as regards specific indices) with the garland version, being advantageously distinguished from the latter by its simplicity and reliability of construction.

The aim of the present tests was to verify the efficiency of individual units and assemblies with single-fuel-element converters in the field of radiation of the reactor, to discover the temperature distributions, and to study the output parameters of converters of this type. An extremely important constructional and technological question in the development of single-fuel-element electrical-generating units is that of the stability of the interelectrode gap over long periods of service at working temperatures. Since preliminary theoretical and experimental data indicated the possibility of making electrical-generating elements with

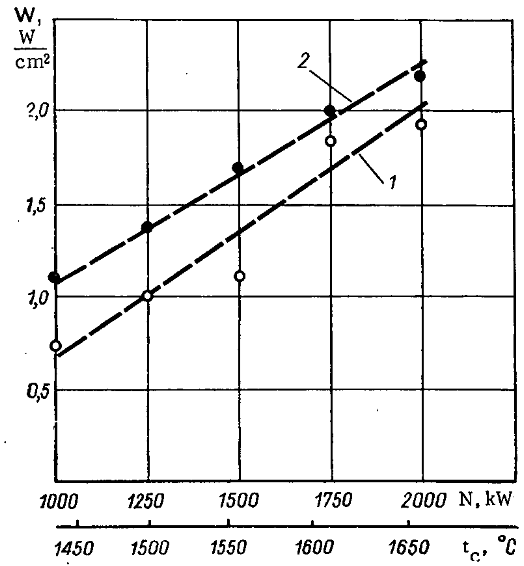

Fig. 4. Dependence of the maximum specific power of the thermionic converters on the reactor power and cathode temperature: (1) for the TÉP-I; 2) for the TÉP-II.

end fixing only, one of the most important points in the test program was that of confirming the efficiency of the cathode over long periods in the absence of intermediate fixing elements in the cathode–anode system.

In view of the fact that the height of the active zone in the water-cooled, water-moderated reactor equalled 50 cm, while the electrical-generating element was symmetrical with respect to the central plane as regards current take-off, only one half element of the single-fuel-element electrical-generating system was tested, i.e., a region including comparatively slight changes in neutron flux was employed. At the same time, in order to simulate the temperature conditions in the central plane, the test assemblies also contained a shortened auxiliary electrical-generating element, playing the part of an additional source of neutron and thermal flux for the main half element and furnished with its own current and potential leads.

The electrical-generating part of the channel is shown in Fig. 1. The principal and auxiliary cathodes 1 and 2 of the thermionic converter, 14 mm in diameter, are inserted coaxially into the common anode 3, the interelectrode distance being 0.5 mm. The lengths of the working part of the cathodes are 200 and 80 mm respectively. Inside the cathode shells, which are made from polycrystalline (thermionic converter TÉP-I) and single-crystal (thermionic converter TÉP-II) molybdenum 1 mm thick, are uranium dioxide insertion pieces in a molybdenum matrix. The central aperature in the fuel element serves for removing the fission products and accommodating the tungsten–rhenium thermocouples. These spaces may at the same time be used for siting the heaters used in the preliminary degassing of the assembly. The interelectrode gap is maintained by means of special metalloceramic elements 4 placed at the ends of the cathode, and forms a common cavity with the cesium vapor source 5 placed in the lower part of the assembly. The cathodes are separated electrically from the anode by hermetically sealed ceramic insulators 6. The anode is made of niobium tube 1.5 mm thick. In order to maintain the temperature required for the operation of the converter at the anode while cooling the channel itself with water, Alundum is applied to its outer surface in the form of discrete longitudinal bands in such a way as to ensure the necessary temperature drop for any specified thermal flux from the cathode. In order to absorb the residual gases passing into the interelectrode space during operation, titanium getters 7 are installed in the lower part of the assembly. The generating part of the assembly is surrounded by an aluminum alloy displacer 8 and is inserted into an external carrying jacket made of stainless steel 9. The working temperature of the cesium reservoir is maintained by means of a special electrical furnace 10.

The assembly is furnished with thirteen thermocouples for monitoring the temperature of the cathode, anode, cesium reservoir, and other parts. The principal and auxiliary electrical-generating elements have their own individual current (11) and potential leads.

By means of the outer casing, the assembly as a whole is sealed into the channel, which at its upper end has a head-piece with vacuum-tight electrical connections and a shut-off vacuum valve. After assembly, the electrical-generating element was subjected to laboratory tests for 200 h with an electrical simulator representing the nuclear fuel, electrical power being generated during this period. Before installation in the reactor, the channel was subjected to final vacuum conditioning and tests in a special test-bed.

The experimental apparatus incorporates a system for evacuating the inside of the channel, a system of receivers for the ejection and storage of the radioactive gases, and electrical supply, monitoring, and measuring desks. The volt–ampere characteristics were plotted by both the compensation and oscillograph methods.

The assemblies of the series under consideration, TÉP-I and TÉP-II, were operated in the reactor at powers of 1000 kW and over (the cathode temperature was never lower than 1480°C) for 900 and 1440 h respectively. In these experiments, the reactor power level was kept constant for specific intervals varied from 1000 to 2000 kW in steps of 250 kW during the tests. The temperatures of the cathode, anode, cesium reservoir, and individual structural units were recorded continuously, and the volt–ampere characteristics of the converter were also plotted periodically; the temperature of the reservoir containing the cesium was corrected to the value corresponding to the maximum electrical power of the thermionic converter in the mode under consideration.

The temperature of the anode was not adjusted as the power varied; on changing the power from 1000 to 2000 kW it rose from 450 to 750°C.

In view of the fact that the cathode temperature was measured with thermocouples situated in the central cavity of the fuel element, a calculated correction was introduced in order to determine the temperature of the working surface of the cathode.

By way of illustration, Fig. 2 shows some typical volt–ampere characteristics of the assembly TÉP-I, obtained for various levels of energy evolution at the cathode surface (12.8-26 W/cm^2), corresponding to reactor powers of 1000-2000 kW. For each level of energy evolution the cesium vapor pressure was kept constant so as to ensure almost optimum efficiency. The same figure illustrates the power characteristics of the thermionic converters for the corresponding modes in the region of optimum voltage (thin lines). For all levels of energy evolution the converters operated in the arc mode, as indicated by the almost linear dependence of current on voltage. The no-load voltage for all the characteristics shown in Fig. 2 equals 1.8-2 V. The optimum output voltage increases with increasing energy evolution, from 0.7 to 1.0 V.

Figure 3 illustrates a typical relationship between the electrical power of the TÉP-I and the temperature of the cesium reservoir t_{Cs}. The optimum values of t_{Cs} for the majority of the operating modes considered lay in the range 305-325°C.

Figure 4 shows the dependence of the maximum specific electrical power of the thermionic converters on the reactor power and the cathode temperature of both assemblies, plotted under almost optimum conditions. The slight difference in the specific electrical powers of the two assemblies is evidently due to the fact that in the TÉP-I the cathode shell was made of polycrystalline molybdenum and in the TÉP-II of a single crystal. We see from Fig. 4 that in the cathode temperature range 1550-1650°C an electrical power density of 1.5-2 W/cm^2 is realised.

By using the temperature measurements and determining the thermal balance of the converter, we may estimate the specific thermal flux. This is ~16 W/cm^2 for a power of 1250 kW and varies in proportion to the power. The efficiency varies from 6 to 9% in various operating modes of the assembly.

On testing the assemblies over several hundreds of hours operation, we sometimes noted a sudden fall in their output parameters; analysis showed that this was due to poor construction of the lower fixing system, which ruptured as the cathode underwent linear expansion. In subsequent work these inferior parameters remained unaltered, indicating that the remainder of the structural components were still intact.

The auxiliary electrical-generating elements generated electrical energy in a stable manner during the whole period of testing the two channels. However, in view of the fact that these auxiliary elements lay considerably below the center of the active zone of the reactor, their specific electrical power was no greater than 1-1.5 W/cm^2 at the maximum reactor power.

The following conclusions may be drawn from the foregoing analysis.

1. A reactor-based thermionic electrical-generating element of the single-fuel-element type has been successfully developed and manufactured.

2. We have carried out loop tests on channels containing thermionic-converter assemblies. The reactor experiments have confirmed the correctness of the construction and technological designs adopted, and the fundamental efficiency of the electrical-generating elements under test.

3. An electrical power density of 2 W/cm^2 has been achieved, the total power being 180 W and the efficiency 8-9% for a cathode temperature of 1650°C and time-stable volt–ampere characteristics.

4. The duration of the tests, with cathode temperature of at least 1480°C, were 900 and 1440 h respectively for the two electrical-generating elements tested, not counting the operating time of these elements in preliminary laboratory tests (200h).

5. The specific electrical power attained, together with the relative simplicity of the thermionic-converter channel construction, justifies our recommending the construction here discussed rather than the garland construction for use in reactor thermionic converters of relatively low volumetric specific power.

LITERATURE CITED

1. Yu. I. Danilov and D. V. Karetnikov, At. Énerg., 28, 33 (1970).
2. B. A. Ushakov, At. Tekh. za Rubezhom, No. 11, 7 (1969).
3. V. V. Goncharov et al., Soviet Contributions to the Second Geneva Conference (1959), Vol. 2 [in Russian], Atomizdat, Moscow (1959), p. 243.
4. A. Schock et al., "Direct conversion of thermal energy into electrical energy and the corresponding fuel elements," VINITI Report [Russian translation], No. 7 (84) (1969), p. 169.
5. G. Sawyer et al., ibid., No. 1 (78) (1969), p. 169.

NEUTRON PRODUCTION IN VARIOUS MATERIALS WITH 46 MeV ALPHA PARTICLES

V. K. Daruga and E. S. Matusevich

UDC 539.125.52

This paper presents more accurate data on the production of neutrons in thick targets by alpha particles. Preliminary results were published previously [1, 2].

Targets of Li, Be, C, Mg, Al, Ti, Fe, Co, Ni, Cu, Zn, Zr, Nb, Mo, Ag, Cd, Ta, W, Au, Pb, Bi, and U of natural isotopic composition were bombarded with a 46 MeV α-particle cyclotron beam. Target thicknesses were equal to the α-particle ionization range in the target material or were somewhat greater than this range.

In the experiments, measurements were made of secondary neutron spectra at angles of 0° and 90° to the beam of bombarding particles, of angular distributions in the range θ = 0-140°, and of the absolute neutron yields for energies $E_n > 0$ and $E_n \geq 1.8$ MeV.

Measurements were made with a single-crystal stilbene spectrometer having a pulse-shaped discrimination against γ-rays, a standard "long" counter containing an SNM-5 (BF_3) neutron detector, a ZnS $\cdot$(Ag) + Plexiglas fast neutron detector, and a wide-range ZnS(Ag) + B^{10} detector with polyethylene moderator. Detector characteristics were investigated in detail [3] in beams of monoenergetic neutrons and with radioactive neutron sources calibrated to better than 5% [4].

Spectra. Data on secondary neutron spectra from both thick and thin targets are very scarce in the literature for α-particle bombarding energies above 25 MeV. Measurements of the differential energy distributions of neutrons from thin targets of Al, Co, Nb, and Au were made [5] for 42 MeV α-particles. Thick C, Al, and Fe targets were investigated [6] with 39 MeV α-particles.

Secondary neutron spectra from thick targets obtained in our experiments $E_n < 2$ MeV, the energy distribution curves $N(E_n)$ were extrapolated to low E_n values with consideration given to the trend and variation in shape of the distribution curves in the region of the spectrometer threshold and to measured

TABLE 1. Average Energy of Spectral Neutrons

Target	$<E_n>$ M.		Target	$<E_n>$	
	$\theta = 0°$	$\theta = 90°$		$\theta = 0°$	$\theta = 90°$
Li	$\geq$5,2	3	Zr	—	2,2
Be	$\geqslant$7	2,6	Nb	3,1	2,1
C	$\geqslant$6,9	3,4	Ag	2,9	2,1
Mg	5	3,3	Cd	2,9	—
Al	4,6	3	Ta	2,4	1,65
Ti	3,9	—	W	2,7	—
Fe	3,4	2,4	Au	—	1,65
Co	3,3	2,4	Pb	2,6	1,7
Ni	4,6	2,6	Bi	2,4	—
Cu	3,7	—	U	2,5	2,2
Zn	—	2,5			

TABLE 2. Parametric Characteristics of Spectra

Target	$<E_\alpha>$	$T^*_{(L)}$,	T,
C	33	1,96—2,94	2,3 [6]†
Al	33,5	2,02—2,62	2 [6]; 2,1 [5]‡
Fe	34	1,69—2,02	1,6 [6]
Co	34,1	1,58—2,02	1,8 [5]
Nb	35,9	1,37—1,77	1,6 [5]
Au	39,05	0,98—1,4	1,0 [5]

*Two values for the spectral regions $E_n < 4$ MeV and $4 < E_n < 10$ MeV.

†Thick target, E_α = 39 MeV.

‡Thin target, E_α = 42 MeV.

Translated from Atomnaya Énergiya, Vol. 33, No. 3, pp. 757-765, September, 1972. Original article submitted December 20, 1971.

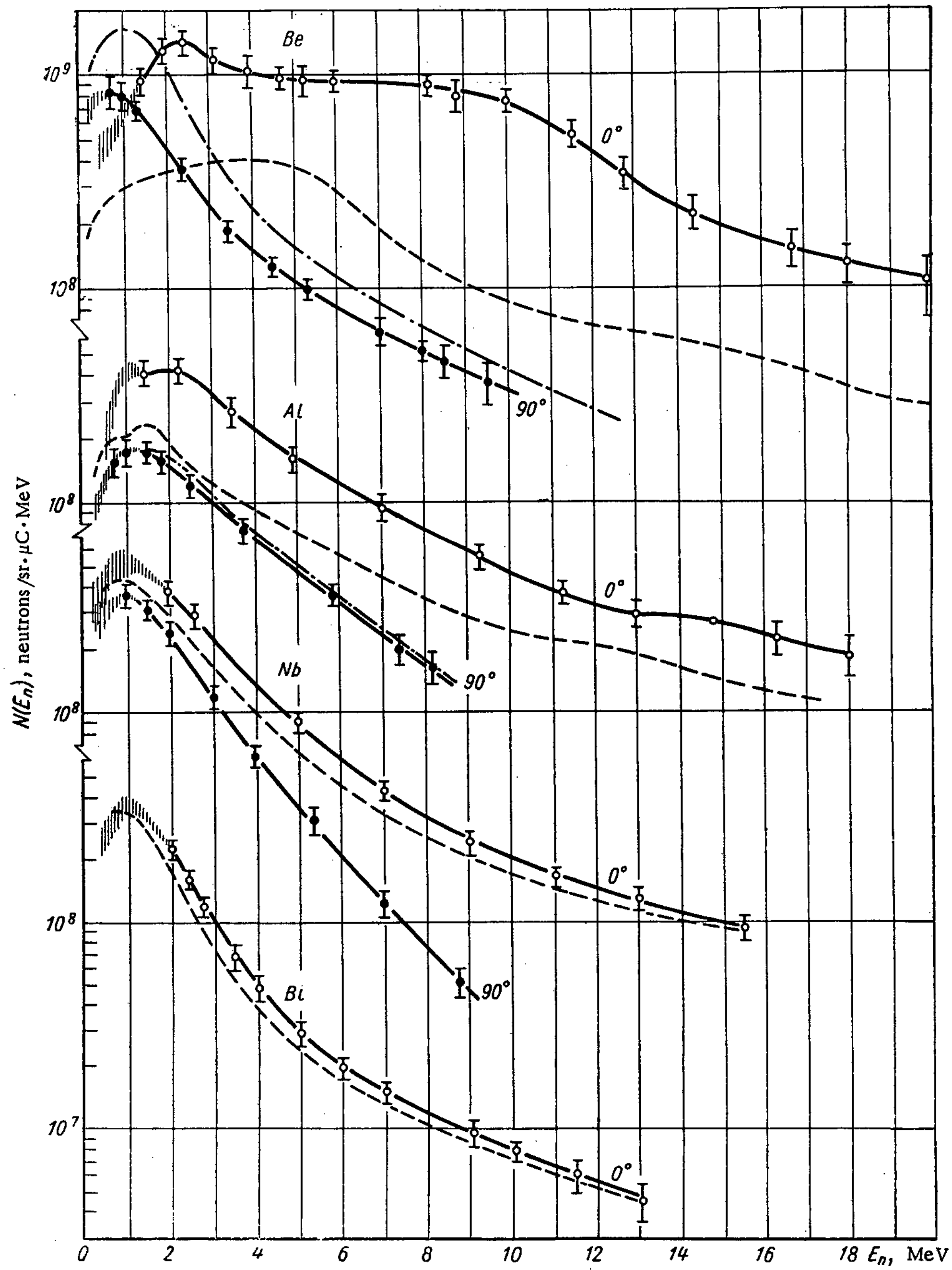

Fig. 1. Neutron spectra from Be, Al, Nb, and Bi targets. Dashed and dot-dash curves are the spectral shapes in the center-of-mass system.

absolute yields of neutrons in this energy region. In the figures, the vertical shading indicates the range of possible $N(E_n)$ in this part of the spectrum.

Table 1 gives values of $\langle E_n \rangle$, the average energy of the spectral neutrons estimated from the data in Figs. 1-5.

As a qualitative comparison between the energy distributions we obtained and the measurements of others at similar α-particle bombarding energies, values of T_L were determined, where T_L is a parametric characteristic of the spectra when they are analytically represented in the form $N(E_n) \sim E_n^{5/11} \cdot \exp(-E_n/T_L)$ [7] (see Fig. 3, Ti). In Table 2, values of $T_L = (12/11)T_L$ found for some spectra at an angle $\theta_{cm} = 90°$ are compared with similarly obtained values of the parameter T [5, 6] for the spectral region $E_n < 10$ MeV.

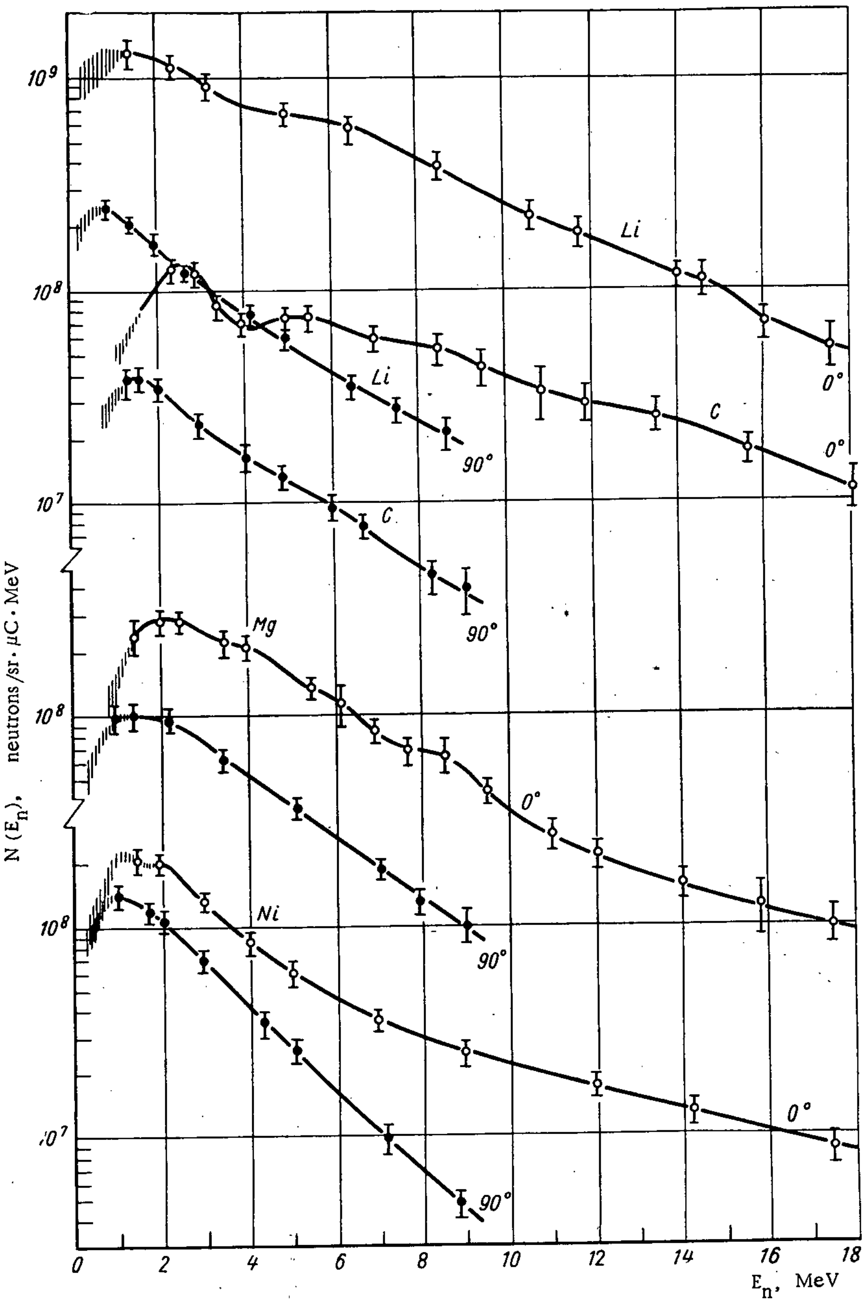

Fig. 2. Neutron spectra from Li, C, Mg, and Ni targets (E_α = 46 MeV).

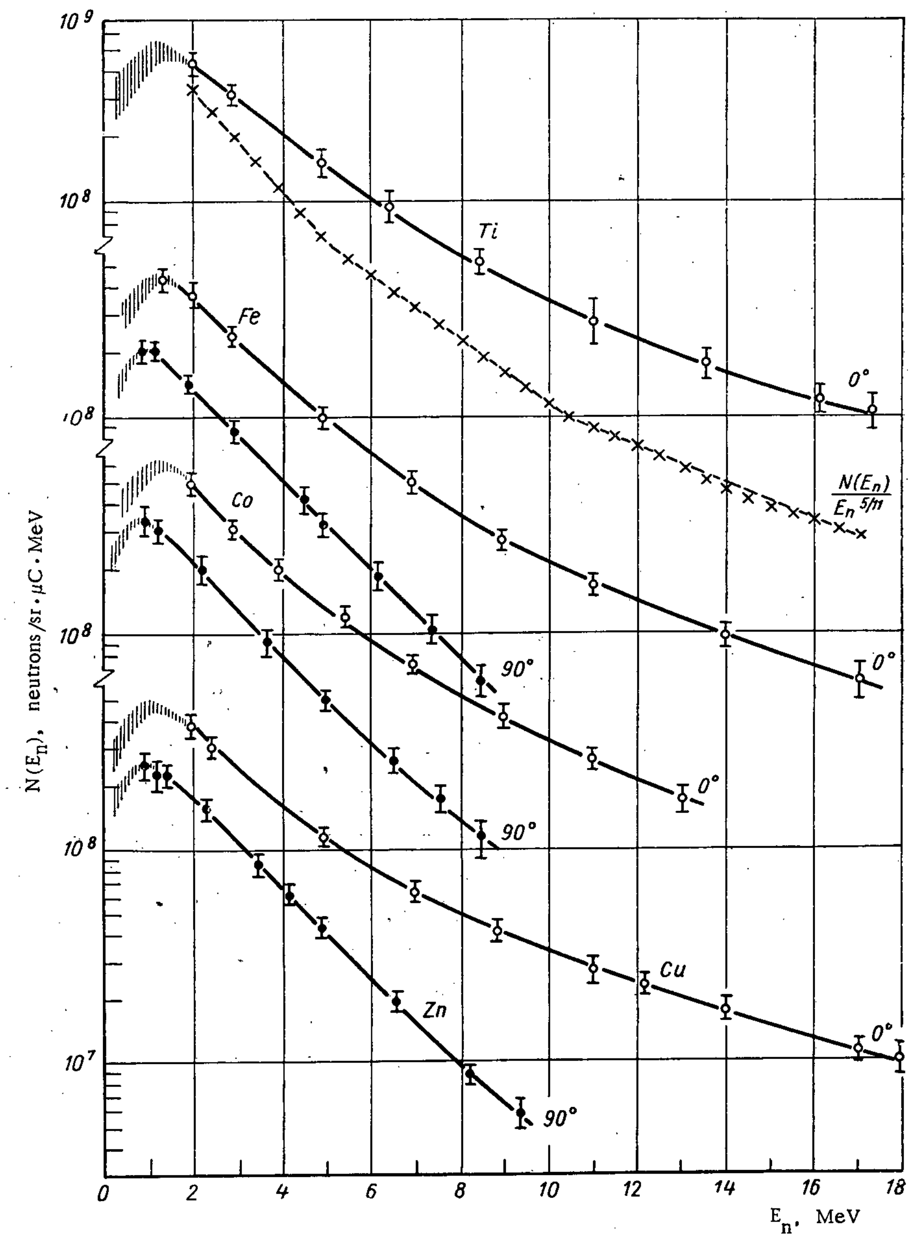

Fig. 3. Neutron spectra from Ti, Fe, Co, Cu, and Ta targets (E_α = 46 MeV).

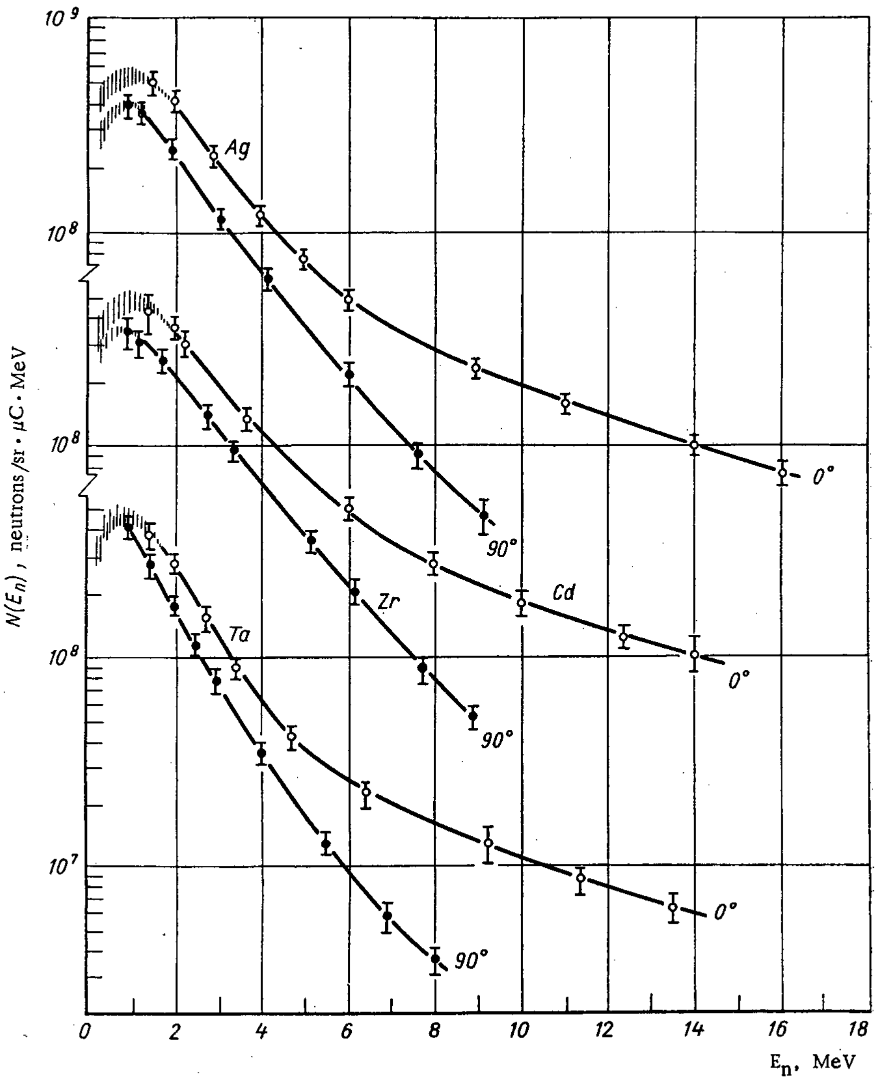

Fig. 4. Neutron spectra from Ag, Cd, Zr, and Ta targets (E_α = 46 MeV).

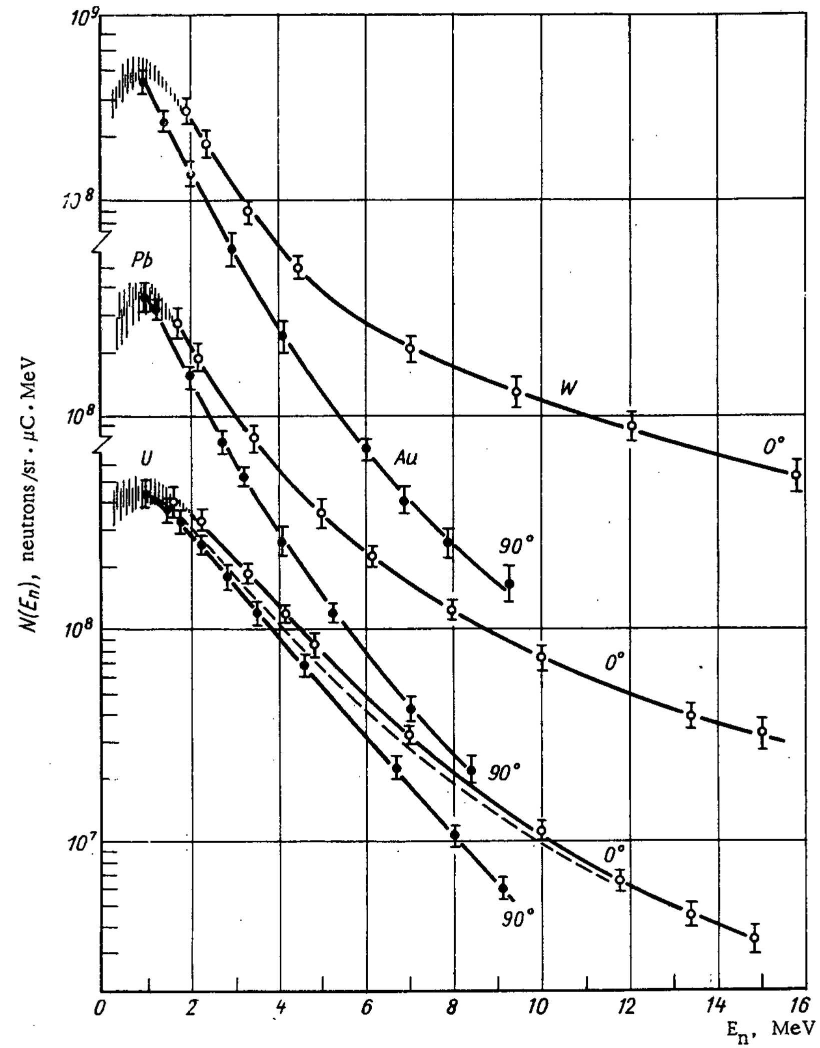

Fig. 5. Neutron spectra from W, Au, Pb, and U targets (E_α = 46 MeV).

Declassified and Approved For Release 2013/02/27 : CIA-RDP10-02196R000300110003-7

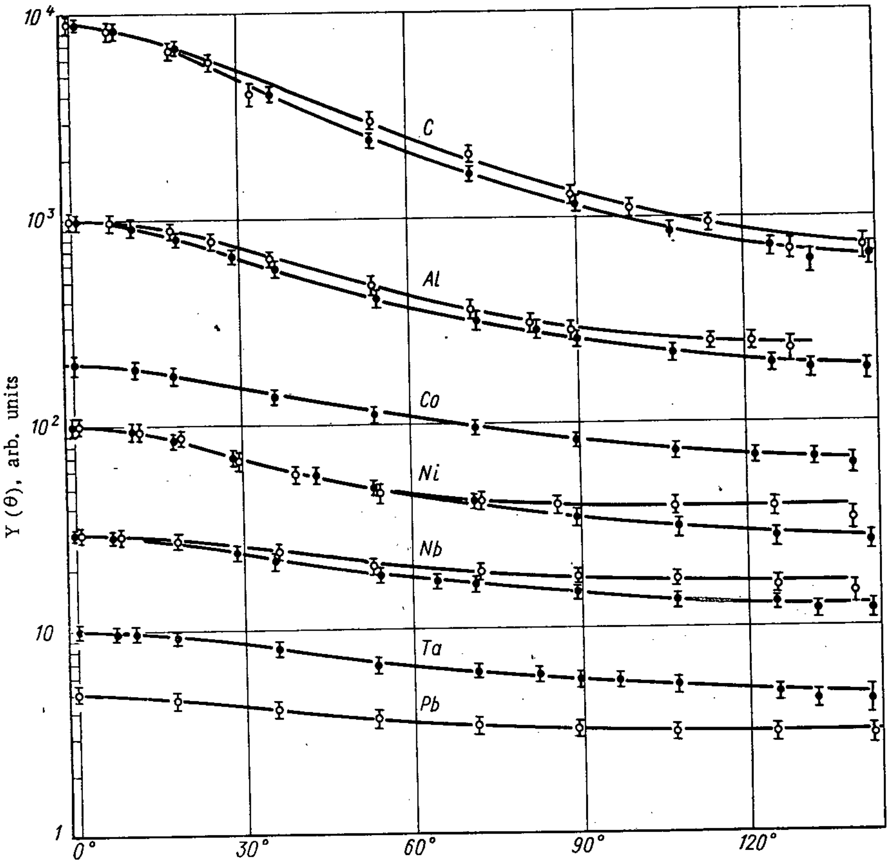

Fig. 6. Angular distribution of neutrons from certain targets: ○) $E_n > 0$; ●) $E_n > 1.8$ MeV.

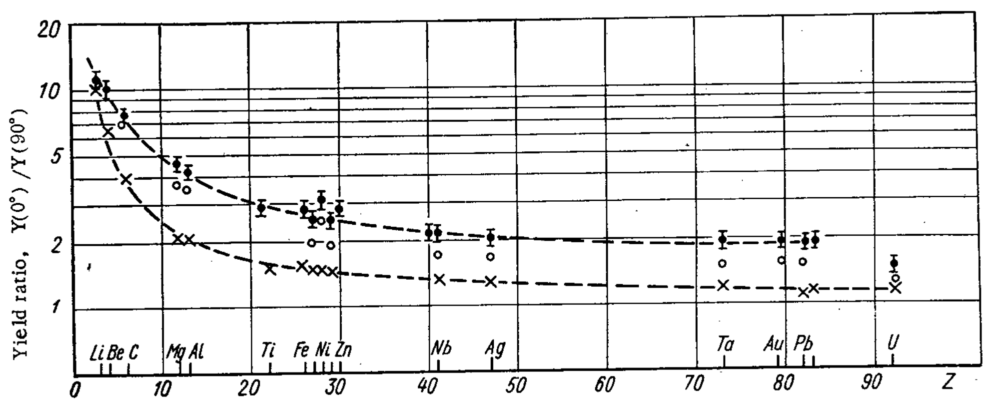

Fig. 7. Dependence of neutron yield ratio at $\theta = 0°$ and $\theta = 90°$ on atomic number Z of the target: ○) $E_n > 0$; ●) $E_n > 1.8$ MeV.

The second column in Table 2 gives the average effective (with respect to neutron yield) energy $\langle E_\alpha \rangle$ of the bombarding α-particles for nuclear interactions in a thick target. This quantity was calculated [3] on the basis of known data about the partial cross section of reactions yielding neutrons.

Angular Distributions. The angular distributions of neutron yields for energies $E_n > 0$ and $E_n \geq 1.8$ MeV (Fig. 6) from thick targets are smooth functions $Y(\theta)$ and are characterized by some degree of peaking in the direction $\theta = 0°$. Even for the heaviest elements, the yield ratio $Y(0°)/Y(90°)$ is about 1.6 for $E_n > 0$ and about 2 for $E_n \geq 1.8$ MeV. It is only in the case of α-particle bombardment of uranium that this ratio

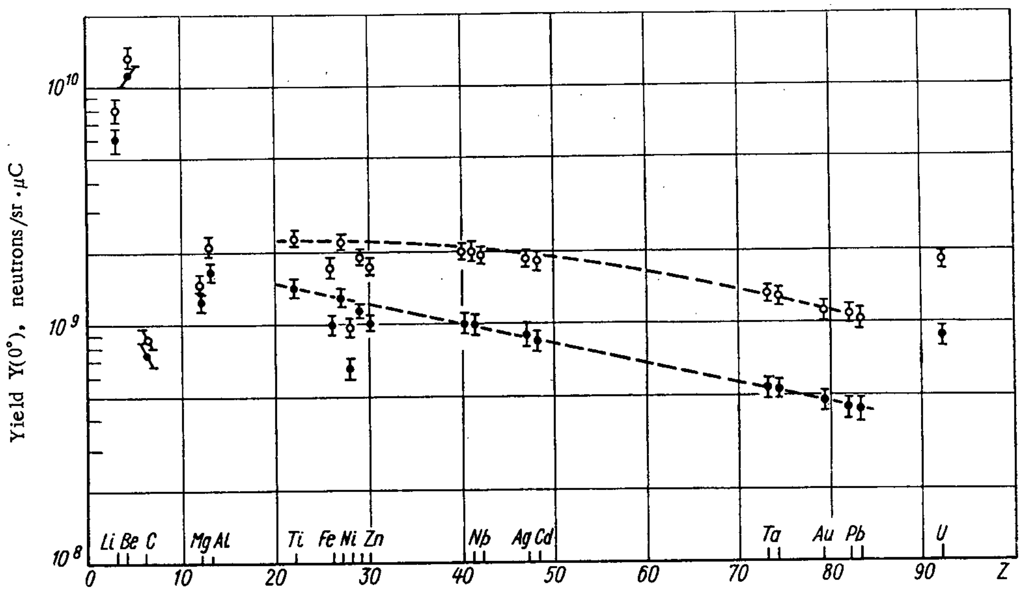

Fig. 8. Z dependence of absolute neutron yields in the direction $\theta = 0°$ ($\theta_{lab} = 0°$; $E_\alpha = 46$ MeV); ○) $E_n > 0$; ●) $E_n > 1.85$ MeV.

TABLE 3. Total Integral Neutron Yields

Target	$Y_{4\pi}$, neutrons / μC (calc.)	$Y_{4\pi}$, neutrons /μC (expt.)
Li	$1,7 \cdot 10^{10} \pm 20\%$	—
Be	$2,9 \cdot 10^{10} \pm 17\%$	—
C	$0,25 \cdot 10^{10} \pm 15\%$	—
Mg	$0,67 \cdot 10^{10} \pm 13\%$	—
Al	$1,0 \cdot 10^{10} \pm 13\%$	—
Fe	$1,15 \cdot 10^{10} \pm 14\%$	—
Co	$1,6 \cdot 10^{10} \pm 15\%$	$> 1,1 \cdot 10^{10}$
Ni	$0,55 \cdot 10^{10} \pm 13\%$	$0,56 \cdot 10^{10} \pm 20\%$
Cu	$1,4 \cdot 10^{10} \pm 14\%$	$> 1,1 \cdot 10^{10}$
Zn	$1,25 \cdot 10^{10} \pm 15\%$	$> 0,57 \cdot 10^{10}$
Zr	$1,7 \cdot 10^{10} \pm 13\%$	—
Nb	$1,6 \cdot 10^{10} \pm 13\%$	$1,4 \cdot 10^{10} \pm 30\%$
Mo	$1,6 \cdot 10^{10} \pm 14\%$	—
Ag	$1,6 \cdot 10^{10} \pm 13\%$	$1,8 \cdot 10^{10} \mp 20\%$
Cd	$1,5 \cdot 10^{10} \pm 14\%$	$1,25 \cdot 10^{10} \pm 30\%$
Ta	$1,15 \cdot 10^{10} \pm 13\%$	$1,2 \cdot 10^{10} \pm 15\%$
Au	$1,0 \cdot 10^{10} \pm 13\%$	$1,03 \cdot 10^{10} \pm 15\%$
Pb	$0,95 \cdot 10^{10} \pm 12\%$	$1,05 \cdot 10^{10} \pm 15\%$
Bi	$0,9 \cdot 10^{10} \pm 13\%$	$0,94 \cdot 10^{10} \pm 15\%$
U	$1,75 \cdot 10^{10} \pm 11\%$	$1,85 \cdot 10^{10} \pm 15\%$

will be lower (1.27 and 1.5, respectively) because of the large contribution from fission neutrons, the angular distribution of which is almost isotropic. Figure 7 shows the dependence of the ratio Y(0°)/Y(90°) on Z – the atomic number of the target nuclei.

It is not possible to select a single analytical form to describe the experimental distributions $Y(\theta)$ of secondary neutrons from thick targets for all angles θ and all Z. One can propose the following approximate expression which describes the distribution $Y(\theta)$ for $\theta = 0$–$90°$ and $Z > 10$:

$$Y(\theta, Z)/Y(0°, Z) \approx [1 + (\eta - 1)\sin^k \theta]^{-1},$$

where $\eta = Y(0°)/Y(90°)$ (see Fig. 7), and $k = f(Z) \approx 2 + (\theta°/45°)$.

The accuracy of this expression in describing the relative shape of the neutron angular distributions is no worse than ± 20%.

Introducing the idea of average effective energy of the bombarding particles $\langle E_\alpha \rangle$ and making certain assumptions [3] in the transformation of spectra from the laboratory system to the center-of-mass system (see Figs. 1 and 5), one can estimate the effect of the average translational velocity of the "compound nucleus" on the neutron angular distribution. The lower curve in Fig. 7 (crosses) shows the Z dependence of calculated values of the ratio Y(0°)/Y(90°) in the laboratory system under the assumption that neutron angular distribution ($E_n > 0$) is isotropic in the center-of-mass system (taking into account only the effect of translational velocity).

Absolute Yields. Figure 8 shows absolute neutron yields measured at $\theta = 0°$ for various thick targets. Yield measurements were made for neutrons with energies $E_n > 0$ and energies above the threshold of the ZnS(Ag) + Plexiglas detector. The general picture of the yield distribution as a function of Z is similar to that which was observed in the case of 23.5 MeV proton bombardment of thick targets [8]. One should notice the reduced yields from targets in the closed-shell region (Z = 28) and the increase by more than a factor of two for uranium (in comparison with the value extrapolated from the yield values for Ta–Bi) resulting from the fission of the residual nucleus.

The experimentally obtained values for absolute neutron yields and angular distributions were used for the determination of the integral total yields $Y_{4\pi}$ ($E_n > 0$) of neutrons from thick targets bombarded by 46 MeV α-particles. The resultant values are given in Table 3.

The third column in Table 3 gives the integral total neutron yield calculated from the experimental data on absolute values of the production cross section for neutrons in α-particle reactions [3]. In those cases where there was complete information about partial cross section in the energy $E_n \leq 46$ MeV (heavy nuclei), the experimental and calculated yields agreed within the limits of error.

The authors thank V. A. Dulin, V. G. Dvusherstnov, and N. N. Pal'chikov for help with the measurements.

LITERATURE CITED

1. A. T. Bakov et al., Bulletin of the Information Center for Nuclear Data [in Russian], No. 3, Atomizdat, Moscow (1966), p. 266.
2. V. K. Daruga et al., in: Radiation Dosimetry and Shielding Physics at Charged-Particle Accelerators [in Russian], JINR, Dubna (1970), p. 85.
3. V. K. Daruga, Dissertation [in Russian], JINR, Dubna (1971).
4. V. K. Daruga et al., Applied Nuclear Spectroscopy [in Russian], No. 2, Atomizdat, Moscow (1971), p. 3.
5. D. Drake et al., Direct Interactions and Nuclear Reaction Mechanism, Vol. 1, New York–London (1963), p. 282.
6. O. D. Brill' et al., Nuclear Interactions in Shielding of Space Ships [in Russian], Atomizdat, Moscow (1968), p. 147.
7. K. LeCouteur, in: Nuclear Reactions [Russian translation], Vol. 1, Gosatomizdat, Moscow (1962), p. 323.
8. V. K. Daruga and E. S. Matusevich, At. Énerg., 29, 456 (1970).

NEUTRON YIELD FROM SPONTANEOUS FISSION OF EVEN – EVEN CURIUM ISOTOPES

L. I. Prokhorova, V. G. Nesterov,
G. N. Smirenkin, G. V. Grishin,
E. A. Nikitin, V. N. Polynov,
and V. V. Rachev

UDC 539.173.84

The importance of data on the average neutron yield per fission ($\bar{\nu}$) for basic reactor materials determines the considerable scale of investigation into refinement of this data. There is very much less information about $\bar{\nu}$ for other isotopes, particularly transplutonium elements. At the same time, a knowledge of $\bar{\nu}$ for induced and spontaneous fission is necessary for the solution of various problems connected with the reactor production of these elements, their chemical treatment, and their practical use as neutron sources. This information is also of definite interest for the physics of the fission process.

In the present work, $\bar{\nu}$ was measured for the spontaneous fission of the heavy isotopes of curium Cm^{246} and Cm^{248}, data for which was lacking at the time the experiment was planned [1, 2]. In addition, the value of $\bar{\nu}$ for Cm^{244}, which has been rather well investigated in a number of papers that are in

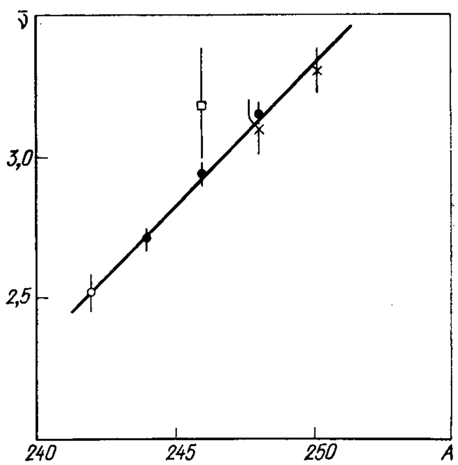

Fig. 1

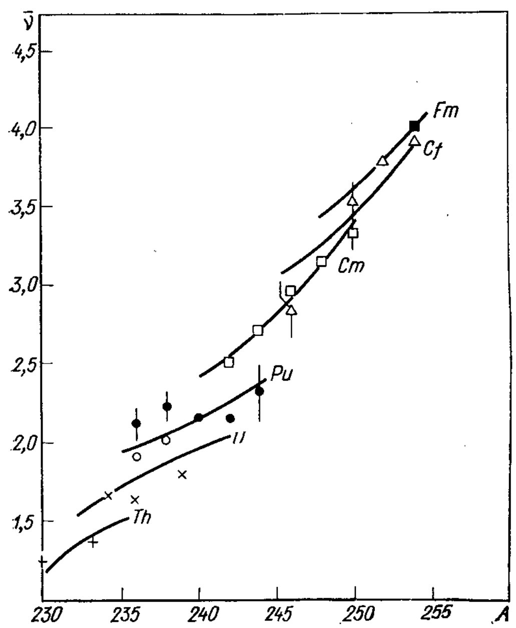

Fig. 2

Fig. 1. Average neutron yield per spontaneous fission of curium isotopes; ×) [1]: □) [2]; ○) [17]; ●) present work.

Fig. 2. Comparison of calculated results for $\bar{\nu}$ [18] (solid curves) with experiment for spontaneous fission of: ○) uranium; ●) plutonium; □) curium; Δ) californium; ■) ferium; +, ×) extrapolated values of $\bar{\nu}$ for thorium and uranium respectively.

Translated from Atomnaya Énergiya, Vol. 33, No. 3, pp. 767-770, September, 1972. Original article submitted November 25, 1971.

TABLE 1. Target Composition

Target	Amount of material, μg	Isotopic composition, % *			$\bar{\nu}$
		Cm^{244}	Cm^{246}	Cm^{248}	
Cm^{244}	0,9	~100	—	—	2,700±0,014
Cm^{246}	1,9	~0,6	99,4	—	2,950±0,015
Cm^{248}	1,3	5,6	2,0	92,2	3,157±0,015

*Admixture of odd isotopes, which make no significant contribution to the number of spontaneous fissions, is not shown.

TABLE 2. Experimental Values of $\bar{\nu}$ for Spontaneous Fission of Cm^{244}

Year experiment performed	$\bar{\nu}$	Reference
1955	2,83±0,12	[11]
1956	2,784±0,070 *	[12]
1956	2,677±0,056	[13]
1956	2,709±0,064	[14]
1964	2,690~0,039	[16]
1970	2,693—0,024	[15]
1970	2,750±0,080	[16]
1970	2,671±0,015	[7]
	2,700±0,014	This work
Weighted mean value	2,690±0,009	

*Value of $\bar{\nu}$ calculated from the ratio $\bar{\nu}$ (Cm^{244})/$\bar{\nu}$ (Cf^{252}), obtained in this experiment.

agreement [3-8], was measured in order to monitor operation of the equipment. A relative method of measurement [7, 9] was used in the experiment. Fission events and prompt neutrons were recorded simultaneously for the material under investigation and a Cf^{252} standard. The experimental equipment was a heterogeneous neutron detector consisting of 24 He^3 counters arranged in a cylindrical paraffin block in the central channel of which there was a fission detector. The well-known value $\bar{\nu}$ (Cf^{252}) = 3.756 [10] was used as a standard. A layer of curium oxide prepared from the separated isotopes, which was deposited on a platinum backing, served as a target. Characteristics of the targets are given in Table 1, where the results are also shown.

The value obtained for $\bar{\nu}$ (Cm^{248}) agrees within limits of experimental error with the data from [1]: 3.11 ± 0.09. The only known data for Cm^{246} is that in the Thompson paper [2], where $\bar{\nu}$ = 3.19 ± 0.22. We obtained a smaller value with no overlap of experimental errors. The value of $\bar{\nu}$ (Cm^{246}) taken from [2] lies off the monotonic and practically linear dependence of $\bar{\nu}$ on A (Fig. 1). It is likely the value is too high.

The results of this experiment for $\bar{\nu}$ (Cm^{244}) are in good agreement with other data, as can be seen from Table 2. The weighted mean value $\langle\nu\rangle$ for spontaneous fission of Cm^{244}, which equals 2.690 ± 0.009, can serve as quite a good standard for measurements.

In Fig. 2, the results of this work together with other data on $\langle\nu\rangle$ for spontaneous fission of even–even isotopes from uranium to fermium [17] are compared with the results of calculations performed in 1958 [18] based on an analysis of fission energy balance. Values for the transplutonium nuclei, measured later, are in good agreement with predictions [18] despite considerable simplification in the calculations. For example, in calculating

$$\bar{\nu}=\frac{\bar{E}_F-\bar{E}_k-\bar{E}_\gamma}{\bar{E}_\nu} \tag{1}$$

(here $\bar{E}_F = \overline{(M - M_L - M_H)}$ is the mean fission energy; M is the mass of the fissioning nucleus; $\bar{E}_k$, $\bar{E}_\gamma$, and $\bar{E}_\nu$ are respectively the average kinetic energies of fragments, prompt γ rays, and neutron emission), it was assumed that the mass of the heavy fragment, M_H, was independent of the Z and A of the fissioning nucleus and was 140 and that the average kinetic energy of the fragments depended linearly on Z^2/A:

$$\bar{E}_k = c_1 Z^2/A^{1/3} - c_2, \tag{2}$$

with the constants c_1 and c_2 being chosen so that the best agreement of calculation with experiment was obtained for $\bar{\nu}$.

It was later pointed out [6] that neither of these assumptions are satisfied with sufficient accuracy in the Z and A range of the fissioning nuclei under consideration; in the range Z ≥ 95 and A ≥ 245, the quantity M_H increases (for heavy isotopes, M_H reaches 143-145) and, at the same time, $\bar{E}_k$ deviates from the relation (2) in the direction of lower values [17, 19]. Since $\bar{E}_F$ in the region of most probable fragment masses is a decreasing function of M_H/M_L, the use of an underestimate for M_H in Eq. (1) in [18] led to an increase in $\bar{E}_F$ which was compensated by an approximately equal overestimate of the quantity $\bar{E}_k$. This circumstance explains the insensitivity of the computed results in [18] to the inaccuracies of the assumptions used there and the consequent agreement with experiment.

TABLE 3. Comparison of $\bar{\nu}$ Values for Various Methods of Fission and for Various Nuclei

Compound nucleus	Spontaneous fission, $\bar{\nu}_{sp}$	Induced fission, $\bar{\nu}(E)$	$\bar{\nu}(E)-\bar{\nu}_{sp}$	E/E_ν
U^{236}	1,90±0,05 [17]	2,41±0,01 [8]	0,51±0,05	0,96
U^{238}	1,99±0,07 [8]	2,77±0,13 [23]	0,78±0,15	1,05
Pu^{240}	2,15±0,02 [17]	2,87±0,01 [8]	0,72±0,02	0,96
Pu^{242}	2,14±0,01 [17]	2,92±0,01 [8]	0,78±0,02	0,93
Cm^{244}	2,70±0,02 (this work)	3,43±0,05 [15]	0,73±0,06	1,00
Cm^{246}	2,93±0,03 (this work)	3,83±0,03 [15]	0,90±0,05	0,94
Cf^{250}	3,53±0,09 [1]	4,06±0,04 [19]	0,53±0,10	0,96

Note. In all cases except U^{238}, the given $\bar{\nu}(E)$ for nucleus X^A refers to thermal neutron fission of the target nucleus X^{A-1}, i. e., $E = B_n$; for U^{238}, $\bar{\nu}(E)$ was determined in the reaction $U^{238}(\gamma, f)$ at E = 7,0 MeV [23]. In the measurements, the value $\bar{E}_\nu^{-1}$ = 0,17 MeV^{-1} [20] was used, which corresponds to the theoretical evaluation of $d\bar{\nu}/d\bar{E}_k$ for the most probable method of fission; binding energy values B_n were taken from [24].

The divergence between calculation and experiment in the region of "light" nuclei is explained by the fact that in the analysis (more precisely, in the selection of the constants c_1 and c_2 in Eq. (2)), extrapolated values rather than direct values, which did not exist at the time (there is still no data for thorium), were considered as source data for the $\bar{\nu}$ of uranium and thorium. In the extrapolation of data for induced fission to spontaneous fission, they used the relation

$$\bar{\nu}(0)=\bar{\nu}(E)-\frac{E}{\bar{E}_\nu}, \tag{3}$$

where it was assumed $\bar{E}_F$, $\bar{E}_k$, and $\bar{E}_\gamma$ remain constant when the excitation energy changes. There are a number of considerations and examples [20-22] pointing to the nonfulfilment of this condition. It is apparently for this reason that the results of direct measurements on U^{238} and U^{236} (1.9-2.0 [8]) were markedly higher than those from extrapolation (1.5-1.7 [18]). Table 3 presents several examples which make it possible to compare $\bar{\nu}$ for spontaneous fission with $\bar{\nu}$(E) for induced fission and with values of $\bar{\nu}$ extrapolated in accordance with Eq. (3).

Table 3 indicates the observed difference, $\Delta\bar{\nu}_{obs} = \bar{\nu}(E)-\bar{\nu}_{sp}$, varies markedly from nucleus to nucleus and these values are less than $\Delta\bar{\nu} = E/E_\nu \approx 0.9$-$1.0$ in most cases. A similar effect, $(d\bar{\nu}/dE)_{obs} < E_\nu^{-1}$, appears in several of the nuclei (U^{236}, U^{239}, and Pu^{240}) in the region $E > B_n$, i.e., for fast neutron fission [20] and probably results from a systematic decrease of $\bar{E}_F$ with an increase in excitation energy as was proposed in [20]. The variation in $\Delta\nu_{obs}$ in two cases studied (Pu^{240} and U^{238}) was explained by different changes in $\bar{E}_k$ in the transition from induced fission to spontaneous fission [21]. From what has been said, one can conclude that it is reasonable to use an average value $\langle\Delta\bar{\nu}\rangle \approx 0.75$ for estimating $\bar{\nu}_{sp}$ from data for induced fission and for extrapolated values of $\bar{\nu}$ with the understanding the error may amount to 0.2. On the basis of this value of $\langle\Delta\bar{\nu}\rangle$, the estimated derivative $(\partial\bar{\nu}/\partial E)_{obs} = \langle\Delta\bar{\nu}\rangle/E \approx 0.12$ MeV^{-1}.

In conclusion, we consider the relationship $\bar{\nu}$(A, Z). Published attempts to obtain some kind of simple interpolation formula for this relationship over a sufficiently broad range of fissile nuclei [17, 22, 15] can hardly be called successful [17]. The deviation of $\bar{\nu}$ reaches 0.2-0.3 mainly in the region of heavy nuclei. Obviously, there are reasons which explain the difficulties in such a description. One has been pointed out [6, 19]. In the region $Z \geq 95$ and $A \geq 245$, an abrupt change in the nature of the $\bar{\nu}$(A, Z) dependence occurs. At A and Z values less than 245 and 95 respectively, $\bar{\nu}$ is very slightly dependent on A ($d\bar{\nu}/dA < 0.04$) while $d\bar{\nu}/dZ \approx 0.2$; on the other hand, for large A and Z there is the following dependence of $\bar{\nu}$ on A and Z: $d\bar{\nu}/dA \approx 0.2$, $d\bar{\nu}/dZ \approx 0.05$-$0.07$ (see Fig. 1). This phenomenon was related to the influence of shell effects [22] on the magnitude of the realizable energy $\bar{E}_F$ and its distribution between excitation energy and $\bar{E}_k$ [6, 19]. A second reason influencing the behavior of $\bar{\nu}$ for induced fission and characterized by large scale individual deviations from a smooth dependence in comparison with $\bar{\nu}_{sp}$ was noted above. It consists of marked variations in $\Delta\bar{\nu}_{obs} \times E_\nu/B_n$ resulting from changes in $\bar{E}_F$ and $\bar{E}_k$ with increase in excitation [20, 21].

The authors are grateful to K. E. Volodin, B. Nurpeisov, and Yu. M. Turchin for assistance.

LITERATURE CITED

1. C. Orth, Nucl. Sci. and Engng., 43, 54 (1971).
2. M. Thompson, Phys. Rev., C2, 763 (1970).
3. W. Crane, G. Higgins, and H. Bowman, Phys. Rev., 101, 1804 (1956).
4. B. Diven et al., Phys. Rev., 101, 1012 (1956).
5. D. Hicks, Y. Ise, Jr., and R. Pyle, Phys. Rev., 101, 1016 (1956).
6. V. I. Pol'shov et al., At. Énerg., 17, 28 (1964).
7. L. I. Prokhorova et al., At. Énerg., 30, 250 (1971).
8. V. Konshin and F. Manero, Report INDC (NDS) 19/N (1970).
9. V. G. Nesterov et al., Nuclear Data for Reactors, Vol. II, IAEA, Vienna (1970), p. 167.
10. C. Hanna et al., Atomic Energy Review, VII, 4 (1969).
11. D. Hicks, Y. Ise, and R. Pyle, Phys. Rev., 98, 1521 (1955).
12. W. Crane, C. Higgins, and H. Bowman, Phys. Rev., 101, 1804 (1956).
13. B. Diven et al., Phys. Rev. 101, 1012 (1956).
14. D. Hicks, Y. Ise, Jr., and R. Pyle, Phys. Rev., 101, 1016 (1956).
15. A. Yaffey and Y. Lerner, Nucl. Phys., A145, 1 (1970).
16. Yu. S. Zamyatnin et al., Nuclear Data for Reactors, Vol. II, IAEA, Vienna (1970), p. 183.
17. V. A. Kon'shin, Nuclear Physics Constants for Transplutonium Elements, IAEA, Vienna (1971).
18. I. Bondarenko et al., Proc. of the Second Intern. Conf. on the Peaceful Uses of Atomic Energy, Vol. 15, United Nations, Geneva (1958), p. 353.
19. K. E. Volodin, V. G. Nesterov, B. Nurpeisov, et al., Yad. Fiz., 15, 29 (1972).
20. L. I. Prokhorova and G. N. Smirenkin, Yad. Fiz., 13, 1170 (1970).
21. V. N. Okolovich and G. N. Smirenkin, Zh. Éksp. Teor. Fiz., 43, 1861 (1962).
22. L. D. Gordeeva and G. N. Smirenkin, At. Énerg., 14, 530 (1963).
23. H. Conde and M. Holmberg, Physics and Chemistry of Fission, Vol. II, IAEA, Vienna (1965), p. 57.
24. I. V. Gordeev, D. A. Kardashev, and A. V. Malyshev, Nuclear Physics Constants [in Russian], Atomizdat, Moscow (1963).

AVERAGING CROSS SECTIONS AND RECIPROCAL VELOCITIES TO CALCULATE THE EIGENNUMBERS OF THE NONSTEADY-STATE BOLTZMANN EQUATION

B. D. Abramov

UDC 621.039.51.134

In pulsed experiments it is assumed that the behavior of the neutron flux for some time after the beginning of the pulse can be described by

$$\psi(\mathbf{r}, \mathbf{\Omega}, v, t) \sim a_0\psi_0(\mathbf{r}, \mathbf{\Omega}, v)\, e^{\alpha_0 t} + a_1\psi_1(\mathbf{r}, \mathbf{\Omega}, v)\, e^{\alpha_1 t} + \ldots, \tag{1}$$

where successful measurement of α_0 and ψ_0 depends on satisfaction of the relations

$$|\alpha_0| \ll |\alpha_k|; \quad a_0 \gg |a_k|; \quad k=1, 2, \ldots. \tag{2}$$

Here $\psi_k(\mathbf{r}, \Omega, v)$ is the eigenfunction of the nonsteady-state neutron-transport equation corresponding to the eigennumber $\alpha = \alpha_k$, and a_k are some numbers.

It therefore becomes necessary to calculate several eigenfunctions and eigennumbers of the nonsteady-state Boltzmann equation. The most effective way to solve this equation is to use the multigroup method, in which the energy dependence of the cross section is approximated by piecewise-constant functions. This approximation can be used in various methods, depending on which characteristics must be calculated most accurately. In particular, existing systems of constants are averaged over the neutron spectrum characteristic of a critical (steady-state) reactor, so calculations incorporating these constants generally lead to the correct values of the parameters characterizing a critical reactor. However, the use of these constants to calculate the parameters for a nonsteady-state reactor (e.g., to calculate the eigennumbers α_k) can result in large errors because of the difference between the spectra of critical and noncritical reactors.

We are concerned here with which constants should be used for a correct calculation of the various eigennumbers α_k and with the extent to which these constants differ from the usual ones. For this purpose we use the method of [1], used to average the cross sections for a multigroup calculation of the positive solution of the critical problem, to average the cross sections for a multigroup calculation of the various (simple) eigennumbers α_k and eigenfunctions ψ_k of the nonsteady-state Boltzmann equation with an account of delayed neutrons.

The appropriate equations are written out for averaging the cross sections and for averaging a new constant, the group-average reciprocal velocity 1/v, characteristic of only the nonsteady-state theory. Because of the ambiguity in the definition of the multigroup nonsteady-state conjugate equation, two versions of these equations are possible. Equations are derived for an approximate calculation of 1/v and for estimating the effect of the error in the 1/v calculation on the value of the eigennumber α_k. Analysis of the equations found shows that the constants required to calculate the various eigennumbers α_k may differ greatly (e.g., the constants required to calculate the complex eigennumbers α_k must be complex, etc.). It is concluded on this basis that the eigennumbers α_k calculated on the basis of the ordinary constants may under certain conditions have little in common with the eigennumbers α_k of the kinetic equation.

No successive-approximation algorithms are necessary for a practical averaging of cross sections on the basis of these equations. The construction of such algorithms to calculate the higher-order

Translated from Atomnaya Énergiya, Vol. 33, No. 3, p. 771, September, 1972. Original article submitted May 11, 1971; revision submitted December 9, 1971.

eigennumbers may be extremely difficult (e.g., in the case of multiple or complex roots), but α_0 and the corresponding positive solution ψ_0 can be calculated on the basis of the algorithm given in [1] for the steady-state case.

LITERATURE CITED

1. G. I. Marchuk, Methods for Designing Nuclear Reactors [in Russian], Gosatomizdat, Moscow (1961).

PERTURBATION OF γ-RADIATION FIELD WHEN OBJECTS IN FILLER ARE EXAMINED

F. M. Zav'yalkin

UDC 539.166.2

The dependence of the characteristics of the field of scattered radiation, when an object is lodged in the filler, on the parameters of both the object and the filler at different radiation energies was investigated.

Results of Monte Carlo calculations [1, 2] of the differential flux $N(\omega, E, H)$ of the photons, and of the intensity $\Phi(\omega, E, H)$ of the scattered radiation from a plane unidirectional source emitting photons of energy $E_0 = 1.25$ MeV beyond an iron barrier of thickness up to $\mu H = 8$ and filler [melt of a tin–lead mixture (30%)], and also of aluminum and filler (91% CH_2I_2 solution in C_6H_6), for a source such that $E_0 = 0.66$ MeV, were used in the analysis (see Fig. 1).

A formula for the relative variation $\delta_\Phi(H)$ of the intensity or for the variation $\delta_N(H)$ of the radiation flux beyond the barrier when the object was removed from the filler was derived:

$$\delta_\Phi(H)=1-\frac{B^*_\Phi(H)}{B_\Phi(H)}; \quad \delta_N(N)=1-\frac{B^*_N(H)}{B_N(H)},$$

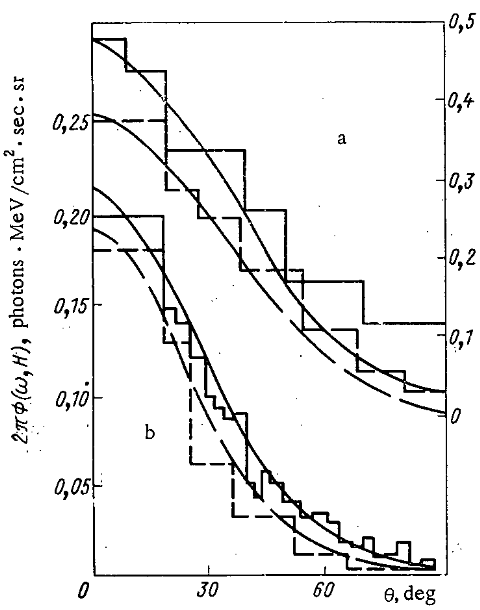

Fig. 1. Angular distribution of scattered radiation intensity beyond barriers. a) ———) aluminum barrier 5 cm thick; ----) filler barrier; b) ———) iron barrier 10 cm thick; ----) filler barrier. Curves based on approximation formula (1). Histograms plotted on basis of Monte Carlo calculations.

Translated from Atomnaya Énergiya, Vol. 33, No. 3, p. 772, September, 1972.

here $B_\Phi(H)$ and $B_N(H)$ are the buildup factors for a barrier made of the material comprising the object; $B^*_\Phi(H)$ and $B^*_N(H)$ are their counterparts for a heterogeneous barrier (object–filter).

Results of calculations of $\delta_\Phi(H)$ and $\delta_N(H)$ with the object completely replaced by filler are tabulated in the article. As the thickness is increased, the values of $\delta_\Phi(H)$ and $\delta_N(H)$ tend asymptotically to a saturation level, attaining 30-45% at $\mu H \approx 4$. The angular distribution is approximated by a Gaussian function of the form

$$\Phi(\omega, H) = \mathrm{const}\, e^{-(\theta/\theta_0)^2}. \tag{1}$$

These values of the characteristic angles θ_0 for iron and aluminum are greater than for the corresponding fillers.

It is shown that the relative difference between the distributions of the scattered radiation beyond the object material and the filler increases with decreasing energy E and with increasing angle θ. In the limit as $\theta \to 0$ and as $E \to E_0$, i.e., in the case of collimated radiation, the intensity ratio or the flux ratio of the scattered radiation becomes proportional to the density ratio of the electrons of the materials used. Note also that $\delta_\Phi(H) < \delta_N(H)$ at different values.

In conclusion, the author thanks A. M. Kol'chuzhkin for valuable suggestions, and S. I. Durinov for assistance in the calculations.

LITERATURE CITED

1. U. Fano, Gamma Radiation Transport [Russian translation], Gosatomizdat, Moscow (1963).
2. A. Kol'chuzhkin et al., in: Large-Dose Dosimetry [in Russian], Generalova (editor), FAM, Tashkent (1966), p. 56.

INSTRUMENTAL ACTIVATION DETERMINATION OF TRACE AMOUNTS OF COPPER

I. A. Miranskii and R. Sh. Ramazanov

UDC 543.53

Copper determinations in rocks and ores on the basis of the annihilation radiation of the isotope Cu^{64} involves difficulties due to the presence of Na^{24}; the interaction between the hard γ-radiation of Na^{24} and the surrounding host materials can also lead to annihilation radiation interfering with the determination. Single-crystal spectrometry techniques are ruled out as feasible solutions of the problem of noise associated with the sodium, so that analyses of copper in rocks and ores always depend on the use of instrumental activation analysis employing coincidence spectrometers which exhibit some degree of selectivity depending on the spectrometer arrangement.

Investigations using fast-coincidence, fast–slow coincidence, and total-coincidence spectrometers have shown that the highest sensitivity for copper determinations against a background of masking radiations is that offered by the total-coincidence spectrometer (a spectrometer in which signals from two detectors are added), because of the different nature of pattern of formation of annihilation radiation emitted by the isotopes Cu^{64} and Na^{24}. When a total-coincidence spectrometer is employed, it becomes possible to make successful copper determinations even when the sodium content is three whole orders of magnitude greater than the copper content. The optimum weighed specimen and optimum spectrometer loading must be selected here, and a special method of standardization is needed, since there is a relationship observed between the count rate of coincidences in γ-radiation emitted by the isotope Cu^{64} and the spectrometer loading.

Translated from Atomnaya Énergiya, Vol. 33, No. 3, pp. 772-773, September, 1972. Original article submitted November 11, 1971.

Investigations have shown that the optimum weighed portion of rock for an analysis must weigh 50 mg, the weight of the standard must be 10^{-5} g, the irradiation time 3-4 min in a thermal column with a flux of $1.2 \cdot 10^{12}$ neutrons/cm^2 · sec, exposure time 12 h, measurement time 15 min, and the spectrometer loading must not be in excess of $3 \cdot 10^3$ to $4 \cdot 10^3$ pulses/sec.

By observing these constraints, the authors were able to make copper determinations in rock and ore samples with a sensitivity of 10^{-3}% with satisfactory reliability, and with sensitivity of 10^{-4}% in the case of specimens reported in the literature. The data were monitored by radiochemical methods. Excellent agreement was found in the results.

TRACK-DELINEATING AUTORADIOGRAPHY IN METALLOGRAPHIC INSPECTION OF TARGETS OF THE TRANSURANIUM ELEMENTS

V. G. Polyukhov, V. N. Syuzev,
Yu. V. Chushkin, and M. M. Antipina

UDC 621.039.548

The method of track-delineating autoradiography on photosensitive glass has been used to study the distribution of active grains with transuranium elements over the cross section of polished sections made from two dispersion type targets irradiated in the central channel of an SM-2 reactor. In the specimens investigated, 96-99% of all of the events of spontaneous fission of heavy nuclides were accounted for by Cf^{252}, amounting to $7 \cdot 10^4$ to $4 \cdot 10^5$ fissions/min per mg of the starting plutonium – aluminum composition.

Autoradiographs of two types were used: one with an aluminum filter (thickness ~ 3 mg/cm^2) between the photosensitive glass and the surface of the specimen, the other without a filter. In the first case,

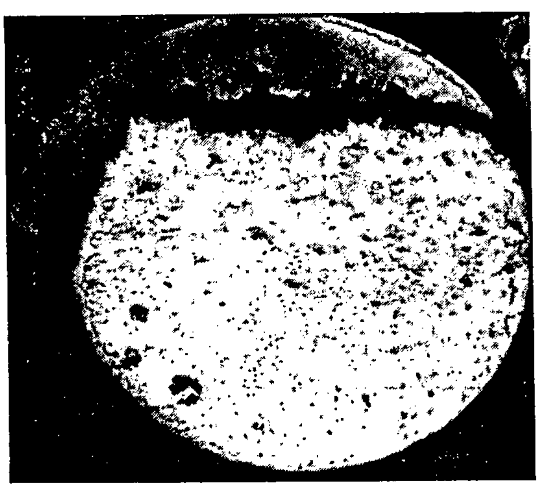

a

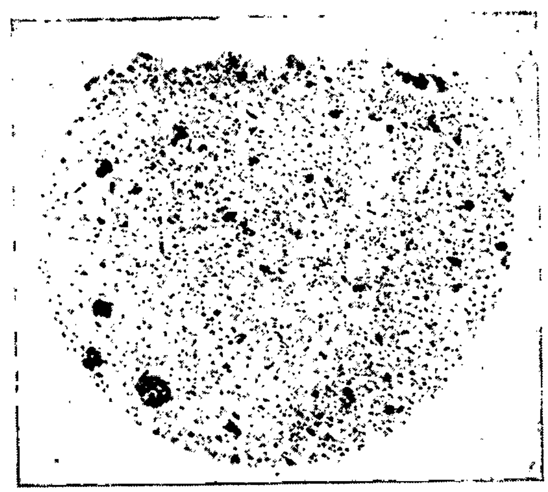

b

Fig. 1. Macrostructure of transverse section through target made with aid of a photograph (a) and an autoradiograph (b) (× 5).

Translated from Atomnaya Énergiya, Vol. 33, No. 3, pp. 773-774, September, 1972. Original article submitted January 3, 1972; revision submitted March 28, 1972.

products of spontaneous fission ejected in practice solely from the surface of the specimen become recorded in the authoradiographs, while in the second case products originate in layers located within the specimen. The exposure time was from 15 to 60 min.

Objective data on the distribution pattern of grains containing Cf^{252} were obtained through photometric scans of the autoradiographs taken on an MF-4 microphotometer. The integral and differential distribution curves of the grains were studied. The resulting autoradiographs made it possible to determine the rate of erosion of the envelope, and of the assumed migration of active material into the envelope. An MBI-3 microscope was used to study the microstructure of individual grains on the autoradiographs.

Comparison of the results obtained and data from investigations using the method of analysis of microphotographs of the same polished sections disclosed that the use of track-delineating autoradiography on glass considerably broadens the options of metallographic investigations of targets irradiated in a reactor, with minimum effort and cost in producing the targets.

YIELDS OF Ge^{68} IN IRRADIATION OF GALLIUM BY PROTONS AND DEUTERONS, AND IRRADIATION OF ZINC BY α-PARTICLES

P. P. Dmitriev, N. N. Krasnov, G. A. Molin, and M. V. Panarin

UDC 539.172.13 + 539.172.16

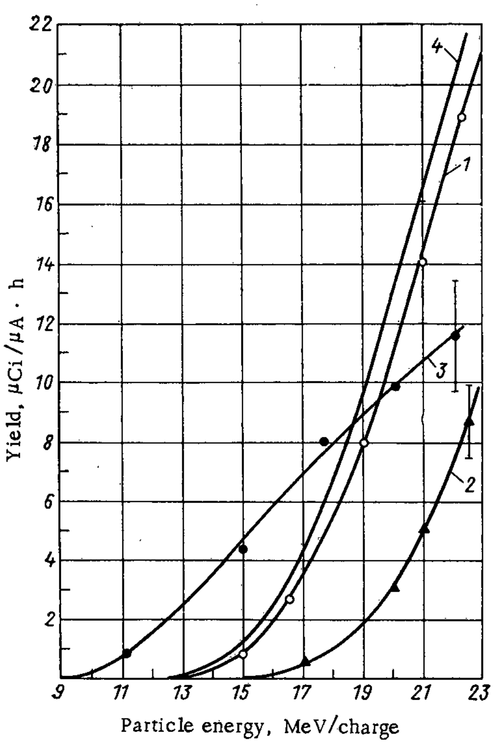

Fig. 1. Yield of Ge^{68} as a function of energy of bombarding particles in irradiation of thick targets: 1) Ga + p; 2) Ga + d (increased fivefold); 3) Zn + α (increased fivefold); 4) Ga + p, data borrowed from [2] (integration of excitation functions).

Translated from Atomnaya Énergiya, Vol. 33, No. 3, p. 774, September, 1972. Original article submitted February 7, 1972; revision submitted March 24, 1972.

Dependences of yields of Ge^{68} on the energy of bombarding particles in the irradiation of thick gallium and zinc targets by charged particles from the deflected beam emitted by the FÉI [Physics and Engineering Institute] cyclotron were measured. The activity of the Ge^{68} was measured on the basis of annihilation radiation emitted by its daughter Ga^{68} (yield 1.76 photon/decay event). The procedure followed in measuring the yields is similar to that described in [1].

Yields of Ge^{68} are plotted on the curves in Fig. 1.

LITERATURE CITED

1. N. N. Krasnov and P. P. Dmitriev, Atomnaya Énergiya, 20, 57 (1966); 20, 154 (1966).
2. N. Porile et al., Nucl. Phys., 40, 500 (1963).

RESOLVING POWER OF ELECTRON MICROSCOPE AUTORADIOGRAPHY FOR α-EMITTERS

V. N. Chernikov, A. P. Zakharov, and V. M. Luk'yanovich

UDC 620.18 (083.4)

A combination of high autoradiographic resolution and sensitivity and the possibility of studying the surface of the specimen simultaneously with the aid of the electron microscope is the typical feature of the method of electron-microscopic autoradiography [1, 2].

To date, theoretical and experimental research in this area has been restricted to dealing with the effective use of preponderantly soft-emitters. This article uses calculations to show that the procedure of electron microscopic autoradiography is superior in its resolving power to the method of analysis based on recording tracks of α-particles in thick emulsion detectors and in other layer type detectors, when the use of α-active isotopes is involved.

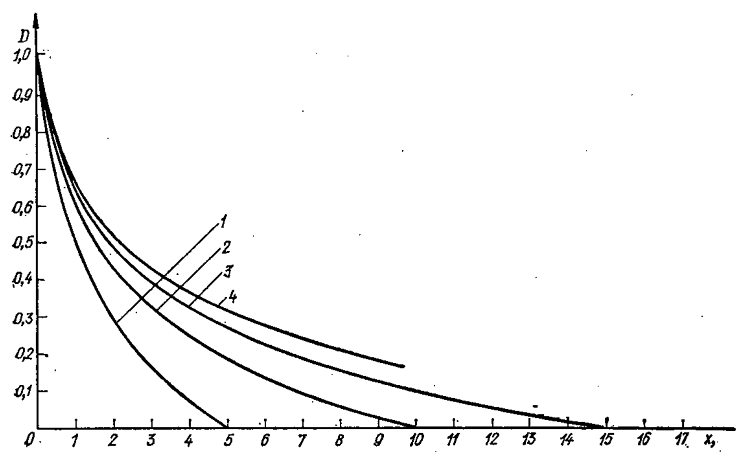

Fig. 1. Curves of D(x) for a monolayer of "M" emulsion in the case of a plane α-active source. Curves 1-4 correspond to α-partice free path lengths of 5, 10, 15, and 20 μ.

Translated from Atomnaya Énergiya, Vol. 33, No. 3, pp. 775-776, September, 1972. Original article submitted February 14, 1972.

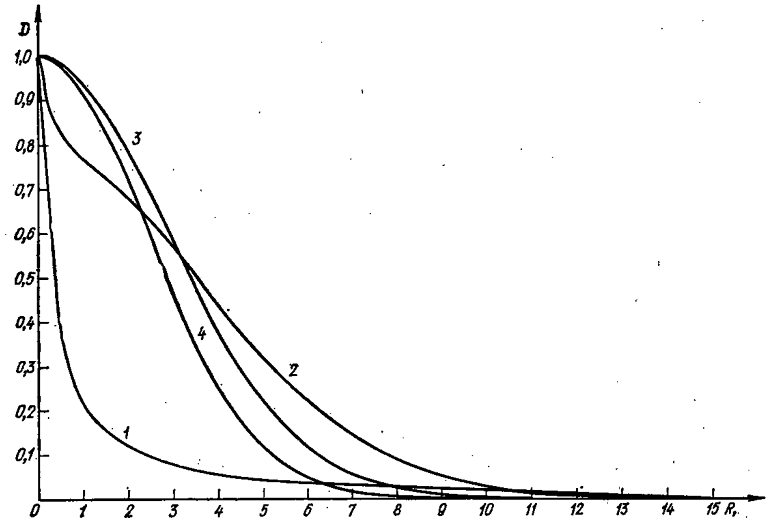

Fig. 2. Curves D(x) plotted for a monolayer of "M" emulsion in the case of a linear α-active source. Curves 1-4 correspond to different distribution patterns of isotope over length of source, for R = 15μ.

Digital computers were employed to analyze the functional relations between the photographic density D (density of distribution of crystals of reduced silver) in ultrathin layers of a fine-grained nuclear emulsion placed above the α-active source of interest, and the distance x to that source. The sources in question formed a semi-infinite straight line and a semi-infinite plane oriented in the test specimen at right angles to the surface of the specimen (Fig. 1, Fig. 2), and a point source and spherical sources of different diameters set at different depths in the specimen. In all cases, the minimum distances d at which two photographic densities could still be resolved were calculated on the basis of the criterion used. The effect of such factors as the free path length of the α-particles, the thickness of the emulsion layer and the thickness of the carbon layer, the geometry of the source proper, and the pattern in which the source was arranged within the specimen, and also the nonuniformity of the distribution of radioactive isotope throughout the depth of the source (in the case of the semi-infinite straight line and semi-infinite plane), on the shape of the D = D(x) curves and accordingly on the resolving power, was calculated.

The numerical results of these calculations make it possible to arrive at a priori estimates of the effectiveness of applying that method, or several other nonphotographic methods, to the task without having to resort to additional experimentation, and also make it possible to interpret the resulting data correctly.

NEW DEVICE FOR IN-PILE MEASUREMENTS OF INTERNAL FRICTION AND SHEAR MODULUS OF SPECIMEN

V. S. Karasev, É. U. Grinik, V. S. Landsman, and A. I. Efimov

UDC 620.178.311.62

Investigation of internal friction and shear modulus of materials undergoing irradiation in a reactor makes it possible to secure information on the kinetics of the buildup of radiation defects and on annealing out of radiation defects, important since the radiation defects determine the physicomechanical properties of reactor design materials [1, 2].

The arrangement we developed for such measurements incorporates an inverted torsion pendulum driven into forced oscillations, and a remote-controlled electronic recording system. When the diameters of the test specimens are in the 0.5 to 2.5 mm range (lengths 50 to 100 mm), the frequency of the oscillations is 20 Hz, and the amplitude of the relative deformation is specified with a range from 10^{-4} to 10^{-7}. The error in internal-friction determinations is not greater than 2%, the error in shear-modulus determinations is not greater than 1.2%. The procedure followed in measuring internal friction, and the estimates of accuracy of the results, do not differ in principle from the description appearing in [3]. The shear

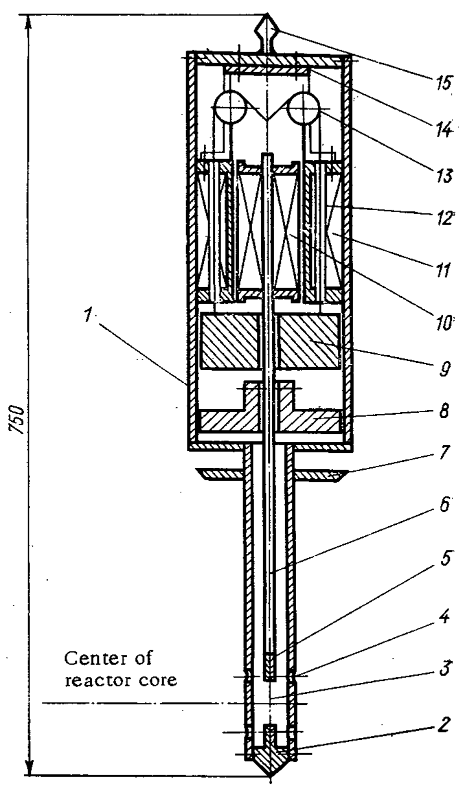

Fig. 1. Design of capsule holding specimens for in-pile measurements of internal friction and shear modulus.

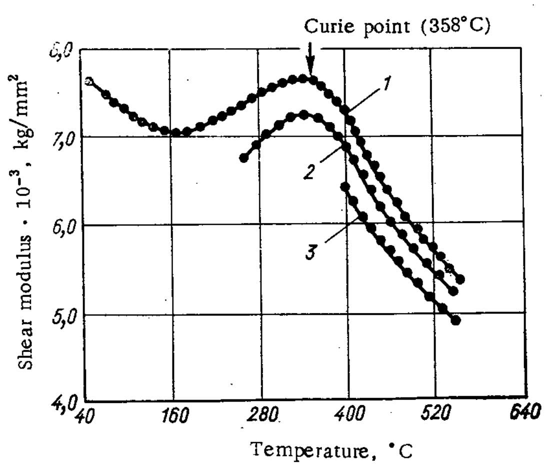

Fig. 2. Effect of reactor radiation intensity on temperature variation of shear modulus of nickel: 1) prior to reactor startup; 2) during irradiation process with reactor power at 5 MW; 3) the same, with reactor power at 10 MW.

Translated from Atomnaya Énergiya, Vol. 33, No. 3, pp. 777-778, September, 1972. Original article submitted December 27, 1971.

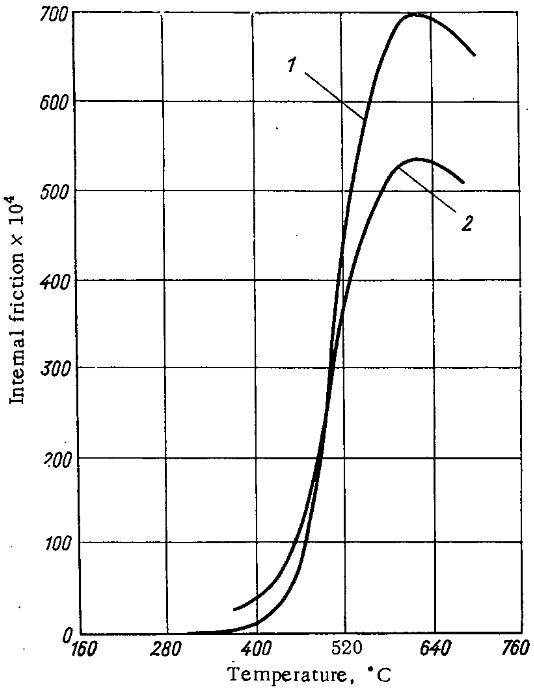

Fig. 3. Effect of reactor radiation intensity on temperature variation of internal friction of iron: 1) prior to reactor startup; 2) during irradiation, with reactor power at 10 MW.

TABLE 1. Temperature Distribution in the Test Specimen (1) and in the Blank Specimen (2) during In-Pile Irradiation, °C

Distance from center of specimen, mm	Specimen	Reactor power output, MW					
		3,0	3,5	4,0	4,0	10,0	10,0
+30	1	254	276	307	565	520	872
	2	252	274	307	569	516	870
0	1	250	273	303	563	515	867
	2	250	272	303	567	515	866
—30	1	258	280	310	560	517	864
	2	256	279	309	560	514	862

modulus is determined from the frequency of the oscillations of the test specimen, as measured by a PP-15 scaler with 0.1% error.

This arrangement differs from the one described in [3] principally in the design of the measuring instrument, which is encapsulated. The design of the instrument capsule is seen in Fig. 1. The capsule contains a housing 1 the bottom of which provides a mount for the fixed clamp 2. The moving clamp 5 is mounted on the rod 6 of the inverted torsion pendulum. Clamps 2 and 5 serve to secure the test specimen 3. The holes 4 in the body of the capsule are needed for mounting the specimen in place. The spacing ring 7, welded to the body of the capsule, allows the capsule to be mounted in a well of the reactor materials testing channel. The rod 6 of the torsion pendulum provides mounts for the inertia flywheel 8 and moving coil 11 of the contactless sensor. The balancing device contains two units 13, a specially designed mounting bracket 14 and counterweight 9, supports for which pass through the tubes 10 in the fixed coil 12. The counterweight 9 counterbalances the weight of the moving portion of the inverted torsion pendulum. The tapered rod 15 is useful for remote loading and unloading of the capsule in and out of the reactor materials testing channel. The capsule is ≈ 750 mm long, which makes it possible to discharge the capsule in the usual manner via the reactor transfer hole.

The capsule described above was inserted in the vertical channel of a water-cooled, water-moderated (VVR-M) reactor equipped with a temperature control system [4]. The temperature distribution over the length of the test specimen is determined during the measurements from readings of Chromel – Alumel thermocouples welded to a blank specimen at three points along its length; the blank specimen is mounted in the bottom (fixed) holder of the capsule parallel to the test specimen and spaced 2 mm apart from the latter. Results of measurements of the temperature distribution in one of the test specimens and in the blank specimen, at different reactor power output levels, are presented in Table 1.

Clearly, the irradiation temperature of the specimen is determined with sufficient accuracy from the readings of the thermocouples mounted on the blank specimen. The maximum temperature difference at the corresponding points is not greater than 4°C, and not greater than 10°C over the height of the specimens.

The reliability of the arrangement was confirmed by staging 700-h tests of the capsule inserted in the materials testing channel of the VVR-M reactor built at the Institute of Nuclear Research of the Academy of Sciences of the Ukrainian SSR, with the specimen exposed to irradiation at intensity ≈ 10^{14} neutrons /$cm^2 \cdot$sec ($E \geq 0.1$ MeV). The temperature of the specimen fluctuated within the 350-750°C range.

Results of the investigation of the effect of the neutron irradiation intensity on the temperature variations of the shear modulus of electron-beam-remelted nickel of 99.99% purity, and of the internal friction of electron-beam-remelted iron of 99.99% purity, are plotted in Figs. 2 and 3.

LITERATURE CITED

1. V. S. Karasev, Dokl. Akad. Nauk SSSR, 171, 84 (1966).
2. S. Harkness et al., Nucl. Appl. and Technol., 9, 24 (1970).
3. R. Butera and R. Craig, Pribory dlya Nauchnykh Issledovanii, No. 4, 11 (1966).
4. V. S. Karasev et al., At. Énerg., 22, 492 (1967).

Declassified and Approved For Release 2013/02/27 : CIA-RDP10-02196R000300110003-7

MEASUREMENT OF THE SPECTRAL AND ANGULAR DISTRIBUTIONS OF BACK-SCATTERED ELECTRONS

P. L. Gruzin, Yu. V. Petrikin, and A. M. Rodin

UDC 539.124.17

We present the results of measuring the spectral and angular distributions of back-scattered electrons. The electrons had primary energies of 0.15 to 1.5 MeV and were incident normally on semi-infinite targets. The experimental apparatus consists of a monochromator and an electron spectrometer. The monochromator is basically a double-focusing magnetic β-ray spectrometer. The vacuum chamber is shut off from both sides by flanges, on one of which is mounted a BIS-10 type $Sr^{90} + Y^{90}$ β-particle source having an activity of 500 mCi. A cylindrical target 15 mm in diameter and 5 mm thick is placed at the other end of the chamber at the focus of the β-ray spectrometer. For a source diameter of 10 mm the β-ray spectrometer has a momentum resolution of 3.5% and a transmission of 2.5%.

The electron spectrometer is built around a type DDC-8/2A Si (Li) detector cooled with liquid nitrogen to −70°C through a vacuum heat pipe. The detector pulses pass through an amplifying circuit to an AI-100 pulse analyzer and simultaneously to a scaling circuit. The resolution of the Si (Li) spectrometer for the 624 keV K line of Ba^{137m} is 12 keV. The position of the maximum of the energy distribution of the electrons

TABLE 1. Values of η_N, n, and k

E_0, keV	$\eta_N(\theta, E_0, Z)$ θ=15°	θ=30°	θ=45°	θ=65°	θ=80°	n	k
Aluminum							
150	0,0473	0,0405	0,0305	0,0152	—	1,5	0,138
200	0,0475	0,0405	0,0304	0,0152	—	1,6	0,137
300	0,0471	0,0405	0,0304	0,0152	—	1,7	0,137
400	0,0478	0,0405	0,0298	0,0150	—	1,8	0,134
600	0,0462	0,0393	0,0288	0,0149	—	1,9	0,132
800	0,0434	0,0364	0,0266	0,0141	—	2,0	0,131
1000	0,0403	0,0339	0,0252	0,0139	—	2,0	0,123
1300	0,0357	0,0297	0,0217	0,0135	—	2,0	0,118
Copper							
150	0,0951	0,0796	0,0574	0,0270	0,0128	1,8	0,258
200	0,0998	0,0830	0,0587	0,0270	0,0130	1,9	0,264
300	0,1030	0,0836	0,0595	0,0270	0,0130	2,0	0,270
400	0,102	0,0848	0,0587	0,0264	0,0122	2,0	0,265
600	0,0987	0,0815	0,0565	0,0257	0,0115	2,0	0,254
800	0,0931	0,0770	0,0540	0,0250	0,0102	2,0	0,240
1000	0,0901	0,0709	0,0513	0,0236	0,0095	2,0	0,228
1300	0,0828	0,0682	0,0480	0,0216	0,0088	2,0	0,212
Tin							
150	0,144	0,118	0,0831	0,0352	0,0150	1,9	0,356
200	0,150	0,122	0,0845	0,0362	0,0156	2,0	0,370
300	0,156	0,126	0,0868	0,0374	0,0156	2,1	0,385
400	0,157	0,125	0,0865	0,0362	0,0156	2,2	0,376
600	0,148	0,119	0,0828	0,0352	0,0156	2,2	0,362
800	0,142	0,114	0,0780	0,0345	0,0154	2,2	0,341
1000	0,135	0,110	0,0747	0,0332	0,0144	2,2	0,339
1300	0,128	0,104	0,0704	0,0312	0,0135	2,2	0,315
Lead							
150	0,193	0,154	0,106	0,460	0,0183	2,2	0,475
200	0,204	0,162	0,110	0,463	0,0190	2,3	0,496
300	0,212	0,169	0,113	0,467	0,0197	2,4	0,510
400	0,211	0,168	0,112	0,467	0,0197	3,4	0,505
600	0,205	0,163	0,109	0,453	0,0195	2,4	0,493
800	0,200	0,157	0,106	0,448	0,0190	2,4	0,478
1000	0,193	0,153	0,102	0,429	0,0190	2,4	0,464
1300	0,181	0,143	0,094	0,406	0,0172	2,4	0,432
Uranium							
150	0,206	0,166	0,113	0,0460	0,0202	2,2	0,500
200	0,218	0,174	0,115	0,0480	0,0209	2,3	0,518
300	0,222	0,177	0,116	0,0480	0,0209	2,4	0,526
400	0,222	0,176	0,115	0,0480	0,0202	2,4	0,523
600	0,215	0,169	0,111	0,0470	0,0200	2,4	0,505
800	0,207	0,162	0,106	0,0450	0,0180	2,4	0,484
1000	0,200	0,157	0,102	0,0430	0,0189	2,4	0,468
1300	0,188	0,148	0,094	0,0420	0,0176	2,4	0,448

Translated from Atomnaya Énergiya, Vol. 33, No. 3, pp. 779-781, September, 1972. Original article submitted December 30, 1971.

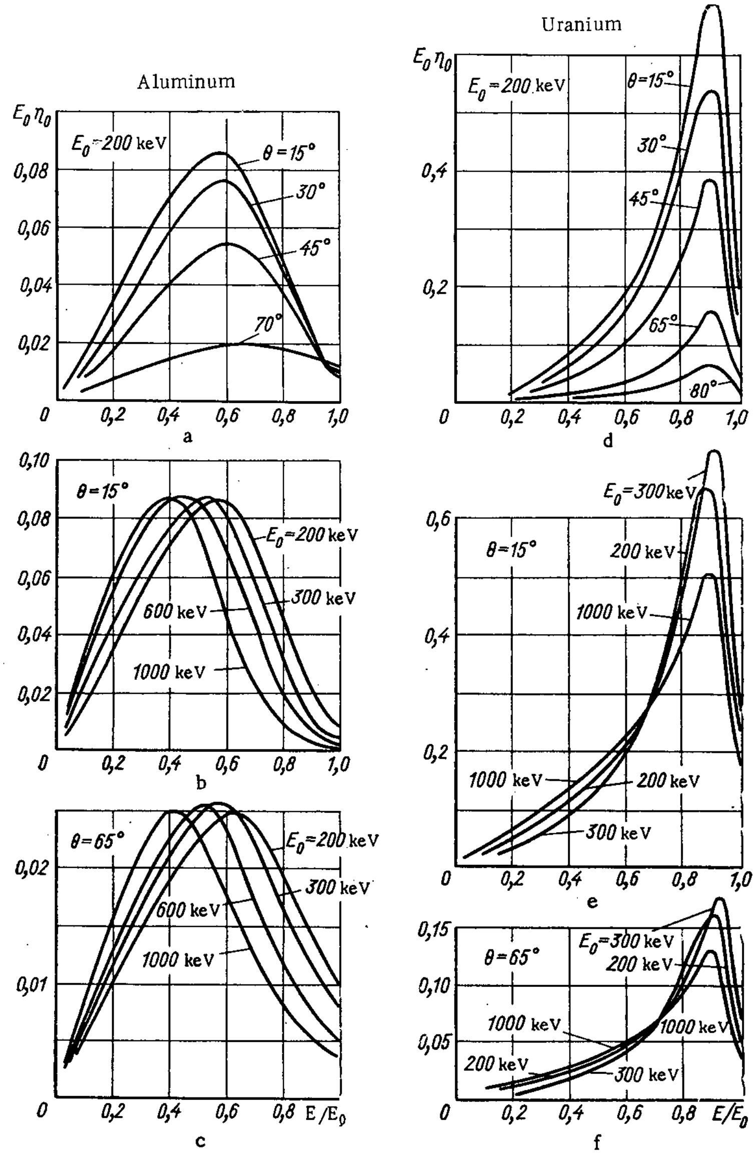

Fig. 1. Energy distribution of electrons back scattered from aluminum and uranium.

incident on the target was determined on the analyzer scale by placing the detector in a stopped-down beam. The Si (Li) spectrometer energy scale was calibrated with the 482 and 975 keV K lines from a Bi^{207} source which could be fed to the detector during the measuring process without breaking vacuum.

The targets were made of Al, Cu, Sn, Pb, and U. The angle θ between the axis of the detector and the normal to the target was set at 15, 30, 45, 65, and 80°.

The differential back-scattering coefficient can be determined from measured quantities:

$$\delta_N = \frac{N(\theta, E_0, Z)}{N_0 \Delta\Omega}, \tag{1}$$

where N (θ, E_0, Z) is the number of electrons recorded by the detector per unit time in the solid angle $\Delta\Omega$ in the direction θ. N_0 is the incident electron flux and Z is the atomic number of the target material.

The function N (θ, E_0, Z) takes account of the pulses which are intercepted by the discriminator, and the detector and preamplifier noise. The number of pulses was determined after extrapolating the measured amplitude distribution to zero amplitude. The thickness of the detector dead layer was estimated to

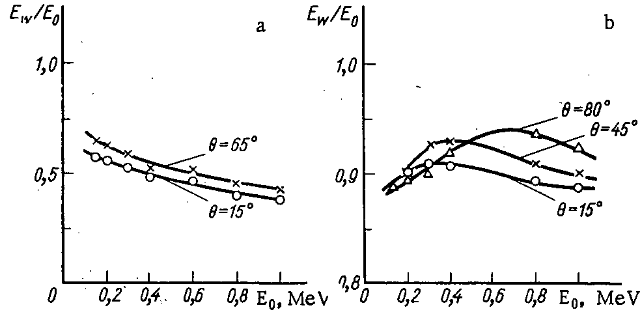

Fig. 2. E_W/E_0 as a function of E_0 for aluminum (a) and uranium (b).

be less than 5 keV, and therefore the counting efficiency was practically 100% for energies above 10 keV. The values of $N_0\,\Delta\Omega$ were calculated for each θ by taking account of the distribution of the beam density over the target.

The differential back-scattering coefficient η_D, characterizing the spectral distribution of the scattered radiation, is given by

$$\eta_D = \frac{N'(\theta, E, E_0, Z)}{N_0 \Delta\Omega \Delta E}, \tag{2}$$

where $N'(\theta, E, E_0, Z)$ is the number of electrons counted per unit time in the solid angle $\Delta\Omega$ in the direction θ in the energy interval from E to E + ΔE. The values of $N'(\theta, E, E_0, Z)$ were calculated on an M-20 computer from the spectrograms by introducing corrections for the back scattering of electrons from the detector, its finite resolution, and the fact that the beam incident on the target was not monoenergetic.

The results of measuring η_N for the targets listed are shown in Table 1. The angular distribution of back-scattered electrons in the energy range investigated depends not only on Z but also on the beam energy E_0. The dependence of η_N on θ up to angles to 80° can be written in the form

$$\eta_N = A(E_0, Z)\cos^{n(E_0, Z)} + B(E_0, Z), \tag{3}$$

where for given values of E_0 and Z, A is an order of magnitude larger than B. The values of $n(E_0, Z)$ are listed in Table 1. It is clear that for elements of intermediate and particularly of large Z (uranium, lead) η_N passes through a pronounced maximum for beam energies in the 300-400 keV range, while for aluminum η_N decreases slowly as the energy increases. Table 1 also gives values of the integrated back-scattering coefficient k obtained by integrating $\eta_N = f(\theta)$ numerically over the solid angle. These values of k are in good agreement with the results in [1]. If the measured dependence of η_N on E is extrapolated into the low-energy region the values of η_N obtained agree with the data in [2, 3] within the limits of the experimental error.

The measurements of η_D were performed for the targets indicated at the same angles θ. As an example Fig. 1 shows the spectra of radiation scattered from aluminum and uranium. The parameters are the angle θ (Fig. 1a, d) and the beam energy E_0 (Fig. 1b-e). For elements with large Z the most probable energy of the E_W spectrum is almost independent of θ. For elements with small Z (aluminum) the ratio E_W/E_0 increases with increasing θ up to energies $\sim$ 1 MeV.

It is clear from Fig. 2a, b that the carefully measured dependence of E_W/E_0 on E_0 for aluminum and uranium is of the same character as the dependence of η_N on E_0; i.e., the maximum of E_W/E_0 for uranium occurs at 300-400 keV just as for η_N, while E_W/E_0 for aluminum decreases with energy.

The error in determining η_N arises because of the error in $N_0\Delta\Omega$ (± 5%) and $N(\theta, E_0, Z)$ (± 1%), the inaccuracies in positioning the target and detector, the spread in the angles of incidence of the beam etc. The maximum error in η_N should be taken as ± 10%. The error in η_D is somewhat larger since it involves in addition the error in the selected energy interval ΔE, the error in $N(\theta, E, E_0, Z)$, which depends on the target material and lies in the 2-7% range, and the errors in the introduction of corrections in the processing of the spectrograms. The possible total error in η_D should be taken at $\pm$ 15%. The values of η_N and k in Table 1 are intentionally given to higher accuracy in order to show more graphically the energy dependence of these quantities. The behavior of this curve is determined with a very much smaller error since practically only the errors in determining N and N_0 enter into it.

LITERATURE CITED

1. P. Yerdier and F. Arnal, Compt. Rend., 267, 1443 (1968).
2. H. Kulenkampf and K. Ruttiger, Zeit. Phys., 137, 426 (1954).
3. H. Kanter, Ann. Phys., 20, 144 (1957).

RADIATIVE CAPTURE OF NEUTRONS BY U^{238} IN THE 1.2-4.0 MeV RANGE

Yu. G. Panitkin and V. A. Tolstikov

UDC 539.172.4.162.2

The cross section for the radiative capture of neutrons by U^{238} is important in fast reactor calculations and is also of interest from the point of view of refining our model concepts of nuclei and nuclear reactions. The present paper is a continuation of [1, 2] on the study of the U^{238} radiative capture cross section over a broad energy range.

In the present article we report measurements of the U^{238} radiative capture cross section in the 1.2-4.0 MeV range. The measurements were made by the activation method at an electrostatic accelerator with a maximum energy of 5 MeV. The neutrons were obtained from the T (p, n)He^3 reaction. The neutron flux was monitored by an ionization chamber with a layer of U^{235}. The specimen was placed directly on the fission chamber wall. The induced activity was measured with a Ge(Li) detector using the 74 keV γ-line of U^{239}. The recording range of the γ-spectrometer and the resolution of the spectrometer were checked during the measurements with the γ-spectrum of Tm^{170}. The fluctuations in neutron flux during the irradiation process were measured and appropriate corrections were introduced in the processing of the results. For energies above the U^{238} fission threshold the U^{238} fission products were removed from the specimen by chemical purification before measuring the induced activity.

The background of neutrons scattered in the target chamber of the accelerator was determined by the deviation from the inverse square law at various distances from the target; it amounted to < 1% of the magnitudes measured in the direct flux.

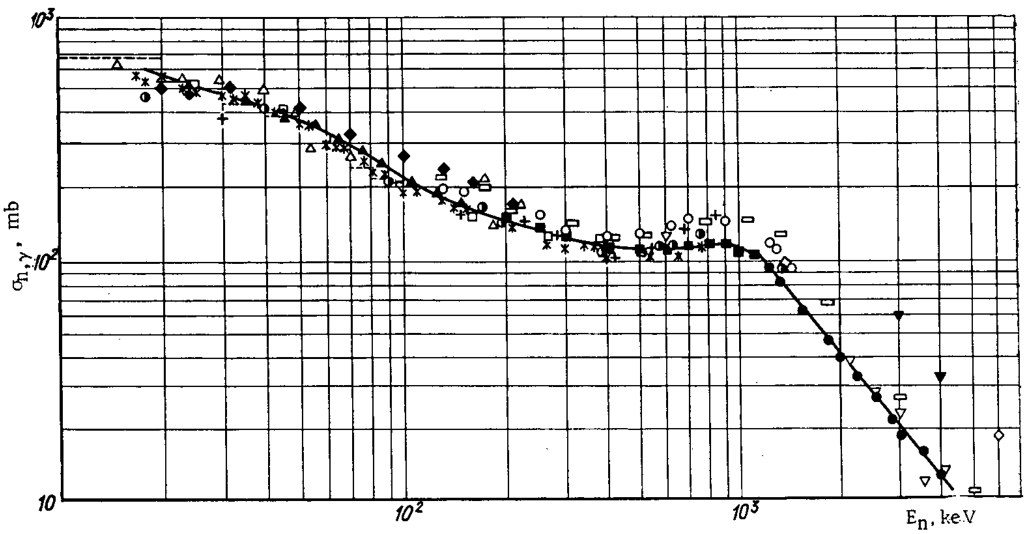

Fig. 1. Cross section for the radiative capture of neutrons by U^{238}. ●) Our data 1971; ▲) [1]; ■) [2]; ●) [7]; ○) [8] *) [9]; ⊂) [5]; □) [3]; +) [10]; ◆) [11]; ----) [12]; ▽) [4]; ◇) [14]; ▼) [6]; △) [13].

Translated from Atomnaya Énergiya, Vol. 33, No. 3, pp. 782-783, September, 1972. Original article submitted February 16, 1972.

TABLE 1. Cross Section of the Radiative Capture of Neutrons by U^{238}

E_n, MeV	N^8/N^5	σ_5	σ_8
1,2±0,043	0,61±0,01	1,23	94±2
1,3±0,045	0,529±0,01	1,24	82±1,7
1,5±0,049	0,391±0,008	1,26	62±1,5
1,8±0,054	0,315±0,007	1,287	48±1
2,0±0,057	0,264±0,05	1,306	40±1
2,2±0,061	0,219±0,006	1,314	33±1
2,5±0,067	0,176±0,005	1,287	27±0,8
2,8±0,073	0,149±0,005	1,257	22±0,8
3,0±0,078	0,127±0,004	1,230	19±0,8
3,5±0,094	0,112±0,009	1,186	16±1,5
4,0±0,110	0,0992±0,007	1,140	13±1

At proton energies above ~ 3 MeV neutrons begin to be produced in the molybdenum backing of the targets. The contribution of these neutrons is very important for the quantities being measured since their energies are low in comparison with the energy of the direct beam of neutrons from the $T(p, n)He^3$ reaction. This contribution is determined by irradiating the specimen and chamber with the tritium target replaced by the molybdenum backing. The contributions of these neutrons to the fission chamber counting rate and to the induced activity of the specimen are significantly different. This is due to the fact that in this energy range the U^{238} radiative capture cross section is falling rapidly while the U^{235} fission cross section remains approximately constant. The contribution to the fission chamber counting rate was 30-50%. The contribution to the induced activity of the specimen was 60-85%.

Since the U^{235} fission cross section and the U^{238} radiative capture cross section are approximately constant for neutron energies up to ~ 2 MeV the contribution of neutrons scattered by target and chamber components can be neglected. With increasing neutron energy inelastic scattering from structural materials of the target, chamber, and specimen gives rise to low-energy neutrons having a very much larger capture probability than neutrons from the $T(p, n)He^3$ reaction. In addition the U^{235} layer contains an admixture of other fissionable nuclei which contribute to the fission chamber counts. The correction for these effects can be calculated as follows:

for the specimen

$$N_8^k = \frac{N_8^{1k}}{1 + n_H \sigma_{Hk} \frac{\bar{\sigma}_8^k}{\sigma_8^k} + \sum_{i,n} N_i \sigma_{ink} \frac{\sigma_8^{nk}}{\sigma_8^k}};$$

for the chamber

$$N_5^k = \frac{N_5^{1k} \cdot N_5 \sigma_5^k}{\sum_m N_m \sigma_{mk} + n_H \sigma_{Hk} \sum_m N_m \bar{\sigma}_m^k + \sum_{i,n,m} N_i \sigma_{ink} N_m \sigma_m^{nk}},$$

where N_8^k is the "true" count of the specimen for neutrons of energy k; N_8^{1k} is the measured count of the specimen for neutrons of energy k; N_i is the number of nuclei of the i-th component of the structural materials; σ_{ink} is the cross section for the inelastic scattering of a neutron of energy k by the i-th component of the structural materials with the nucleus left in level n; σ_8^{nk} is the cross section for radiative capture by U^{238} of a neutron which has been inelastically scattered leaving the nucleus in level n; σ_8^k is the U^{238} radiative capture cross section for neutrons of energy k; $\bar{\sigma}_8^k$ is the U^{238} radiative capture cross section averaged over the spectrum of neutrons of initial energy k which have been scattered by hydrogen; n_H is the number of hydrogen nuclei; σ_{Hk} is the cross section for the scattering by hydrogen of neutrons of energy k; N_m is the fraction of fissionable nuclei of the m-th component in the fission chamber layer; σ_{mk} is the fission cross section of the m-th component of the fission chamber layer for neutrons of energy k; N_5 is the fraction of U^{235} nuclei in the fission chamber layer; σ_5^k is the U^{235} fission cross section for neutrons of energy k; $\bar{\sigma}_5^k$ is the U^{235} fission cross section averaged over the spectrum of neutrons of initial energy k which have been scattered by hydrogen; N_5^{1k} is the experimental fission chamber count; N_5^k is the "true" fission chamber count; $\bar{\sigma}_m^k$ is the cross section for the fission of the m-th component of the layer averaged over the spectrum of neutrons of initial energy k which have been scattered by hydrogen; the cross section of a pertinent component taking part in the calculation of the correction averaged over the spectrum of neutrons of initial energy E which have been scattered by hydrogen has the form

$$\bar{\sigma} = \frac{\int_0^{E_0} \Phi(E)\sigma(E)\,dE}{\int_0^{E_0} \Phi(E)\,dE} = \frac{\int_0^{E_0} \sigma(E)\,dE}{E_0}.$$

These corrections amount to 5-8% of the measured value. The corrections were calculated to ~ 15%.

The results of the measurements are presented in Table 1 and Fig. 1. Figure 1 shows our earlier result [1, 2] and for comparison the results of other experimenters [3, 4]. The error in the derived value of the cross section for the radiative capture of neutrons by U^{238} is the mean square error of the experiment taking account of the errors in the corrections introduced, but not taking account of the errors in the U^{235} fission cross section or in the U^{238} reference cross section. The reference value of the U^{238} radiative capture cross section was taken as 516 mb at 24.4 keV [3]. The U^{235} fission cross section was taken from [15].

The data of [12] are normalized at 30 keV to the value of the average radiative capture cross section [16]. Figure 1 shows that in the range of neutron energies considered, our results agree with those of [4] but are 20-30% lower than the results in [5] and lower than the results in [6] by about a factor of three.

LITERATURE CITED

1. Yu. G. Panitkin, Yu. Ya. Stavisskii, and V. A. Tolstikov, Nucl. Data for Reactors, Vol. 2, IAEA, Vienna (1970), p. 57.
2. Yu. G. Panitkin, Yu. Ya. Stavisskii, and V. A. Tolstikov, Data from a Conference on Neutron Physics [in Russian], Naukova Dumka, Kiev (1972).
3. H. Mehlove and W. Pöenitz, Nucl. Sci. and Engng., 33, 24 (1968).
4. E. Broda and D. Wilkinson, Report BR-574, AERE-NP/R-1743, Harwell (1955).
5. J. Barry, J. Bunce, and P. White, J. Nucl. Energy, 18, 481 (1964).
6. A. Leipunskii et al., Second Geneva Conference (1958), Vol. 15, UN (1959), p. 50.
7. C. Linenberger, J. Miskel, and E. Segre, Report LA-179, Dec. (1944).
8. W. Pöenitz, Nucl. Sci. and Engng., 40, 383 (1970).
9. M. Fricke et al., IAEA Conf. on Nucl. Data, Vol. 2, Helsinki (1970), p. 265; Report NASA-CR-72745, DA-10194 (1970).
10. R. Hanna and B. Rose, J. Nucl. Engng., 8, 197 (1959).
11. E. Bilpuch, L. Weston, and H. Newson, Ann. Phys., 10, 455 (1960).
12. M. Maxon, Report AERE-R6074 (1969).
13. V. Tolstikov, L. Sherman, and Yu. Stavisskii, J. Nucl. Engng., A/13 18, 599 (1964).
14. D. Hughes and R. Schwartz, Neutron Cross Sections, BNL, New York (1958), p. 342.
15. W. Hart, Evaluated Fission Cross Section in the Energy Range 1 keV to 15 MeV. Paper UK-10, UK–USSR Seminar, June, 1968. Intern. Atomic Energy Review, July, 1971. To be published in Atomic Energy Review.
16. T. Byer and V. Konshin, Report IAEA, Nuclear Data Section, IAEA, Vienna (1971).

LOW-ENERGY PORTION OF THE SPECTRUM OF PROMPT NEUTRONS FROM THE SPONTANEOUS FISSION OF Cf^{252}

L. Jaki, Gy. Kluge,
A. Lajtai, P. P. D'yachenko,
and B. D. Kuz'minov

UDC 539.173.84

The extensive use of Cf^{252} for the standardization of neutron measurements presumes accurate knowledge not only of the number of neutrons emitted in spontaneous fission but also their spectral distribution. However, the information presently available on the spectrum of prompt neutrons from the spontaneous fission of Cf^{252} is very contradictory. In particular the results reported in [1, 2] on the low-energy

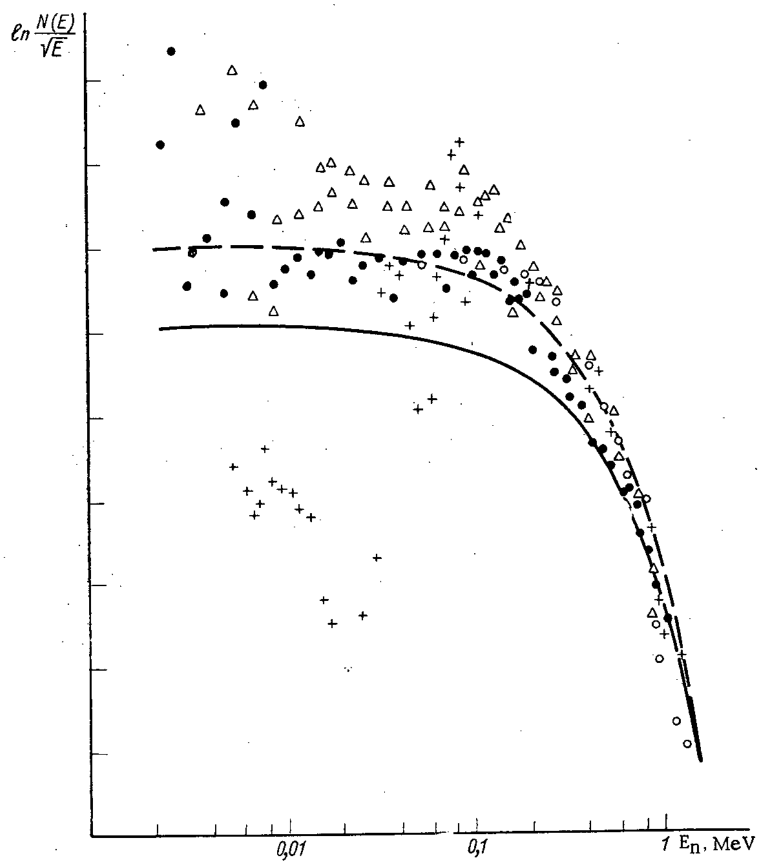

Fig. 1. Spectrum of prompt neutrons from the spontaneous fission of Cf^{252}. ●) Our data; △) [1]; +) [2]; ○) [3]. Maxwellian spectrum for temperatures of 1.57 MeV (———) and 1.30 MeV (----).

Central Institute of Physical Research of the Hungarian Academy of Sciences, Budapest. Physics-Power Institute, Obninsk. Translated from Atomnaya Énergiya, Vol. 33, No. 3, pp. 784–785, September, 1972. Original article submitted March 21, 1972.

(E_n < 0.2 MeV) portion of the fission neutron spectrum for this isotope do not agree. Meadows [1] emphasizes the deviation of the low-energy neutron spectrum from the traditionally assumed Maxwellian distribution $N(E) \approx \sqrt{E} \exp(-E/T)$. This result has a more general significance since it raises a doubt as to the applicability of the Maxwellian distribution over the whole range of energies of prompt neutrons from the induced fission of U^{233}, U^{235}, and Pu^{239} used as fuel in nuclear power reactors.

We have measured the neutron spectrum over the energy range from 0.002 to 1 MeV for the spontaneous fission of Cf^{252}. The neutron energy was determined from the time of flight from the Cf^{252} layer to the neutron detector. The neutrons were recorded by a glass scintillator containing 7.3% lithium enriched in Li^6 (to 96%). The detector was 7.6 cm in diameter and 0.3 cm thick. In processing the experimental data we used the same energy dependence of the neutron counting efficiency as in [1] where a similar detector was employed.

Fission products were counted in a gas scintillation chamber 10 cm in diameter and 6 cm long. In order to decrease the background of scattered neutrons the chamber was made of aluminum 0.1 cm thick with an end window 0.03 cm thick. The chamber was filled with a mixture of 80% argon and 20% nitrogen at a pressure of 1 atm. In various series of measurements two Cf^{252} targets were used with strengths of $1.7 \cdot 10^5$ and $1.1 \cdot 10^6$ fissions/min.

Flight paths 15.5, 30, and 57.5 cm long were used, and the time of flight was measured down to 400 nsec. The converter was started up by a signal from the neutron detector. The stop signal proceeded from the fission product detector with a 400 nsec time delay. The zero of the time scale was determined by the position of the peak of the prompt fission gammas, correcting for their time of flight to the neutron detector. The time scale was calibrated by the displacement of the position of the prompt fission γ-peak when various calibrated delay lines were connected. The value of one channel of the time scale was 0.39 nsec. The time resolution, determined by the width of the prompt fission γ-peak, was 4.5 nsec (the total width at half height).

We took account of three kinds of backgrounds.

1. Two components of the background due to random coincidences. Random coincidences due to the charge of the detectors were determined by introducing appropriate delay lines. Random coincidences in which the start and stop signals arose in different fissions were calculated using the experimentally known fission rate and the time spectrum of fission neutrons.

2. The background of scattered neutrons. To measure the background we placed a brass cone 13 cm long between the fragment and neutron detectors on the 57.5 cm flight path and one 7 cm long on the two shorter flight paths.

3. Background of delayed γ-rays. Measurements of the background were made on the 3.5 cm flight path and then scaled to normal measuring conditions by taking account of the difference in solid angles and the number of fissions recorded.

The results of the measurements are shown in Fig. 1 together with results reported by others. The data from the various sources were joined in the 0.7-1 MeV range of neutron energies. Our results and those of [1] are in satisfactory agreement. The experimental data for E_n < 0.2 MeV deviate from the Maxwellian distribution for T = 1.57 MeV and lie rather close to the distribution for T = 1.3 MeV. Measurements of the spectrum of neutrons from the spontaneous fission of Cf^{252} are reported in [1-8] for a wide range of energies (0.1-8 MeV). The temperatures obtained in these papers vary from 1.37 to 1.59 MeV. However an analysis in [9] of the existing experimental data on the spectra of prompt neutrons from the spontaneous fission of Cf^{252} showed that as a rule values of the temperature are obtained in those cases where no corrections are introduced, increasing the mean energy of the fission neutrons. As a result Jeki et al. [9] conclude that the temperature of the Maxwellian distribution describing the spectrum of neutrons from the prompt fission of Cf^{252} must be close to 1.57 MeV. In this case our experiments confirm the conclusion in [1] that the fission neutron spectrum of Cf^{252} deviates from Maxwellian in the low-energy region.

The spectrum of neutrons from the spontaneous fission of Cf^{252} should be investigated further over a wide range of energies, and the low-energy portion of the spectrum should be measured with detectors whose variation of efficiency with energy is different from that of lithium glass.

LITERATURE CITED

1. I. Meadows, Phys. Rev., 157. 1076 (1967).
2. Yu. S. Zamyatnin et al., Nucl. Data for Reactors, Vol. 2, IAEA, Vienna (1970), p. 183.
3. H. Werle, Report INR-4/70-25 (1970).
4. E. Hjalmar, H. Slätis, and S. Thompson, Arkiv Fys., 10, 357 (1955).
5. A. Smith, P. Fields, and I. Roberts, Phys. Rev., 108, 411 (1957).
6. T. Bonner, Nucl. Phys., 23, 116 (1961).
7. H. Bowman et al., Phys. Rev., 126, 2120 (1962).
8. H. Conde and C. During, Arkiv Fys., 29, 313 (1965).
9. L. Jeki, Gy. Kluge, and A. Lajtai, Report KF, KI-71-9 (1971).

γ-RADIATION FIELD IN THE UPPER LAYER OF THE BLACK SEA

G. F. Batrakov, B. N. Belyaev,
A. S. Vinogradov, K. G. Vinogradova,
B. A. Nelepo, and A. G. Trusov

UDC 551.463:539.1

The γ-radiation field in sea water is produced by radioactive isotopes in the water, by cosmic-ray electron–photon showers, and by radioactive isotopes in living organisms and suspensions. Sea water contains natural and man-made isotopes whose decays involve γ-emission. The specific activity of one such isotope (K^{40}) is much higher than that of the others [1], so the effect of other isotopes and of cosmic rays on the γ-radiation field of sea water can be treated as a perturbing factor.

Basic Characteristics of the γ-Radiation Field. Experiments have shown that the intensity and spectral composition of the γ-radiation of sea water are highly constant [2-7]. Only in the upper layer and near the bottom do we find an appreciable intensity increase; right at the surface, there is a higher count rate in the soft part of the spectrum. It is very difficult to identify other isotopes against the K^{40} background because of their low specific activity; accordingly, this identification has been carried out only in a few studies [2, 8, 9].

Sea water is a highly dispersive medium. Calculations show that the scattered-radiation flux in sea water considerably exceeds the primary flux for nearly all isotopes [10]. The basic contribution comes from the intense multiple-scattering peak in the soft part of the spectrum. The shape and height of this peak do not depend on the energy of the initial γ-radiation, so the total flux of γ-rays in the soft part of the spectrum is proportional to the net specific γ-activity of the sea water. Accordingly, the perturbing factor of the γ-radiation field of sea water must have the greatest effect near the scattered-radiation peak.

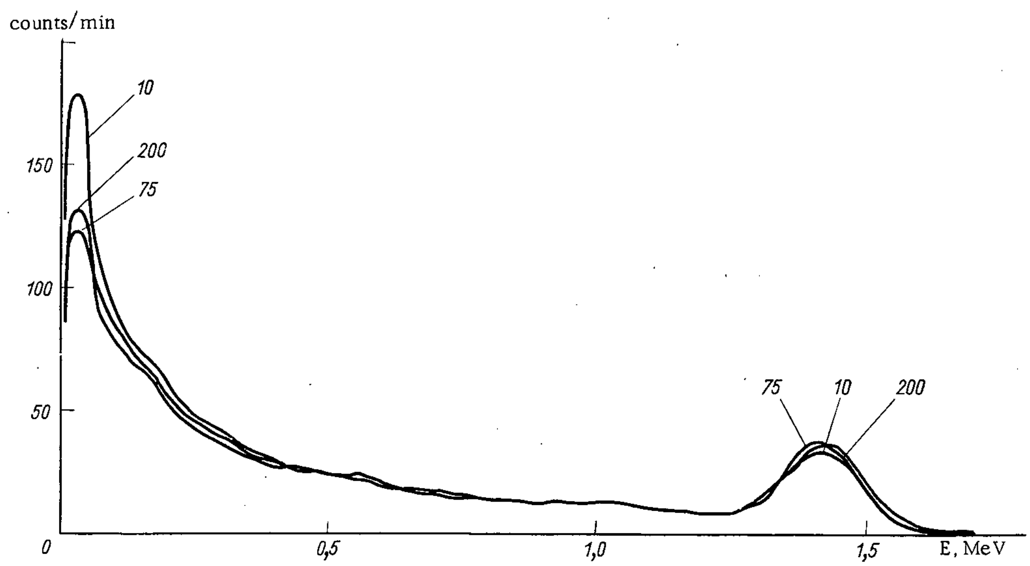

Fig. 1. The γ-radiation spectrum of the sea water at depths of 10, 75, and 200 m.

Translated from Atomnaya Énergiya, Vol. 33, No. 3, pp. 785-788, September, 1972. Original article submitted April 4, 1972; revision submitted April 18, 1972.

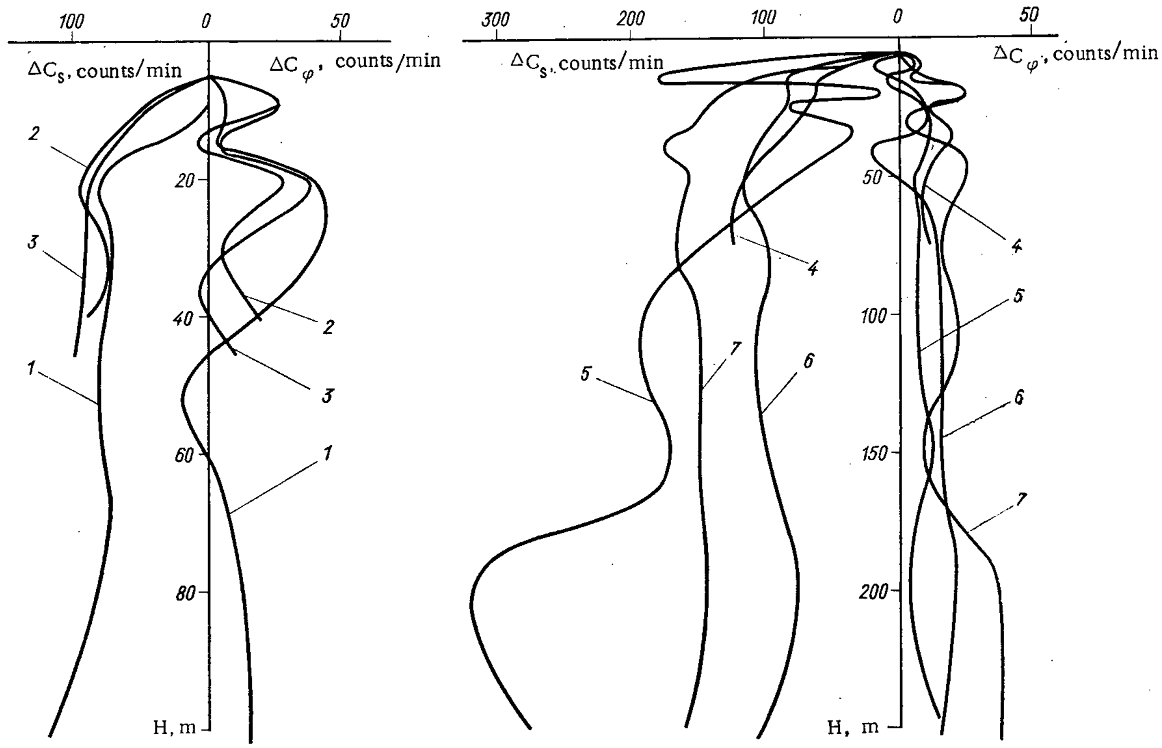

Fig. 2. Depth dependence of the count rate at the K^{40} photopeak and soft part of the spectrum at stations 1-7.

Experimental Procedure. In an effort to determine the nature of the variations of the γ-radiation field we carried out two series of measurements in the upper layer of the Black Sea. Measurements were carried out at three stations in the eastern part of the sea in June and at four stations in the central and eastern parts during the following March. The experimental apparatus consisted of a multichannel γ-spectrometer with a submerged scintillation detector.

Most of the measurements were carried out with a single-crystal sodium iodide detector 150 mm in diameter and 100 mm high. The measurement time at the horizon was from 1.0 to 1.5 h, sufficient for a determination of the count rate at the K^{40} photopeak with a statistical error of 1.5%. Measurements were carried out at 5-m steps down to a depth of 20-25 m; below that they were carried out at 10-m or larger steps.

To eliminate the effect of the spectrometer drift on the results, we converted all the experimental spectra to a standard energy scale; we determined the count rate in the K^{40} photopeak by a more refined procedure, which does not introduce any appreciable additional error [11].

Experimental Results. The overall nature of the experimental spectra is consistent with that of previously published spectra; in the soft part of the spectrum there is a clearly defined and intense scattered-radiation peak (Fig. 1), whose position and shape agree well with those calculated in [10]. The spectra reveal a clearly defined K^{40} photopeak and weak systematic increases which can apparently be identified as the photopeaks of other isotopes.

Near the scattered-radiation peak we observe large variations in the count rate as a function of the depth; the other parts of the spectrum remain relatively constant (Fig. 1). This behavior was also found in a comparison of the spectra obtained at a given depth in different parts of the sea.

In analyzing the experimental data we found certain regularities in the depth dependence of the count rate in both the soft part of the spectrum and near the K^{40} photopeak. Figure 2 shows the count-rate change ΔC_S in the soft part of the spectrum (57-257 keV) and that of ΔC_{ph} at the K^{40} photopeak 5 m below sea level. The experimental results are in satisfactory agreement, despite the seasonal differences among the properties of the sea water and the wide spacing of stations. Supplementary experiments showed the results to be quite reproducible (curves 2 and 3).

Comparison of the count rates at the various stations showed a systematic difference at all depths in the soft part of the spectrum. The flux of primary K^{40} γ-radiation does not follow the salinity distribution, instead simply displays a tendency to increase with depth. The strongest variations in count rate are found in the upper, relatively fresh layer of the Black Sea [12].

Analysis of the basic observed features shows that in the regions displaying sharp inhomogeneities in the properties of the sea water the count rate at the K^{40} photopeak more accurately reflects the distribution of these inhomogeneities. The count rate at the photopeak displays greater variations than that in the soft part of the spectrum, since the scattered-radiation flux smooths the effect of these inhomogeneities. This circumstance furnished a partial explanation for the observation that the count-rate variations at the K^{40} photopeak do not have any analogy in the soft part of the spectrum.

The count rate in this soft part of the spectrum is due to the fluxes of scattered γ-radiation from the various sources: isotopes dissolved in the water, isotopes in suspended material, and cosmic rays (the contribution of the latter should be the same at all stations). In addition, some contribution could come from the primary soft γ-radiation (50-200 keV) of natural radioactive isotopes of the uranium and thorium family. These γ-lines are not resolved in the instrumental spectrum of the scintillation spectrometer; instead they merely contribute to an overall increase in the count rate.

Changes in the density and composition of the sea water were found to have a very slight effect on the count rate at the K^{40} photopeak. Appreciable count-rate changes can be caused only by a change in the specific avtivity of the K^{40} dissolved in the water and held in the suspended material. An estimate of the potassium concentration in this suspended material and in plankton showed that the observed count-rate variations could not be explained by features of the depth distribution of the suspended material and plankton.

Comparison of the results found in measurements, in regions differing in the content of suspended material, shows that the contribution of K^{40} in this suspended material could be comparable to the change in the activity of the dissolved K^{40} only in rare cases.

The observed sequence of maxima and minima in the depth dependence of the count rate down to 50 m, is apparently due to the fine stratification of sea water recently discovered through the use of continuously operating thermometers and salinometers.

We can draw some conclusions from these results.

1. It has been shown experimentally that the most sensitive part of the γ-radiation spectrum of sea water is the region near the scattered-radiation peak, in which the effects of all the perturbing factors are summed. This region makes the principal contribution to the change in the integral intensity of the γ-radiation field of sea water. In measurements incorporating a high discrimination level, the integral intensity of the γ-field of the sea water changes much less significantly, as has been shown in many radiometric measurements. Only in [7], in which measurements were carried with a radiometer having a 60-keV threshold, was a large scatter in intensity observed in the upper layer of the ocean.
2. It has been shown that the intensity decrease in the soft part of the spectrum near the surface of the ocean is due not only to the absorption of cosmic rays, but also to a change in the net specific activity of isotopes in the water.
3. The K^{40} specific activity undergoes important variations as a function of the depth, displaying an overall tendency to increase with depth in various regions of the sea.
4. By studying the variations in the γ-field one can determine the structure of hydrophysical fields having characteristic dimensions of the order of 10^{-1}-10 m.

The authors thank A. G. Kolesnikov for discussion of this study, and V. I. Man'kovskii and L. A. Koveshnikov for furnishing data on the transparency and salinity of the sea water.

LITERATURE CITED

1. V. P. Shvedov and S. A. Patin, Radioactive Contamination of the Oceans and Seas [in Russian], Atomizdat, Moscow (1968).
2. B. A. Nelepo, Dokl. Akad. Nauk SSSR, 134, No. 4, 810 (1960).

3. B. A. Nelepo, Vestnik MGU. Seriya 3. Fizika-Astronomiya, No. 5, 36 (1960).
4. V. N. Lavrenchik and G. N. Sofiev, Izv. Akad. Nauk SSSR, Seriya Geofizicheskaya, No. 2, 275 (1962).
5. L. M. Khitrov and K. A. Kotlyarov, Okeanologiya, No. 2, 334 (1962).
6. G. V. Samokhin and A. F. Fedorov, in: Radioactive Contamination of the Oceans and Seas [in Russian], Nauka, Moscow (1964).
7. Akiyama Tsutomu, Oceanogr. Mag., 17, Nos. 1-2, 69 (1965).
8. R. Chesselet and D. Nordeman, Bull. Inst. Oceanogr., 60, No. 1266, 14 (1963).
9. M. Gross and C. Barnes, Science, 149, No. 3688, 1088 (1965).
10. A. S. Vinogradov, in: Research in the Physics of Oceans [in Russian], MGI AN USSR, Sevastopol' (1969), p. 106.
11. A. S. Vinogradov and K. G. Vinogradova, Morskie Gidrofizicheskie Issledovaniya, No. 1, 212 (1969).
12. A. K. Leonov, Regional Oceanography [in Russian], Gidrometeoizdat, Leningrad (1960), Part 1.

AVERAGE YIELD OF NEUTRONS PER SPONTANEOUS FISSION OF Bk^{249}

V. N. Kosyakov, V. G. Nesterov,
B. Nurpeisov, L. I. Prokhorova,
G. N. Smirenkin, and I. K. Shvetsov

UDC 539.173.7

Interest in the study of the dependence of the fission neutron yield $\overline{\nu}$ on the A and Z of the fissioning nucleus has increased markedly in the last few years. This is explained by the increase in the possibilities and scales of producing transuranium elements. The necessity of a detailed study of their properties is dictated by both scientific and practical considerations.

The most detailed information on $\overline{\nu}$ for transuranium elements is for spontaneous fission. The known data for even–even nuclei from curium to ferium show that $\overline{\nu}$ is a linear function of A to within about 4% (Fig. 1). The value 3.63 ± 0.16 for $\overline{\nu}$ (Bk^{249}) is somewhat out of line with the other data. It was reported in 1957 in an unpublished paper by Pyle [1]* and cited later in [2, 3]. This is the only value of $\overline{\nu}$ for the spontaneous fission of odd nuclei in general and for Bk^{249} in particular.

The preparation of Bk^{249} ($\sim 7\,\mu g$) used in our work was obtained by treating a curium target irradiated in the SM-2 reactor. Separation and purification were performed by the oxidation–reduction extractive-chromatographic method [4]. The last stage of purification was performed in a quartz apparatus which had previously been leached out using specially pure reagents and doubly distilled water. After triple

* The value 3.72 ± 0.16 was given in the original paper. The value in the text was obtained by renormalization, taking account of the change in $\overline{\nu}$ for the standards Pu^{240} (2.23–2.15) and Cf^{252} (3.28–3.756).

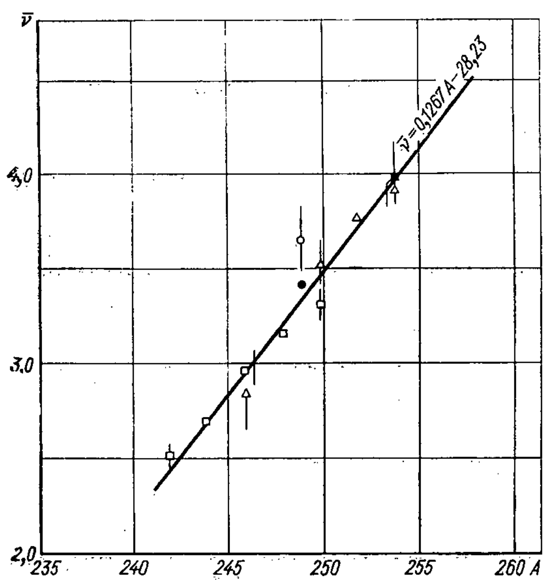

Fig. 1. $\overline{\nu}$ as a function of A for spontaneously fissionable nuclei. The straight line is a least-square fit. ●, ○) values of $\overline{\nu}$ (Bk^{249}) from our data and [1] respectively; ■) fermium [12]; □, △) curium and californium from average values of experimental data in [3] and [10] respectively.

Translated from Atomnaya Énergiya, Vol. 33, No. 3, pp. 788–789, September, 1972. Original article submitted April 14, 1972.

purification the Cf^{252} content in the Bk^{249} did not exceed 10^{-10} which, for the ratio of decay constants of these isotopes ($\sim 2 \cdot 10^7$ [5, 6]), guarantees practically no background due to the spontaneous fission of Cf^{252}. The amount of Cf^{249} built up during the experiment from the instant of the last stage of purification amounted to $\leq 0.3\%$. According to data in [5, 7] the contribution of Cf^{249} to the observed number of spontaneous fissions was still less by about a factor of 30.

$\bar{\nu}$ for Bk^{249} was measured by the ratio method [8], which is based on recording coincidences between pulses from detectors of prompt neutrons (24 He^3 counters in a paraffin block with an efficiency of $\sim 25\%$) and fragments from spontaneous fission (ionization chamber) for the isotope under study and a standard, in our case Cf^{252}. We recorded about $3.6 \cdot 10^4$ fissions of Bk^{249} and $2.2 \cdot 10^6$ of Cf^{252}. After making small corrections [8] to the experimentally observed ratio we obtained $\bar{\nu}$ $(Bk^{249})/\bar{\nu}$ $(Cf^{252}) = 0.9039 \pm 0.0069$. Using $\bar{\nu}$ $(Cf^{252}) = 3.756$ [9], $\bar{\nu}$ $(Bk^{249}) = 3.395 \pm 0.026$.

Our value of $\bar{\nu}$ (Bk^{249}) is lower than that in [1] and is in reasonable agreement with the general behavior of $\bar{\nu}$ shown in Fig. 1; i.e., it lies between the values of $\bar{\nu}$ for the neighboring nuclei Cm^{248} (3.157 ± 0.015) [10] and Cf^{250} (3.53 ± 0.09) [11].

The authors thank V. A. Borisenk and V. E. Rudnikov for helping with the measurements.

LITERATURE CITED

1. R. Pyle, The Multiplicities of Neutrons from Spontaneous Fission, Paper Presented at Gordon Conference (1957).
2. I. I. Bondarenko et al., Second Geneva Conference (1958), Vol. 15, U.N., Geneva (1959), p. 353.
3. V. A. Kon'shin, Nuclear Physics Constants for Transplutonium Elements [in Russian], IAEA, Vienna (1971).
4. A. A. Zaitsev et al., Paper No. 689 [in Russian], Fourth Geneva Conference (1971).
5. J. Milsted et al., J. Inorg. Nucl. Chem., 31, 1561 (1969).
6. D. Metta et al., J. Inorg. Nucl. Chem., 27, 33 (1965).
7. D. Metta et al., ibid., 31, 1245 (1969).
8. L. I. Prokhorova et al., Atomnaya Énergiya, 30, 250 (1971).
9. C. Hanna et al., Atomic Energy Rev., 7, 3, 4 (1969).
10. L. I. Prokhorova, this issue, p. 875.
11. C. Orth, Nucl. Sci. and Engng., 43, 54 (1971).
12. G. Choppin et al., Phys. Rev., 102, 766 (1956).

IV ALL-UNION CONFERENCE ON UTILIZATION OF NEUTRON SCATTERING IN SOLID-STATE PHYSICS

M. G. Zemlyanov

The IV All-Union Conference on the utilization of neutron scattering in solid-state physics was held in March 1972, at Sverdlovsk, under the joint auspices of the Council on the complex Solid-State Physics of the Academy of Sciences of the USSR and the USSR State Committee on the Peaceful Uses of Atomic Energy [GKIAÉ SSSR], with the participation of the Institute of Metal Physics of the Urals Scientific Center, Academy of Sciences of the USSR. The conference attracted over 130 scientists; 71 reports were heard. The topics discussed included: ferrites, the magnetic structure of metals and alloys, structural neutron diffraction, interaction of polarized neutrons, diffraction on imperfect crystals, ideal crystals, inelastic scattering, experimental procedure, and experimental equipment.

Almost half of the reports were devoted to the study of magnetic systems, i.e., to that branch of solid-state physics in which the method of neutron scattering is most advantageous compared to other research techniques.

E. G. Brovman's paper was one of the more interesting theoretical contributions. In this paper the effect of the electronic system on the formation of the phonon spectrum of metals was discussed. Treatment of the unpaired interaction between covalent type ions, which takes place as a consequence of the interaction of three or more ions through the intermediary of conduction electrons, enables the authors to account for many of the experimental results within the framework of a unified treatment. The unpaired interaction leads to pronounced singularities in the dispersion relations for the phonon branch of the excitation. The experimental detection of those special features provides direct proof of the effect of the unpaired interaction.

M. A. Ivanov discussed the effect of introducing very heavy impurity atoms on the excitation spectrum of the lattice of the original matrix. The introducing of impurities can bring about the formation of not only quasilocal states, but also an energy gap traceable to vibrations of the impurity atoms out of phase with the atoms belonging to the host matrix.

Among the reports devoted to ferrites, the one most deserving of attention was submitted by R. A. Sizov and K. N. Zaitsev, dealing with the spatial distribution of magnetic moments in a lattice of hexagonal ferrites. In order to explain the results they obtained, the authors made use of a DNA type (deoxyribonucleic acid) helical chain structure, and showed that the magnetic moment is delocalized with respect to the nucleus. The delocalization is temperature dependent, and could possibly be accounted for in terms of polarization of the electron shells. A displacement of this type has also been reported by other authors, but the magnitude reported was much smaller.

Application of various experimental techniques to the study of the same system has greatly expanded the information obtainable. For example, a paper by G. M. Drabkin et al., discussed a magnetic phase transition in yttrium ferrite–garnet, studied with the aid of polarized neutrons and radio-frequency susceptibility measurements. These complex investigations enabled the authors to not only determine the value of the Curie point with great accuracy, but also to establish the validity of the hydrodynamical description of long-wavelength fluctuations in the critical region.

The depolarization effect accompanying passage of neutrons through a magnetic system was found, with the aid of polarized neutrons, to depend essentially on the mutual orientation of the polarization vector

Translated from Atomnaya Énergiya, Vol. 33, No. 3, pp. 791-792, September, 1972.

and the neutron velocity. In accordance with the theoretical argument advanced by S. V. Maleev, the anisotropy of depolarization must be 3/2, as confirmed experimentally in the case of nickel (A. I. Okorokov and associates).

Several reports on studies of invar alloys were presented by the Institute of Metal Physics of the Urals Scientific Center, Academy of Sciences of the USSR. The spatially inhomogeneous magnetic structure of those alloys was detected, and new data were obtained on the magnetic structure of alloys with mixed ferromagnetic and antiferromagnetic interaction.

Great opportunities are opening up for the application of neutron scattering methods in the study of ideal crystal systems. A report by S. Sh. Shil'shtein cited research findings on the transmission and reflection of neutron radiation by ideal crystals. These measurements provide experimental confirmation of the anomalous transparency of a perfect absorbing crystal in the Wulff–Bragg position, and the suppression of the (n, γ)-reaction in the case of resonance scattering in CdS. In addition, the measurements make it possible to study neutron refraction on individual grain boundaries, and to obtain complete information on the internal domain structure of massive ferromagnetic crystals.

Several reports dealt with studied of the structure and excitation spectrum of interstitial phases (hydrides, oxides, carbides). For instance, a report by I. R. Éntin et al., on the atomic and magnetic structure of martensite – the basic component of tempered steel – successfully made use of an isotope specimen to reliably establish the arrangement of carbon atoms in the martensite lattice. This provided an explanation of the nature of the tetragonal configuration, and is of great importance in understanding the mechanism underlying martensite transformations.

Reports by I. P. Eremeev and V. I. Gorbachev dealt with how to obtain information on phonon spectra for systems coherently scattering neutrons. In order to secure information on the density of states in coherent systems, the authors resort to averaging over the space of reciprocal vectors based on measurements of neutrons of a given energy scattered on a polycrystalline specimen over a broad range of angles. The minimum error in the restoration of the state density function by the proposed method is 10-20%.

Close attention was given to procedures and equipment in experiments with neutrons (neutron sources, spectrometers, recording techniques, processing of experimental results). A report by M. G. Zemlyanov et al., mentioned two types of neutron spectrometers at the IRT-M nuclear reactor designed for studies of the dynamics of the excited state of matter. One of these spectrometers is a time-of-flight spectrometer and is employed in studies of scattering of cold neutrons. The use of a cryogenic propane source to generate cold neutrons led to a substantial rise in neutron flux. The second spectrometer was a completely automated triaxial neutron crystal spectrometer, outfitted with several thermostating devices. Papers presented by V. G. Shapiro and Ya. G. Gross also reported on neutron crystal spectrometers, but these differed in their design. Reliance of local cooling of the reactor moderator brought about an increase in neutron flux in the long-wavelength region. An interesting paper on this subject was presented by B. G. Goshchitskii et al., proposing natural circulation of a coolant, which appreciably simplifies the technological layout of the source of cold neutrons. Importance is attached to correct handling of the various types of corrections needed in the study of neutron scattering. Reports by A. Z. Men'shikov and S. B. Bogdanov dealt with these points. These papers went into detail on the effect of multiple scattering, as well as secondary extinction, on the reflectivity of single-crystal specimens shaped as plates, cylinders and spheres.

Obtaining the necessary information on the experimental data always involves, in the final analysis, the use of involved mathematical calculations with computers. These topics are dealt with in a report by O. A. Usov. The author compiled an algorithm for calculating the polarization vectors in the most general case of lattice symmetry.

The conference demonstrated that neutron research techniques in solid-state physics persist as basic techniques for obtaining information on the excitation spectra of the crystal lattice and magnetic lattice, on the structure of magnetic and nonmagnetic substances, and imperfections in the crystal lattice.

IAEA SYMPOSIUM ON APPLICATION OF NUCLEAR ACTIVATION TECHNIQUES IN THE NATURAL SCIENCES

R. G. Gambaryan

The International Atomic Energy Agency held a symposium at Bled (Yugoslavia) on April 10-14, 1972, to discuss applications of nuclear activation techniques in the natural sciences, approximately 100 specialists from 24 countries and three international organizations (Euratom, IAEA, JINR) took part. Leading atomic research centers institutes, and organizations of the various countries concerned with medicine and biology were among those represented at the symposium. The reports were concerned with the following general topics: general analytical techniques; toxicology and public health; research on animals and plants; medicine and in vitro research; medicine and in vivo research.

The review papers were very interesting. An introductory review paper delivered by K. Schwartz (USA) dealt with studies of the role played by trace elements (predominantly those whose major role has been established in recent years) in health maintenance and their effect on the progress of illness in humans and in animals. A review paper by D. Parizek (Czechoslovakia) on toxicological investigations using trace elements was especially interesting; Bowen (Great Britain) discussed trace element biochemistry in a review paper.

Ten or so reports were devoted to the use of activation techniques in investigations of the effect of environmental pollution by industrial wastes in water and air on humans. Several papers launched into a discussion of mercury toxicology. The urgency of the problem of environmental pollution is shown by the fact that, comparatively recently (in October, 1970) IAEA had already scheduled a symposium on the use of nuclear techniques to measure and monitor contamination of the environment (At. Énerg., 31, 178 (1971)).

Several reports delivered under the title "Medicine and in vitro research," dealt with more general topics: interrelations between carbohydrate metabolism and trace element metabolism; distribution of trace elements in biological tissues, their role in cardiovascular malfunction, etc.; and some special topics relating to pregnancy functions of (nursing) mothers, children, various specific illnesses (of the urinary bladder, teeth, etc.), and analysis of biomedia (serum, protein).

Most of the reports dealt with work using the conventional method of neutron activation analysis of various biological objects to determine the content of trace elements, with specimens irradiated in a nuclear reactor, or γ-ray spectrometry of irradiated specimens in the instrumental variation, or with chemical separation. Most of the papers reported the use of semiconductor high-resolution γ-ray spectrometry.

One paper on determinations of trace elements in biological specimens with the aid of instantaneous atomic and nuclear reactions was intriguing from the standpoint of technique (University of Namur, Belgium). A specimen of small size was bombarded by a collimated beam (0.2 mm^2) of 2 MeV protons from a Van de Graaff machine, and Si(Li)- and Ge(Li)-detectors were employed to record fluorescent x-ray emission and capture γ-emission, respectively, from the specimens, so that quantitative analysis of various elements could be done on the basis of the emission intensities. The sensitivity threshold of the method is estimated at 10^{-11} g.

Some of the reports contain materials on processing results by computer. The most interesting of these was a paper devoted to compilation of FORTRAN-language programs for automatic processing of

Translated from Atomnaya Énergiya, Vol. 33, No. 3, pp. 792-793, September, 1972.

γ-ray spectra obtained with the aid of Ge(Li)-detectors on desktop computers (Spain). The proposed program is useful for distinguishing the boundaries of photopeaks and the areas under the peaks, in the case of photopeaks that are fully resolved or partially overlapping.

Interesting advances in techniques are the treatment of dead time in a multichannel spectrometer in multicomponent activation analysis (Argentina) and the possibility of effecting determinations of lead (Britain) and iodine (Venezuela) by simple measurements of the induced γ-activity of specimens.

A joint report (USSR and France) described a method and an automatic facility for determinations of P, N, K, and Ca in plant specimens using activation by 14 MeV fast neutrons.

Papers presented by Britain and the USA on arrangements for activation analysis of a patient in vivo will be a special interest to designers of nuclear analytical equipment for medical purposes. A variety of neutron sources were used in carrying out the activation analysis described: a fast (14 MeV) neutron generator, a cyclotron, and isotope (α, n)-sources. The design of the irradiators allowed the options of either partially irradiating the patient, e.g., irradiating the hand only, or irradiating the whole body. The exposure was carried out with the patient in a stationary position or by scanning with the patient and chair moved about cyclically through the neutron field. After neutron irradiation (dose ~ 200-300 mbar) for 3-10 min, the patient is transferred (automatically) to the position for γ-ray spectrum measurements, and the γ-ray spectrum is usually recorded by a scintillation γ-ray spectrometer with back-to-back NaI(Tl) crystals. A Ge(Li)-detector is preferred for taking activity measurements on an irradiated hand. Calibration of the quantitative content of the elements is done on anthropomorphic phantoms. The content of Na, Cl, Al, Ca, P, N, or several of the above elements, is determined. One of the papers (Britain) dealt with a method for irradiating a patient with a pulsed neutron beam generated on a lithium target by a proton beam (10 MeV) from a pulsed cyclotron. The capture γ-radiation emitted by the patient's body is recorded with a time lag following the pulse, as needed, to slow down the fast neutrons to thermal velocities, and this allows for selective determination of the total concentration of nitrogen in the patient. The importance of up-to-the-minute determinations of the content of several elements in separate parts of the human body or in the entire human body is validated for medical practice in the papers.

The symposium showed that activation analysis currently ranks alongside spectrometry, atomic absorption spectrometry, and mass spectrometry as one of the most popular techniques for analysis of trace elements in biological specimens.

The symposium was well organized; the availability of preprints and the care taken to avoid too many papers being delivered orally contributed to the opportunities for fruitful discussions. IAEA plans to publish the proceedings of the symposium in late 1972.

SYMPOSIUM ON DOSIMETRY TECHNIQUES USED IN AGRICULTURE, INDUSTRY, BIOLOGY, AND MEDICINE

V. I. Ivanov

An IAEA symposium held under the joint auspices of the World Health Organization was held in Vienna, April 17-21, 1972. This symposium attracted 112 specialists from 31 countries, and eight representatives from international agencies.

The bulk of the reports dealt with thermoluminescent dosimetry and photoluminescent dosimetry. There were two groups of topics: 1) experience in practical applications of dosimeters; and 2) studies of the luminescence process, of dosimetric properties, and searches for optimum compositions of phosphors. Most of the reports on experience in applications of dosimeters dealt with conventional measurements relying on commercial radioluminescent, photoluminescent, and thermoluminescent detectors. Several interesting reports were given on applications of thermoluminescent detectors in medical and biological work. A report by F. Spires and colleagues (Britain) mentioned applications of powdery LiF in dose measurements in tissue-equivalent material filling a cavity in a cylinder whose walls contained β-active material. Preliminary investigations disclosed that the sensitivity of the pulverized LiF decreased precipitously starting with particle sizes below 40μ. The authors succeeded in producing a practically monodisperse thermoluminescent powder with an average particle size of 1.02μ. They presented data on dose loads on the bone marrow brought about by Sr^{90} contained in bone tissue.

Thermoluminescent dosimetry was used in another investigation (by Unnikrishnan et al., India) to solve the inverse problem: a cavity in a cylinder was filled with a β-active composition and miniaturized thermoluminescent detectors were employed to determine the dose in the cylinder walls; the experimental results were compared with data calculated for isotopes P^{32}, Tl^{204}, and $Sr^{90} + Y^{90}$. The data so obtained can be used in determinations of dose loads on the human alimentary tract after intake of food containing radioactive tracers.

Luminescent methods are now consistently used in dosimetric measurements. The reports presented at the symposium offered examples of their use in radioecology (A. Chapuis et al., France), radiotherapy (V. Labeu, Rumania), in vivo dose measurements (M. Shadev et al., India), etc.

In the second group of topics, attention centered on improvements in the dosimetric characteristics of radiation detectors, expressed preponderantly in minimizing errors in dose determinations by varying the physical properties of the detectors, and minimizing the spread in detector readings. Data cited in the various reports provided evidence of a considerable spread in the readings of commercial detectors. For example, P. Pichlau (West Germany) reported that the spread in the readings of LiF-base thermoluminescent detectors averages ± 2%, which is greater than the spread reported for the Fricke chemical dosimeter (± 0.7%) or ionization chambers (± 0.2%). A paper by D. Regulla (West Germany) cited data on the spread in the sensitivity of TLD-100 detectors. The maximum scatter coefficient was three for one batch of dosimeters, and the standard deviation was ± 15%.

One of the basic causes of the change in the detector characteristics was redistribution of traps with respect to energy levels ("trap dynamics"). Investigations by various authors (P. Pichlau, West Germany; E. Bloom, Britain) show that the CaF_2 heat-sensitive phosphor has advantages over LiF.

D. Regulla (West Germany) investigated thermoluminescence in manganese-doped metaphosphate glasses, since addition of manganese greatly enhances the sensitivity of the glass. Moreover, the

Translated from Atomnaya Énergiya, Vol. 33, No. 3, pp. 793-794, September, 1972.

"trap dynamics" effect is virtually absent in thermoluminescence detectors of this type. It should be noted that similar results were obtained much earlier by Soviet investigators [I. A. Bochvar et al., At. Énerg., 15, 48 (1963)].

How to increase thermoluminescence sensitivity in detectors is the object of special concern at the present time. One plausible approach is to record thermoluminescence from the photon count taken with a photomultiplier tube. T. Niewiadomski (Poland) presented a detailed analysis of sources and spectrum of background emission. This leads to a proposed method for suppressing background by discrimination of pulse amplitudes in output electrical signals, which should expand the range of application of thermoluminescence detectors at the low-dose end to 20 μR. Another report (K. Nollmann and E. Smolko, Argentina) investigated deexcitation curves in the temperature range of thermoluminescence detectors from liquid-nitrogen temperatures to $\approx 400°$K. The research findings are helpful in determining conditions under which measurements of very small doses (of the order of microrads) would be possible.

Chemical dosimetry and applications of plastic materials in dosimetry occupied a prominent place in the deliberations. A comprehensive review paper on the subject was presented by J. Dragonić (Yugoslavia).

It was reported that modern methods for investigating materials based on such phenomena as the Mössbauer effect and electron paramagnetic resonance can be applied fruitfully in dosimetry. The Mössbauer effect has been successfully applied in recent years to the study of the mechanism responsible for radiation-chemical effects in the reduction or oxidation of iron in various compounds. A joint report co-authored by Y. Takashima, Y. Nakayama (Japan), L. Chandler (IAEA) cited results of measurements taken of various solid-state chemical dosimeters based on iron compounds, the number of radiation chemical transformations determined from Mössbauer γ-spectra. The method can be used successfully to measure γ-radiation doses in the range from 10^7 to 10^{10} rad. The electron spin resonance method can also be used to determine products of radiation-chemical reactions. A report by I. Manambelono (Malagasy republic) presented a theory to account for the method, and discussed possible applications of the method in dosimetric work.

The fact that such traditional methods of dosimetry as scintillation dosimetry and photographic dosimetry were hardly discussed at all at the symposium is quite characteristic. But there were a few reports dealing with the development of the ionization method. Reports by French scientists (I. Casanovas et al.), and by F. Horneck (West Germany) offered results of research on ionization chambers filled with liquid dielectrics. The French scientists made use of a liquid ionization chamber to measure pulsed x-ray emission of pulse width $5 \cdot 10^{-8}$ sec. The German specialists studied the voltage–current characteristics of an ionization chamber filled with n-hexane, in the neutron radiation field. Applying the Jaffe theory of column recombination, and authors obtained a value of 26 eV for the average energy of ion production.

One of the Soviet reports (I. A. Avchiev and V. I. Ivanov) pointed out the possibility of broadening the range of measurements using gas ionization chambers in the direction of higher dose rates, by making use of a universal characteristic. Applications of ionization chambers in the range of dose rates from 10^{-3} to 10^{-4} R/sec were reported in a paper submitted by B. V. Mukhachev et al., (USSR). Those authors employed a vacuum radiation component in the 10^{-3} to 10^6 rad/sec range. The dosimetric characteristics of a direct-loading vacuum detector were investigated in a paper submitted by V. I. Ivanov et al. (USSR).

A joint report co-authored by scientists from the Institute of Biophysics, the Institute of Medical Radiology, and the Power Physics Institute (I. B. Keirim-Markus et al., USSR) presented findings based on measurements of the dosimetric characteristics of BR-5 fast reactor channels used in radiobiological research; the LET spectrum was measured with the aid of a set of tissue-equivalent low-efficiency gas-discharge counters in a method worked out by the authors. The neutron spectrum was determined with the aid of a set of fissionable isotopes combined with track-delineating detectors. The use of track-delineating dosimeters for measurements in neutron fields was the subject of a paper by G. M. Obaturov et al. (USSR).

R. Katz (USA) delivered an interesting report. In earlier papers, he had reported on attempts to account for the observed radiation effect on the basis of a discussion of the structure of the tracks left by particles interacting with matter. He developed this concept further in relation to dosimeters of different types, at this symposium. The series of papers by R. Katz developed one of the forms of the microdosimetric approach to the analysis of radiation effects.

The symposium demonstrated the widespread acceptance of various dosimetric techniques in all ranges of nuclear energy applications. The basic efforts of scientists in this area are presently aimed at improving the accuracy of dosimeter readings and at expanding the range of applications of dosimeters.

INTERNATIONAL RADIOECOLOGY CONFERENCE

R. M. Aleksakhin

An international conference devoted to theoretical and practical problems concerning environmental pollution by radioactive materials was held in Starý Smokovec (Czechoslovakia) May 16-19, 1972. A 180 specialists from Hungary, the German Democratic Republic, Poland, Rumania, the USSR, Czechoslovakia, and from IAEA participated in the conference. Seventy papers were heard at the conference, eleven of them by Soviet authors.

The scale and scope of radioecological research has expanded appreciably in recent years, and this research is focused on the regularities of migration of radioactive materials through the environment and the effects of ionizing radiations on living organisms. The purpose of the research is to lay down the scientific groundwork for protection of the environment, in which humans have to live, against radioactive contamination. The attention given to this problem is related to the outlook for peaceful utilization of atomic energy. Special attention is given to radioecological investigations in connection with the expanded construction of nuclear-fuel electric power generating stations.

The reports submitted to the conference encompassed practically all of the basic trends evident in modern radioecology: results of studies of the migration of radioisotopes in the atmosphere, in soils, in natural waters, in the vegetative cover, in wild animals, and in domesticated agricultural animals, were cited. Close attention was given to radioecological research techniques (principles underlying sampling of the environment, development of quick proximate analysis of identification and of quantitative determinations of radioisotopes in specimens featuring a complex radioisotope composition, etc.).

It was pointed out, in the introductory remarks by the chairman of the Czechoslovak Atomic Energy Commission J. Neuman, and in review papers submitted on the most important trends in radioecology by M. Zaduban and J. Fratrič (Czechoslovakia), N. V. Kulikov (USSR), and A. Szabó (Rumania), that research on radioecology and on radiation safety in relation to the operation of nuclear reactors and other major facilities, are crucial in programs worked out for promoting peaceful uses of atomic energy. Attention was directed to the fact that the problem of protecting the external environment from various modes of contamination of the biosphere, including radioactive contamination in particular, is taking on an increasingly broader international character.

One of the principal ways by which radioisotopes gain access to the human organism is through the ingestion of foodstuffs, so that migration of radioisotopes through the system: surface layer of air – soil – plants – agricultural animals was a topic to which special attention was given. The principles underlying estimates of the passage of the basic long-lived fission products Sr^{90} and Cs^{137} into agricultural products made on the basis of collation maps of the content of those isotopes in soils and of the concentrations of those isotopes in global radioactive fallout, were validated in work done by J. Kovács et al. (hungary). The diminution of the rate of Sr^{90} and Cs^{137} fallout in recent years has resulted in an appreciable lowering of the concentration of those isotopes in agricultural plants, in milk, and in meat. According to calculations by Š. Čupka (Czechoslovakia), about 50-70% of the content of Sr^{90} and Cs^{137} in agricultural crop products during the 1970-1971 period was due to uptake of these radioisotopes from the soil, while the role of migration of radioisotopes by routes other than the roots is gradually tapering off.

Estimates of processes by which artificial radioisotopes are taken up by plants from the soil and soil chemistry of fission products and isotopes with induced activity, were the subjects of various papers. I. T. Moiseev et al. (USSR) showed, in a series of field experiments and simulated field experiments,

Translated from Atomnaya Énergiya, Vol. 33, No. 3, pp. 795-796, September, 1972.

that differences in the storage of Cs^{137} by some of the most important agricultural crop plants (grain plants, cereal grains and legumes, potatoes) can be as great as tenfold. Differences in the amount of Sr^{90} stored up amounted to 2.5 to 3 times even in one species of plant studied (different strains of wheat, N. V. Korneeva et al., USSR). A report by J. Beneš (Czechoslovakia) demonstrated that the rate of vertical translocation of the radioisotopes Cs^{137} and Sr^{90} through the soil profile is respectively 10 and 100-1000 times greater, because of vigorous sorption of the two radioisotopes, than the rate of translocation of water. The interaction between Sr^{90} and the organic constituents of soil was shown to be of major importance in Sr^{90} migratory processes in soils (F. I. Pavlotskaya et al., USSR).

A rounded analysis of the behavior of artificial radioactive materials released into the environment is indissolubly bound up with biogeochemical research on the migration of radioisotopes through biological chains and food chains eventually terminating in the human organism. The heightened tempos at which Cs^{137} is incorporated into the ecological migratory cycles in alluvial wooded districts ("polessia") of the Ukrainian SSR and Belorussian SSR, and the effect of those heightened tempos on the role of radioecological processes in concentrating radioisotopes in individual links of the migration chain, were pointed out in a report by A. N. Marei et al. (USSR). Light-textured soils (soils of light mechanical composition) responsible for the low rate of Cs^{137} sorption and the correspondingly ready access of Cs^{137} to plants assimilating the isotope are found in abundance in those districts, so that Cs^{137} concentrations at above-average levels have been recorded in the grass, milk, meat, and in the local inhabitants in these districts. It must be stressed that, even though these Cs^{137} buildup levels are rather high, they are nevertheless far below the levels that could constitute a serious radiation hazard. But this example does illustrate the major role played by biogeochemical factors in radioisotope transport processes. É. B. Tyuryukanova et al. (USSR) pointed out the role played by geochemical factors in the behavior of Sr^{90} and Cs^{137} in USSR soils. The difference in the Cs^{137} distribution in different soils has the effect that the γ-radiation dose rate due to this radioisotope amounts to anywhere from 0.1 to 1.5 μrad/h in different districts; this accounts for about 5 to 15% of the radiation background due to the presence of naturally occurring γ-emitters in the soils (I. M. Nazarov et al., USSR).

This discussion of displacements of radioisotopes through the external environment, from a biogeochemical viewpoint, has made it possible to single out those organisms of the external environment which can act as biotracers of radioactive contamination. Among those organisms are mosses and conifer needles (L. Ryška et al., Czechoslovakia; P. P. Vavilov et al., USSR), and some wild animals (P. Hyacintov et al., Czechoslovakia).

Migration of radioisotopes through the external environment is affected by a host of ecological factors. In order to determine the radiation load on different objects in the environment, or in order to estimate the content of radioisotopes in those objects at fixed intervals of time, we use what are known as models of the migration of radioisotopes through migration chains (soil–plant, soil–human food–human organism, etc.). Regularities of the circulation of radioisotopes are expressed in mathematical form in those models, with the effect of drastically varying conditions of the external environment taken into account. The use of these models, presented in papers by K. P. Makhon'ko, M. P. Grechushkina (USSR) and E. Hladký et al. (Czechoslovakia), makes it possible to fashion a long-term prognosis of the consequences of introducing radioisotopes into the environment.

Some of the reports dealt with radiation safety in the operation of nuclear power generating stations. E. Csongor (Hungary) and T. Wardaszko (Poland) discussed release of tritium and Kr^{85} to the environment. According to the data they reported, the Kr^{85} concentration in the atmosphere has now attained levels of 15 to 20 pCi/m^3, and recent years have seen a trend toward increasing Kr^{85} concentrations. A report by E. Ettenhuber and W. Rensch (East Germany) cited findings of a study of the accumulation of Sr^{90} and Cs^{137} in fish taken from different reservoirs. It was stressed that planned release of radioactivity into water in the vicinity of nuclear power stations now being planned in the German Democratic Republic are far below the concentrations that would lead to accumulation of radioactive materials in fish above the critical tolerance level.

A series of reports dealing with water radioecology included papers by Czechoslovak scientists (M. Zavadský, J. Skalický, A. Velenovský, J. Křepelka, etc.), on pollution of aquatic media by radioisotopes of the uranium–radium series. R. Ilek et al. (Czechoslovakia) proposed several effective biosorbents for cleaning up waters contaminated by uranium and radium.

The basic difficulties in the area of technique in determinations of the content of radioisotopes in objects of the external environment, are generally due to the very low concentrations of the radioisotopes, and also with the complex array of isotopes present in the specimens to be analyzed.

Principles underlying the sampling of the environmental medium were the center of attention in the papers discussing techniques (J. Kovács and J. Negyelkovics, Hungary); the spotlight was also shared by such topics as the study of radioactive aerosols (V. Dvořák et al., Czechoslovakia), and the capabilities of semiconductor spectrometry (H. Procházka et al., Czechoslovakia).

Numerous investigations have demonstrated, consequently, that expansion of the network of nuclear power stations and the replacement of fossil-fuel-burning electric power generating stations by nuclear power stations will not lead to contamination of the external environment, but on the contrary will be helpful in nursing the external environment back to ecological health. Nuclear power eliminates venting to the atmosphere of such pollutants as sulfur dioxide gas, lead oxides, dust, and other toxic chemicals formed in the combustion of organic fossil fuels, while the danger of radioactive contamination of the environment through normal operation of nuclear power stations, and even under emergency conditions, is not great, as demonstrated by the data.

The radioecological conference was helpful in defining the outlook for further research in this area, and will contribute to contacts between scientists of COMECON member nations in the field of protection of the external environment with increasing use of atomic energy in the national economy.

Declassified and Approved For Release 2013/02/27 : CIA-RDP10-02196R000300110003-7

In March, 1972, a group of Soviet scientists traveled to the USA to carry out a joint Soviet–American experiment on small-angle proton–proton scattering. The experiment was staged at the 200 GeV accelerator of the USA National Accelerator Laboratory in Batavia. The experimental equipment (gas-jet hydrogen target, target remote monitoring and control system, etc.) was developed and fabricated in the USSR.

Joint research in this program is scheduled for a one-year period, and is being carried out under the terms of an agreement on joint work in the field of high-energy physics using the accelerators at the Institute of High-Energy Physics (USSR) and the National Accelerator Laboratory (USA), concluded between GKAÉ SSSR [USSR State Committee on the Peaceful Uses of Atomic Energy] and the USAEC on November 30, 1970. An earlier joint experiment using the High-Energy Physics Institute [IFVÉ] accelerator was carried out in 1970-1971, in studies of pion–electron scattering, and received a high estimate in both the USSR and the USA.

* * *

Under the terms of an agreement between the USSR and the GDR [East Germany] on further expansion of collaboration in the cause of peaceful uses of atomic energy, concluded on December 28, 1961, the working plans for scientific and technical collaboration are negotiated and signed on a yearly basis.

From May 10-12, 1972, representatives of the GDR and the USSR met at GKAÉ SSSR to review the balance sheet of collaboration for the years 1970 and 1971, and signed working plans for scientific and technical collaboration between GKAÉ SSSR and the Ministry of the Coal Industry and Power Industry of the GDR for 1972.

The plan provides for mutual assignments of Soviet and German scientists and specialists employed at institutes and enterprises, and engaged in the development of work on problems in atomic science and engineering.

The most fruitful collaboration between the GDR and the USSR is being carried out in the field of scientific research and experimental design work on fast reactors, scientific research and experimental work on water-cooled water-moderated power reactors, and in the field of development and design of radioisotope devices and electron physics equipment, developments and applications of radioactive isotopes and isotope preparations, etc. Joint nuclear physics research on particle accelerator engineering is also in progress.

Some joint developmental projects have been initiated in the recent period on scientific and technical problems, and joint design work in the field of nuclear power is underway.

Active scientific and technical collaboration contributes to technical progress and serves as a shining example of the deepening, improving, and further development of the socialist economic integration of the member nations of COMECON.

* * *

The ninth session of the Franco–Soviet scientific commission, acting in line with the terms of an agreement concluded between GKAÉ SSSR and the French Commissariat de l'Énergie Atomique on conducting joint nuclear research projects in the field of high-energy physics, using the 70 GeV accelerator, was held at Saclay on May 9-12, 1972.

The performance on the French Mirabel liquid-hydrogen bubble chamber on beams produced by the Serpukhov accelerator over the period since the last session of the commission in October, 1971, was

Translated from Atomnaya Énergiya, Vol. 33, No. 3, p. 796, September, 1972.

reviewed. During the physics session in February-March, 1972, the chamber took 40,000 photographs in a beam of 70 GeV protons and 4000 photographs in a beam of 50 GeV π-mesons. The operating conditions of the Mirabel bubble chamber are close to ratings. It was recommended that studies aimed at improving chamber performance, and improving the quality of the photographs still further, be carried out, and that efforts be made to achieve operation with two expansions per cycle.

During February and April, the optics of the seventh channel handling beams of particles on momentum 23 GeV/c and 32 GeV/c obtained from an external target with the aid of an extracted beam were adjusted. The high-frequency separator was adjusted, and separated beams of K-mesons of momentum 32 GeV/c were produced. The results of the measurements showed that over 95% $K^{\pm}$-mesons are contained in the separated beams.

Impressive success on the part of CERN and IFVÉ specialists in producing beams of separated particles in the IFVÉ accelerator was reported. Preliminary results of processing of the data obtained by irradiating the Mirabel bubble chamber with protons, and processing the data at IFVÉ and at Saclay, were discussed. The results showed that the energy dependence of multiple production of particles in proton–proton interactions at energies to 60 GeV differs essentially from the dependence predicted on the basis of cosmic-ray data. A plan for staging future irradiations of the Mirabel bubble chamber during 1972 was discussed and approved. Priority is being given to experiments in separated beams of 32 GeV K-mesons. It is assumed that the new plates of proton–proton interactions at the 70 GeV energy will be taken in October, 1972.

Informational reports were heard on the development of equipment for processing film information at French and Soviet laboratories, and on providing those laboratories with measuring and viewing equipment, and also on providing equipment of this type to the laboratories of CERN member nations interested in participating in the Mirabel bubble-chamber research program.

The work of the commission was carried out successfully.

G. N. Balasanov

STIMULATION AND OPTIMIZATION IN AUTOMATED CONTROL SYSTEMS*

Reviewed by A. M. Rozen and Yu. G. Mitskevich

The above-mentioned book by Balasonov is subtitled: Problems in the Development of Automatic Systems for Control of Continuous Production Processes, with Practical Examples Relating to the Hydrometallurgy of Rare Metals and Radioactive Metals.

G. N. Balasanov is the author of two books devoted to automation of hydrometallurgical processes: Fundamentals of the Automation of Technical Processes in the Hydrometallurgy of Rare Metals and Radioactive Metals (Atomizdat, Moscow, 1960); and Optimum Hydrometallurgical Process Control (Atomizdat, Moscow, 1967). The first book discusses local systems for automatic monitoring and control of production processes, and the second book deals with optimization of production conditions in operational control. This new book by G. N. Balasanov continues the basic trend evident in his work: improvements in production process control. Topics now attracting the greatest attention on the part of specialists in the field of control theory and control systems design, and still covered inadequately in the literature, are treated, included are theoretical and practical problems and questions of techniques in simulation and optimization in the development and utilization of automatic control systems.

The purpose of the book is to provide a reference manual and training manual on simulation and optimization techniques. The need for such a text is beyond question, since the development and implementation of automatic control systems are now being pursued in all branches of industry in the USSR. Specialists in appropriate related fields are trained in crash programs instituted as skill upgrading courses and in automatic control system design departments organized at some college-level institutions in the country. Managers at several echelons in industrial enterprises (plant managers, chief plant engineers, etc.), are also interested to some extent in how automatic control systems are organized. Such a wide range of specialists working at different levels, and such a wide range of students, definitely have a need for training and reference materials of this nature.

The book contains six chapters. The introduction presents concise information on problems encountered in the design of automatic control systems, on the stages of design and development of automatic control systems, and on the structure of automatic control systems. The first chapter contains reference mathematical materials presented by the author as a suitable language for describing the processes, states, and performance of control systems. This chapter includes some basic information on the theory of sets, probability theory, mathematical statistics, matrix algebra, and also on the dynamics of continuous and discrete systems.

The second chapter presents the overall methodology of operations research and systems research (systems analysis), as well as several particular problems in the investigation of optimization of automatic control systems operations, such as the optimum control of production, experimental statistical methods in simulation of automatic control systems, the apparatus of Boolean functions as a means of simulating the logic of systems, the Monte Carlo method, the optimum selection of solutions in a conflict situation and under conditions of risk and indeterminacy. This chapter consequently contains basic problems in the simulation and optimization of control processes in automatic control systems. In order to illustrate the

*Atomizdat, Moscow, 1972.

Translated from Atomnaya Energiya, Vol. 33, No. 3, pp. 797-798, September, 1972.

approach to optimum control of continuous production processes, the author discusses the example of control of hydrometallurgical processes. Examples relating to the field of engineering diagnostics in the automatic control systems installed in a mining and metallurgical combine are also presented, as well as other examples from the field of hydrometallurgy and beneficiation of ores.

In the third chapter, devoted to the principal methods employed in optimum planning in automatic control systems, optimization of the production plan or production program is discussed in the light of an example of setting up a monthly production output plant at a processing plant. This problem is solved by linear programming methods, which are incidentally also elucidated by a concrete example. Methods of dynamic programming, illustrated by the solution of a resources allocation problem, are also described briefly. An example of planning of a stock of reagents at the storehouse of the processing plant is used to illustrate the application of several methods in the theory of inventorying. Methods in scheduling theory are also discussed, from the standpoint of optimized sequencing of operations.

The fourth chapter describes modern methods of research, as well as synthesis and optimization of complex control systems. Theoretical methods of cybernetics and applied mathematics that have found applications not only in control systems but also in the solution of various problems in complex systems in general, are presented for discussion. The theory of the control of discrete systems and continuous systems, the theory of optimal control systems, queuing theory, the theory of mathematical programming, as well as methods of pattern recognition, methods of learning and adaption, are discussed briefly. The methods of queuing theory and Markov chains are applied to the solution of the problem of developing a probabilistic analytical model of a production plant control system. The model can be used to forecast the dynamics of variation in the productivity of the enterprise in terms of one of the products manufactured by the enterprise. The use of methods of pattern recognition, learning, and adaption is illustrated by a learning extremal-control system with compensation of perturbations, employed to control complex technological processes in hydrometallurgical production and in chemical production.

The fifth chapter of the book discusses several examples of systems research applied to technological processes. The organization of systems research is demonstrated. Methods of regression analysis are used to obtain empirical models of the principal hydrometallurgical processes: wet ore extraction, leaching, and solvent extraction. The experimental statistics methods presented earlier, in the second chapter of the book, in the process of developing those models, are illustrated with concrete numerical material. An interesting problem involving a choice of one of several possible models (from the standpoint of the assumed underlying mechanism of the production process) based on experimental findings, is solved. The method of maximum likelihood and the Bayes approach, both discussed in preceding chapters, are used in finding the appropriate model. The problem of how to set up the most representative experiment is solved on the basis of statistical criteria. The development of optimal control algorithms for several hydrometallurgical processes is described in the conclusion to that chapter.

The last chapter deals with human–computer interaction in the control system, computer problems in a control system, and generalized data on cost effectiveness of the use of computers in control systems.

The book consequently offers the reader reference material on basic mathematical topics encountered in the design and development of automatic control systems. Numerous examples illustrating the solution of particular automatic control system problems are most helpful.

The presentation of the material is generally quite successful, but there are some shortcomings. Some of the main points referring to classification problems and to some aspects of design work (cf. the introduction, the beginning of the first chapter) give the impression of being the author's personal opinions, and as such are open to discussion. The selection and composition of the material by chapters occasionally leads to repetition (e.g., linear programming dealt with in both the third and fourth chapters). In some instances, the author was not successful in completely overcoming difficulties associated with the presentation of material of different levels of complexity within the same text, so that some sections will present unexpected difficulties to the reader whose background is adequate for other sections (the sections dealing with the theory of mathematical programming presents such difficulties, for instance). At the same time, the very advanced reader will find sections in which the presentation is too simplified.

The topics involving interaction and interfacing between the human operator, and the computer machine, cost problems, and computer operation and design problems, all now much in the limelight, and dealt with in the sixth chapter (written by M. M. Tsegel'nitskii), are not covered adequately (if we consider

Declassified and Approved For Release 2013/02/27 : CIA-RDP10-02196R000300110003-7

the availability of literature familiar to a broad audience), and the presentation is not free of contradictions.

On the whole, we can state that the author has come off well, handling a rather complicated problem, involving the presentation of basic information on simulation and optimization in the development and utilization of automatic control systems to a broad readership of specialists concerned with the development and implementation of such systems.

L. Kh. Éidus

PHYSICOCHEMICAL FUNDAMENTALS OF RADIOBIOLOGICAL PROCESSES AND RADIATION PROTECTION*

Reviewed by Yu. V. Sivintsev

This monograph by a renowned Soviet specialist in the field of molecular biology contains a consistent description of various stages in the physicochemical process of radiation injury, shielding and protection, and treatment and recovery, of biological objects. Earlier concepts dealing with primary processes, until recently viewed as fundamental in radiobiology, are analyzed critically.

The book begins with a chapter dealing with the properties of ionizing radiations in processes by which they interact with matter. The next two sections are devoted to regularities of direct and indirect radiation effects on biological structures. Here the reader finds primary information on the principles of "hits" and "targets," and also on the schema and products of water radiolysis. The author was successful in presenting these topics with sufficient rigor while relying to a minimum on mathematical formulations. The fourth chapter offers a compressed presentation of reference data on one of the most remarkable discoveries in molecular radiobiology: the process of migration of energy and charge in biological structures. The so-called "oxygen effect," i.e., the enhancement of radiation injury when oxygen is introduced (compared to the level of injury caused by anaerobic irradiation) is the subject of the fifth chapter, in which the description of the oxygen "aftereffect" on potential injuries to biological macromolecules is deserving of special note. A quantitative analysis of the physicochemical mechanism underlying that phenomenon and the nature of latent injuries in the case of several enzymes, is given in the sixth chapter. The next section acquaints the reader with mechanisms of physicochemical recovery of biological macromolecules afflicted with radiation injury. The eight chapter discusses the protection and sensitization mechanisms of biological structure brought about by low-molecular-weight compounds. Here new concepts on the mechanism of protection by chemical impurities in indirect radiation effects are presented in a detailed treatment, making it possible to explain the cause of the direct and inverse oxygen effects.

Hypotheses relating radiosensitivity, protection, and recovery to sulfohydrile groups and to sulfur-containing compounds are analyzed in the ninth chapter. The little-studied modifying effect of water in radiation effects, the physical mechanism of which has not been deciphered to date, is described in the tenth chapter. The next chapter presents data on special features of the biological effects of densely ionizing radiations (the term "strongly ionizing particles" presented in this treatment appears to be an unfortunate choice of term). The concluding section of the book is highly interesting, and deals with results obtained in molecular radiobiology through the method of electron paramagnetic resonance (Chapter 12).

* Atomizdat, Moscow, 1972.

Translated from Atomnaya Énergiya, Vol. 33, No. 3, p. 798, September, 1972.

The monograph being reviewed is recommended as a textbook for students majoring in biology in colleges. The book may be read with interest by radiobiologists, research scientists, and engineers whose work involves ionizing radiations.

I. B. Rubashov and Yu. S. Bortnikov

ELECTROGAS-DYNAMICS*

Reviewed by V. G. Lapchinskii

The book we propose to review is the first monograph to appear in the new field of electromagnetohydrodynamics, or electrogas-dynamics – the study of the flow of unipolar-charged or polarized fluids and gases immersed in a strong electric field.

The center of attention (for several decades) of investigators of electromagnetohydrodynamics, i.e., of that branch of physics combining the concepts of hydrodynamics and electrodynamics, has been magnetohydrodynamics. The decisive factors in magnetohydrodynamics are the strong magnetic field and the electrical conductivity of the quasineutral medium. Comparatively little attention has been given to the study of a broad class of hydrodynamical phenomena in a dielectric medium attributable to the presence of strong electric fields when magnetic fields play only a negligible role. We can only welcome the appearance of this book for that reason, inasmuch as it reviews and generalizes the experience accumulated in this intensely developing branch of science.

The content of the monograph can be divided into two parts. The first part discusses theoretical aspects of EHD (electrohydrodynamics), derives a general system of equations of EHD, formulates a system of electrogas-dynamic criteria, and analyzes fundamental particular cases of the solution of those equations describing the most important EHD flow patterns (one-dimensional flow, completely developed flow, axisymmetric flow, etc.).

The general system of equations is formulated in line with the proposed general definition of an EHD system by the authors (as a system in which the effective electric field is far greater, while the effective magnetic field is of the order of the corresponding induction fields). This definition, while not generally accepted at the present time, enables the authors to build a unique logical construction, and fully answers, in our opinion, the purpose it was intended for.

The sections devoted to the formulation of a system of EHD criteria and to separation of the electrodynamical flow into distinct subregions are deserving of special note. The construction of this part facilitates a comparison of EHD systems and MHD systems. It turns out that some of the EHD criteria and MHD criteria share a common physical meaning, and characterize the relationship between the hydrodynamical forces, viscous forces, and forces associated with the electromagnetic field. The criteria in this class were named by the authors by analogy with their familiar MHD counterparts (e.g., the electrical pressure number, etc.). The specific properties of EHD systems are characterized by criteria which have no analog in MHD systems (such as the space-charge criterion, etc.).

The second part of the book contains sections devoted to the analysis of fundamental EHD patterns and to the application of this analysis to investigations and design calculations of specific engineering devices. The focus in this section is on a reasonably detailed analysis by the authors of one-dimensional

* Atomizdat, Moscow, 1971.

Translated from Atomnaya Energiya, Vol. 33, No. 3, p. 798-799, September, 1972.

and quasi-one-dimensional flow patterns, and the use of the resulting conclusions and regularities in describing an EHD electric power generator and an EHD pump.

Theoretically, interest centers on an analysis of the breaking of the sound barrier in EHD flows, which evince certain special traits. In particular, the speed of sound can be surpassed in two flow regimes, one of which constitutes an analog of the Laval nozzle, the other allowing an analogy with gas-dynamic thermal nozzles.

The theoretical analysis carried out enable the authors to device a suitable procedure for the design and analysis of specific EHD devices, and to design and investigate laboratory models. It must be pointed out that much attention is given in the text to the description of engineering EHD devices, and especially to EHD direct power converters. The principles and design features of such devices are described, along with their ranges of applications, results of experimental investigations and tests, procedures for forecasting ranges of performance parameters, etc. This attention is entirely justified, once we consider the practical potential value and overall outlook of EHD devices.

The monograph, as a first experiment in this new field, is of course not without shortcomings, determined to a partial extent by the nature of the text and subject. The author's efforts to encompass all of the basic topics in electrohydrodynamics inevitably leads to uneven presentation of various divisions of the subject, and a certain marked conciseness in the description of engineering applications. The highly important and quite interesting topics of two-phase EHD flow patterns, boundary layer EHD, and the theory of EHD instabilities, found no reflection in the text.

The widespread use of EHD will lead to further development of the phenomenon, and that will undoubtedly call for a second edition of the book in due time. In that case, we feel the first part of the book should be expanded to include a kinetic description of plasma, the relativistic generalization of plasma, and the transition to the nonrelativistic case. Numerous astrophysical applications should be reviewed in the second part. The problem is that there are instances in the dynamics of cosmic plasma which need not be treated as relativistic, i.e., where the system of EHD equations can be applied entirely in an external Newtonian field, or in the gravitational field proper. The introduction of such problems would make the monograph a more useful reference for a broader range of specialists. At the same time, those additions would expand the volume of the book and render the presentation even more uneven, especially in the second part (Chapters 3 and 4). This contradiction could be overcome in turn by leaving the first part of the monograph without essential changes and developing some particular field in the overall coverage of EHD phenomena (e.g., astrophysical and engineering topics, etc.).

The publication of the book is very timely. The book will attract the attention of a wide range of specialists to this new and promising branch of science.

J. Cronin, D. Greenberg, and V. Telegdi

COLLECTION OF PHYSICS PROBLEMS WITH SOLUTIONS*

Reviewed by V. A. Krivonosov, V. G. Lapchinskii, and B. A. Medvedev

This collection contains problems presented at the degree examination on classical and modern physics taken by graduate students in the physics department of the University of Chicago.

The collection includes 362 solved problems on the following twelve topics: mathematical physics, mechanics, electromagnetism, electronics, optics, quantum mechanics, thermodynamics, statistical physics, atomic physics, solid-state physics, nuclear physics, experimental physics. Solutions are given for all of the problems, except those on experimental physics.

The publication of this translated text will be a great benefit to our young scientific cadres.

On the whole, the level of the physics problems is close to the level of the problems found in the textbook by L. D. Landau and E. M. Lifshits. The collection of problems is also similar to various collections of problems published here on various topics in physics (e.g., the Collection of Problems in Quantum Mechanics by I. I. Gol'dman and V. D. Krivchenkov).

The "Mathematical physics" section contains for the most part fairly elementary problems designed to verify the mathematical level required in the work. This section is placed at the very beginning and contrasts to a certain extent with the interesting physics problems found in the succeeding sections.

As excellent teachers, the authors show an unusually good "feel" in the solution they give for the problems, "urging" the reader onto the correct path. The solutions are designed for a reader with an excellent physics background.

We should like to see alterations in future editions of this collection of problems. In consideration of the broad applications of group theory and of the theory of group representations in modern physics, this important section should be accorded more space (rather than the one long problem allotted in the present edition), but this may possibly reflect the existing program for the minimum in degree qualifications in the USA. The problem on clocks should be formulated more precisely, stipulating spring-drive clocks and not pendulum clocks. And finally, the term "distribution function Z" should be replaced by the term "statistical sum Z" which is the common usage in our literature.

*Russian translation, Atomizdat, Moscow, 1971.

Translated from Atomnaya Énergiya, Vol. 33, No. 3, pp. 799-800, September, 1972.